EVALUATION OF HYBRID BINDER FOR DENSE- AND OPEN-GRADED ASPHALT MIXTURES

By

WEITAO LI

A DISSERTATION PRESENTED TO THE GRADUATE SCHOOL
OF THE UNIVERSITY OF FLORIDA IN PARTIAL FULFILLMENT
OF THE REQUIREMENTS FOR THE DEGREE OF
DOCTOR OF PHILOSOPHY

UNIVERSITY OF FLORIDA

2009

To my beloved parents, Shuling Li and Yuying Meng

ACKNOWLEDGMENTS

It is a great pleasure to thank those people and organizations who offered their self-giving assistance to this research and finally made this dissertation possible.

First of all, I am heartily thankful to my supervisor, Dr. Reynaldo Roque, whose encouragement, supervision and support from the preliminary to the concluding level enabled me to develop a deep understanding of the subject. Without your knowledgeable guidance and mentoring, it would have been impossible for me to finish my doctoral work.

Also I owe my great gratitude and thankfulness to my committee members: Dr. Mang Tia, Dr. Dennis R. Hiltunen and Dr. Bhavani V. Sankar for their invaluable support and advices on accomplishing my work.

Thirdly, special thanks go to Florida Department of Transportation (FDOT) for providing financial support, testing instrumentation, materials that made this research possible. I would like to specifically thank Gale Page, David Webb, Aaron Turner, and Mabel Stickles for their help; their efforts are sincerely appreciated.

I would also like to extend my thanks to Frank Fee from CITGO Petroleum for his assistance in obtaining the control binders for this study, and to the three hybrid binder producers for their time and efforts in producing their different products for this study

In addition, I would like to express my appreciation to Mr. George Lopp for his kind help with material preparation, testing setup and many other technical supports for this research. I also thank Tianying Niu for his hard work and contribution to this project and Dr. Alvaro Guarin for his assistance in helping organize part of the final format of this dissertation.

Lastly, I thank all of my colleagues for spending these wonderful years together.

TABLE OF CONTENTS

page

ACKNOWLEDGMENTS 4

LIST OF TABLES 7

LIST OF FIGURES 9

LIST OF ABBREVIATIONS 13

ABSTRACT 15

CHAPTER

1 INTRODUCTION 17

Background 17
Objectives 20
Scope 21

2 LITERATURE REVIEW 23

Crumb Rubber Used as Asphalt Binder Modifier 23
Polymers Used as Asphalt Binder Modifier 25
Development of Hybrid Binders in Recent Years 26
Methodologies of Evaluating Asphalt Mixtures Healing 28
Pseudo Stiffness Method 28
Ratio of Dissipated Energy Change (RDEC) Method 30
Dissipated Creep Strain Energy (DCSE) Method 32
Elastic Deformation and Strain Recovery 34
Summary 36

3 MATERIALS AND METHODS 38

Binders 38
Aggregates 42
Mixtures 45
Mixture Preparation 46

4 BINDER TEST RESULTS AND ANALYSIS 50

Binders Physical Properties 50
Specific Gravity of Binders 50
Solubility Analysis 51
Mass of Volatiles Loss Analysis 52
Binders Rheological Properties 53

DSR Test Results Analysis 53
BBR Test Results Analysis 57
Multiple Stress Creep Recovery (MSCR) 59
Elastic Recovery 64
Force Ductility Test 65

5 MIXTURE IDT TEST RESULTS AND ANALYSIS 70

Mixture Test Results 70
Analysis of IDT Test Results 77
DG Mixtures 77
OGFC Mixtures 81
Summary 82

6 DEVELOPMENT AND EVALUATION OF HEALING TEST 87

Experimental and Theoretical Background of Healing Test 87
Fatigue Test with Static and Cyclic Loading 87
Damage and Healing 89
Healing Test Development 91
Cyclic Damage Loading (CDL) Mode 91
Loading Amplitude Verification 97
Healing Test Program 101
Data Acquisition 101
Materials Prepared for Healing Test 104
Healing Test Results Analysis 105
Damage Analysis during CDL 105
Healing Analysis of DG Mixtures 111
Summary 115

7 CLOSURE AND RECOMMENDATIONS 117

Summary 117
Conclusions 119
Recommendations 120

APPENDIX

A BINDER TEST RESULTS 122

B HEALING TEST RESULTS 129

C CITGO CERTIFICATES OF ANALYSIS 132

LIST OF REFERENCES 134

BIOGRAPHICAL SKETCH 136

LIST OF TABLES

Table		page
3-1	Asphalt binder and the constituents/formulations	40
3-2	Binder tests summary	41
3-3	Aggregate source	42
3-4	DG mixtures IDs for testing	46
3-5	OGFC mixtures IDs for testing	46
3-6	Dense graded mixture volumetric information	49
3-7	OGFC mixture volumetric information	49
4-1	Specific gravity of binders, 15.6 ºC (60 F)	51
5-1	Summary of total mixture tests	70
5-2	DG mixtures creep and damage test results	71
5-3	DG mixtures strength and fracture test results	72
5-4	DG mixtures energy ratio results	73
5-5	OGFC mixtures creep and damage test results	74
5-6	OGFC mixtures strength and fracture test results	75
5-7	OGFC mixtures energy ratio results	76
6-1	Failure criteria for fatigue test	100
6-2	Materials for healing test	105
6-3	Poisson's ratio comparison	107
6-4	Comparison of DCSE and MR reduction at 20 minutes CDL	115
A-1	G*/sinδ and δ at 67 ºC (152.6 F)	122
A-2	G*/sinδ and δ at 70 ºC (158 F)	122
A-3	G*/sinδ and δ at 76 ºC (168.8 F)	122
A-4	G*/sinδ and δ at 82 ºC (179.6 F)	122

A-5 G*/sinδ and δ at 88 ºC (190.4 F) 123
A-6 G*/sinδ and δ at 90 ºC (194 F) 123
A-7 G*sinδ and δ at 25 ºC (77 F) 123
A-8 G*sinδ and δ at 22 ºC (71.6 F) 123
A-9 G*sinδ and δ at 19 ºC (66.2 F) 124
A-10 G*sinδ and δ at 16 ºC (60.8 F) 124
A-11 BBR test results at -12 ºC (10.4 F) 124
A-12 BBR test results at -18 ºC (0.4 F) 125
A-13 Multiple stress creep recovery, %, RTFOT residue 125
A-14 Non-recoverable creep compliance, kPa^{-1}, RTFOT residue 125
A-17 Elastic recovery at 25 ºC (77 F) (RTFOT residue) 125
A-18 Force ductility test result 126
A-19 Smoke point, flash point and solubility of original binders 126
A-20 Mass loss after RTFOT at 163 ºC (325.4 F) 126

LIST OF FIGURES

Figure		page
1-1	Waste tires use history in Florida	18
2-1	Typical effect of healing due to rest period	30
2-2	Healing test results (1,000 cycles, 75 psi, 15°C)	34
2-3	Normalized healing (after 1000 cycles, 75 psi, 15 °C)	34
2-4	Load controlled cyclic loading and rest periods	35
2-5	A sample plot of the strain versus time during the loading/rest period	36
3-1	DG granite gradation	43
3-2	DG limestone gradation	43
3-3	OGFC granite gradation	44
3-4	OGFC limestone gradation	44
3-5	Mixture testing plan for each mixture and aggregate type	45
3-6	Pill contained with mesh	48
3-7	CoreLok sample weighing equipments	49
4-1	Solubility of original binders	51
4-2	RTFOT, mass loss at 163 ºC (325.4 F)	52
4-3	G*/sinδ, 76 ºC (168.8 F) @ 10 rad/s	55
4-4	Phase angle δ, 76ºC (168.8 F) @ 10 rad/s	55
4-5	G*sinδ, 25 ºC (77 F) @ 10 rad/s	56
4-6	Phase angle δ, 25 ºC (77 F) @ 10 rad/s	56
4-7	S(t), -12 ºC (10.4 F) @ 60 second	58
4-8	m-value, -12 ºC (10.4 F) @ 60 second	58
4-9	Typical ten cycles creep and recovery with creep stress of 100 Pa	60
4-10	Typical creep and recovery cycle with creep stress of 100 Pa	60

4-11 MSCR average recovery at 67.0ºC (152.6 F) (RTFOT residue) 62
4-12 MSCR non-recoverable compliance at 67.0 ºC (152.6 F) (RTFOT residue) 62
4-13 MSCR average recovery at 76 °C (168.8 F) (RTFOT residue) 63
4-14 MSCR non-recoverable compliance at 76 ºC (168.8 F) (RTFOT residue) 63
4-15 Elastic recovery at 25 ºC (77 F) (RTFOT residue) 64
4-16 Force ductility test result, 10 ºC (50 F) 65
4-17 Force ductility test result, 25 ºC (77 F) 66
4-18 Stress-strain diagram of RTFOT residue at 10 ºC (50 F) 67
5-1 $N_{initiation}$ for DG granite mixtures 78
5-2 $N_{propagation}$ for DG granite mixtures 78
5-3 $N_{initiation}$ for DG limestone mixtures 79
5-4 $N_{propagation}$ for DG limestone mixtures 79
5-5 ER for DG granite mixtures 80
5-6 ER for DG limestone mixtures 80
5-7 $N_{initiation}$ for OGFC granite mixtures 83
5-8 $N_{propagation}$ for OGFC granite mixtures 83
5-9 $N_{initiation}$ for OGFC limestone mixtures 84
5-10 $N_{propagation}$ for OGFC limestone mixtures 84
5-11 ER for OGFC granite mixtures 85
5-12 ER for OGFC limestone mixtures 85
6-1 Typical strength test result for DG mixtures, STOA, 10 ºC 89
6-2 HMA material fatigue curve under cyclic loading 90
6-3 Damage recovery curve 91
6-4 Haversine loading waves 93
6-5 Initial resilient deformation with different rest periods, 10 ºC 94

6-6 Rest period effects on resilient deformation, 1755 lbs, 10 ºC 96
6-7 CDL test results, 0.9 second rest, 10 ºC 96
6-8 DG mixtures IDT strength test, 10 ºC 98
6-9 DGUS cyclic loading test results, 0.4 second rest, 10 ºC 98
6-10 DCSE obtained from tensile strength test 99
6-11 Healing test flow chart 102
6-12 Data acquisition during healing phase 103
6-13 Data collection illustration 103
6-14 Resilient deformation 105
6-15 Poisson's ratio comparison, 10 ºC 107
6-16 Damage and healing interpretation with resilient modulus 109
6-17 DG mixtures normalized resilient modulus at damage phase 110
6-18 Relationship between modifier contents and damage rate 110
6-19 Combined regression for healing test 111
6-20 Damage (DCSE) and healing rate comparison 113
6-21 Damage (resilient modulus reduction) and healing rate comparison 114
6-22 Reduced resilient modulus vs reduced DCSE, 20 minutes loading 114
A-1 Original binders stress-strain diagram, 10 °C (50 F) 127
A-2 RTFOT residues stress-strain diagram, 10 ºC (50 F) 127
A-3 PAV residues' stress-strain diagram, 25 ºC (77 F) 128
B-1 M_{RDGUS} at damage and healing, 10 ºC 129
B-2 M_{RDGMS} at damage and healing, 10 ºC 129
B-3 M_{RDGRS} at damage and healing, 10 ºC 130
B-4 M_{RDGAS} at damage and healing, 10 ºC 130
B-5 M_{RDGBS} at damage and healing, 10 ºC 131

B-6 M_{RDGCS} at damage and healing, 10 ºC 131

LIST OF ABBREVIATIONS

AASHTO	American Association of State Highway and Transportation Officials
ARB-12	Asphalt rubber binder with 12% crumb rubber
ARB-5	Asphalt rubber binder with 5% crumb rubber
BBR	Bending Beam Rheometer
CDL	Cyclic damage loading
CRM	Crumb rubber modifier
DG	Dense graded granite
DGUL	Long term oven aged dense graded granite mixture with binder PG 67-22
DGUS	Short term oven aged dense graded granite mixture with binder PG 67-22
DL	Dense graded limestone
DLUL	Long term oven aged dense graded limestone mixture with binder PG 67-22
DLUS	Short term oven aged dense graded limestone mixture with binder PG 67-22
DSR	Dynamic Shear Rheometer
ER	Energy ratio
FDOT	Florida Department of Transportation
HB	Hybrid binder
HMA	Hot Mix Asphalt
IDT	Indirect tension test
MSCR	Multiple Stress Creep Recovery
NCAT	National Center of Asphalt Technology
OGFC	Open graded friction course
PG	Performance grade

RTFOT	Rolling thin film oven test
CDL	Cyclic damage loading
SBS	Styrene Butadiene Styrene

Abstract of Dissertation Presented to the Graduate School
of the University of Florida in Partial Fulfillment of the
Requirements for the Degree of Doctor of Philosophy

EVALUATION OF HYBRID BINDER USE IN SURFACE MIXTURES IN FLORIDA

By

Weitao Li

December 2009

Chair: Reynaldo Roque
Major: Civil Engineering

Binder and mixture tests were performed to evaluate the relative performance of a PG 67-22 base binder and six other commercially available binders produced by modifying the same base binder with the following modifiers: one Styrene Butadiene Styrene (SBS) polymer, three commercially available hybrid binders composed of different percentages of rubber and SBS polymer, and two asphalt rubber binders (5% and 12 % rubber: ARB-5 and ARB-12). Results indicated that hybrid binders (modified with more rubber than SBS) that exceed the cracking performance characteristics of unmodified binder and asphalt rubber binders, and have about the same cracking performance characteristics of SBS polymer modified binder can be produced commercially. Results also indicated that hybrid binder can be suitably specified using existing specification requirements for PG76-22 binder and solubility. Therefore, it appears that hybrid binder has the potential to replace three binders currently used by FDOT in hot mix asphalt: SBS polymer modified asphalt, ARB-5, and ARB-12. It was recommended that FDOT develop a transition plan to accomplish this. The research also showed that existing binder tests do not accurately predict cracking performance at intermediate temperatures, even in a relative sense.

A further Healing testing was performed on the dense-graded granite mixtures to evaluate the healing potential of hybrid binders compared to base binders. Different testing procedures were carried out and analyzed to give a better understanding of healing mechanisms. Results from healing test agreed with those from cracking performance evaluation. However, more healing parameters and procedure need to be fully developed to capture healing characteristics more specifically. It was recommended that FDOT pursue development and evaluation of the healing test.

CHAPTER 1
INTRODUCTION

Background

According to the 2007 estimates of the United States Census Bureau, the State of Florida is the fourth most populous state in the union with a population of approximately 18.25 million people and growing by approximately 1000 residents every day. This population growth not only increases the number of vehicles using the state's infrastructure, but also adds to the state's waste management efforts with respect to the increasing number of waste tires which will eventually accompany the growth in the number of automobiles using Florida's highways.

The Florida Department of Environmental Protection (DEP) reports that prior to 1989, almost all waste tires were either land filled (whole carcasses) or stockpiled. That same year, legislation was passed requiring all tires to be cut or shredded into 8 or more pieces prior to disposal thereby, reducing the total volume of the waste product. This effort consequently sparked the development of alternative uses for this waste product; including asphalt and soil modification; playground or sporting area surfacing or covers; the molding of new rubber-based consumer products, and other applications.

The Florida Department of Transportation (FDOT) utilizes tons of crumb rubber annually, from local producers, for use in FDOT contracted Asphalt Rubber Membrane Interlayer (ARMI), friction courses and sealants used in roadway construction and maintenance. In fact, Florida is the only state which routinely specifies Rubber Modified Asphalts (RMAs) for use in their final surface asphalt mixture (friction courses) on all state highways. The following figure indicates that although both the total number of waste tires and the amount of crumb rubber generated from these waste tires have

remained relatively constant over the period; the usage by FDOT has been decreasing, from approximately 18% to 10% of the total crumb rubber generation.

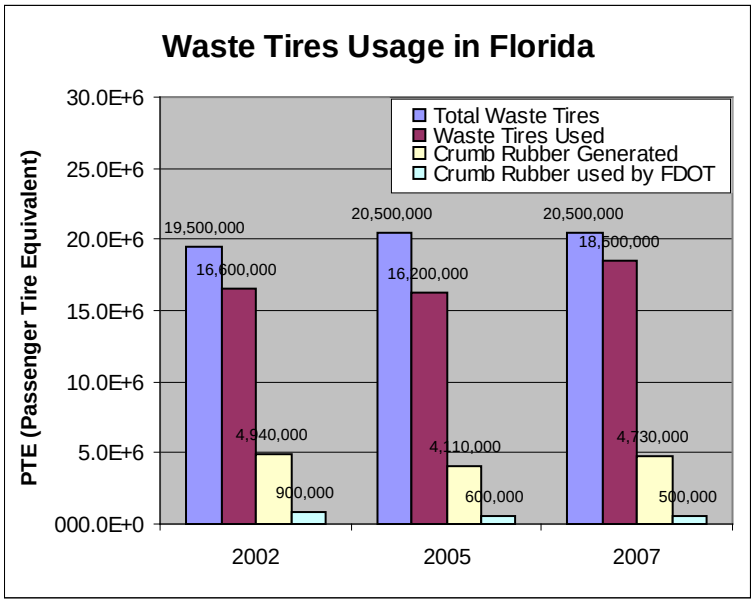

Figure 1-1. Waste tires use history in Florida

Currently, Florida's specifications identify asphalt binders incorporating the use of crumb rubber by binder type and application. These include:

ARB-5 (5% rubber by weight of asphalt), used in Dense Graded Surface Mixtures

ARB-12 (12% rubber by weight of asphalt), used in Open Graded Friction Courses (OGFCs)

ARB-20 (20% rubber by weight of asphalt), used as part of an anti-reflective crack relief layer

The use of these binders was not introduced just to consume crumb rubber as a means to an end, that is, to comply with the comprehensive 1988 Florida State Solid Waste Law. Research conducted in-house by FDOT, the National Center for Asphalt Technology at Auburn University (NCAT) and the University of Florida has shown the beneficial effects of these materials. OGFCs have benefited from asphalt rubber binders

by exhibiting improved short-term raveling resistance, and improved cracking resistance; and Florida's dense graded friction courses, FC-9.5 and FC-12.5, exhibited small improvements in rut resistance over a conventional binder as determined, in an FDOT accelerated pavement analyzer study (Moseley, et al., 2003). In addition, it is generally well accepted that rubber reduces the rate of oxidative age-hardening, which can have a beneficial effect on cracking.

Polymer Modified Asphalts, or PMAs, have been used in Florida since 2001. PMAs are modified by the reacted addition of Styrene Butadiene (SB) polymer or Styrene Butadiene Styrene (SBS) polymers to a base binder. Based on research performed on Florida's Accelerated Pavement Tester (APT) and work performed at NCAT, PMAs have been shown to improve the rutting resistance of good performing asphalt mixtures. Consequently, Florida now uses polymer modified asphalt mixtures for the top layer, or top two layers, on Interstate high truck volume construction projects. In 2004, Florida decided to include the use of PMAs in Interstate high truck volume OGFC based on data from University of Florida testing which indicated better rutting and cracking performance of OGFC (Tia, et al., 2002), and as a method to simplify construction by allowing contractors to purchase larger quantities of a single binder.

The cost of Hot Mix Asphalt (HMA) tripled from about $35 a ton in 1999 to over $100 a ton in 2007. This is mainly due to the reduction in crude oil supply, which therefore, increased the cost of asphalt as a by-product of crude. The increased price of aggregate due to shortages also contributed to the increased cost of HMA. From 1999 to about 2005, asphalt binder prices remained relatively flat, from $100 to $200 a ton, but spiked to almost $500 a ton by 2008. In 2008, a Florida Department of

Transportation commissioned economic study included information regarding the supply shortage of styrene-butadiene polymers for the asphalt industry. This was not new information, just corroboration of well known industry facts. Both reports recommended that alternate asphalt modifiers be considered during supply shortages, including a very interesting alternative: hybrid binders.

A hybrid binder, as described here, is a blending of SB or SBS polymer with digested ground tire rubber (GTR) to produce a cross-linked storage stable polymer-modified asphalt (in some states called Terminal Blend Crumb Rubber). As a consequence of this type hybrid binder, the use of waste tire rubber in Florida pavements would continue and possibly increase. PMAs are normally formulated with about 4% ± SB(S). If the percent SB(S) was reduced and substituted with equal or more GTR, which is more readily available, a likely substitute for the standard PMA could be obtained. We know that both asphalt rubber binders and polymer modified binders can improve the performance of mixtures over the same mixtures produced with unmodified binders. Therefore, it is important to identify and evaluate whether different hybrid binders can perform competitively versus other modified asphalts currently used in Florida's highway applications and identify critical specification properties that must be met.

Objectives

The overall objective of this work is to determine whether a hybrid binder, composed of tire rubber and polymer, results in an asphalt mixture with improved performance related to a mixture produced with unmodified asphalt. More specifically, project objectives include:

- Identify three hybrid binder producers and binders which are currently available or that can be produced for evaluation in this study.
- Characterize the hybrid binders to verify that they can meet all appropriate specifications for polymer–modified binders (PG76-22) and to identify potential issues associated with the specifying and implementing the use of hybrid binders in Florida.
- Compare the performance of OGFC and dense-graded asphalt mixtures produced with hybrid binders to the performance of the same mixtures produced with an unmodified binder, an SBS polymer-modified binder, an ARB-5 binder for dense graded mixtures, and an ARB-12 for OGFCs. Performance will be evaluated in terms of the mixture's resistance to cracking, because one primary concern was that just stiffening the binder could result in brittleness and reduced cracking resistance.
- Develop and further healing test procedures. Interpret damage and healing to HMA mixtures with resilient modulus changes. Characterize dense graded mixtures' damage and healing performances, compare binder's effects on mixtures healing behavior and find relationship between resilient modulus and dissipated creep strain energy.
- Provide recommendations for future work to further understand the behavior of this type of binder, so that blends can be optimized for enhanced performance and to identify properties that accurately reflect the binder's performance in asphalt mixtures and pavement.

Scope

The primary focus of the work will be on three hybrid binders obtained from different producers. Tests were performed to assess the performance of the binders and their controls; and the performance of the mixtures produced with these binders.

Binder performance was characterized using traditional Superpave binder tests (FDOT Standard Specifications 916-1 for PG Superpave asphalt binders) as well as tests for Elastic Recovery (ER) and a newer test called the Multiple Stress Creep Recovery test or MSCR. The MSCR test was primarily developed to identify the presence of polymer in an asphalt binder and to better characterize the high temperature elastic component of polymer modified binders. Force Ductility test was

also adopted because this test method merited further investigation and could be used to characterize the binders.

Mixture performance was evaluated for two mixture types: an OGFC and a dense-graded Superpave mixture. In addition, two different aggregates, limestone and granite, which are extensively used in Florida, were evaluated with each mixture type. For each of the mixtures, hybrid binder performance was compared to the following: unmodified binder (PG 67-22), SBS-modified binder (PG 76-22), and crumb-rubber modified binder (ARB-5) for dense-graded mixtures; SBS-modified binder (PG 76-22), and crumb-rubber modified binder (ARB-12) for OGFC mixtures. Healing potentials were evaluated for dense graded granite mixtures: hybrid binders performance was compared with PG 76-22, ARB-5 and PG 67-22.

Performance evaluation involved the most advanced laboratory tests and interpretation methods available to assess asphalt mixture resistance to cracking in order to ensure that the modified binders did not stiffen the mix to the point that it was brittle and prone to cracking. The primary tools were the Superpave indirect tension test (IDT) along with the HMA fracture mechanics model and energy ratio concept developed at the University of Florida. Also healing test procedures were developed and used to evaluate dense graded granite mixtures healing potentials. Comparison between hybrid binders and control binders was made with respect to their healing performance.

CHAPTER 2
LITERATURE REVIEW

Crumb Rubber Used as Asphalt Binder Modifier

Over the last three decades, many different modifiers have been added to asphalt binders to improve both the rutting and cracking resistance of Hot Mix Asphalt (HMA). Of all the available modifiers, two major categories see extensive use today: Rubber and Polymers.

Rubber, as an asphalt binder modifier most normally referred to as crumb rubber modifier or CRM, is composed of natural rubber (latex), synthetic rubber (polymer), and carbon black. It is known that the natural rubber enhances elastic properties, whereas the synthetic rubber improves thermal stability (NCAT, 1996). CRM is obtained from whole tire recycling and retreading operations.

Heitzman (1992) summarized factors that affect the CRM-binder interaction: production method (ambient versus cryogenic grinding), particle size, specific surface area and chemical composition. Among these, the specific surface area has been reported as the most influential. This document has become the prime source document for specifications for both the recycled tire rubber and asphalt rubber binders. Putman, (2005) found that the CRM-binder interaction can be described by two essential effects: the Interaction Effect (IE) and the Particle Effect (PE). The IE is related to the absorption of aromatic oils from the binder by the rubber, while the PE considers the rubber acting as filler in the binder. He concluded that the IE is greatly influence by the crude source of the binder and could potentially be used as an indicator of a binder's compatibility with CRM. A higher IE value would indicate a more compatible binder.

Currently, there are three methods of incorporating rubber into HMA: the wet process, the dry process, and the terminal blend process. It should be noticed that wet and dry processes are performed at the plant site rather than at a refinery or terminal.

Wet process: the rubber and asphalt binder are mixed together prior to addition with the aggregates (by far, the most widely accepted and used method, in Florida, this is primarily done at the asphalt terminals and can cause confusion with the Terminal blend process definition)

Dry process: the rubber and the aggregates are mixed together prior to the addition of the asphalt binder.

Terminal blend process: the rubber is dissolved in the asphalt binder at the terminal with addition of other additives/modifiers. Generally, a proprietary means using a combination of chemicals, heat and physical processing is used to achieve solubility.

In many different regions of the country, pavements using asphalt rubber binders have exhibited better cracking resistance and increased durability over pavements using conventional asphalts. Several State experiences are summarized by Hicks, et al. (1995):

The Arizona Department of Transportation (ADOT) started using rubber in HMA test sections in the 1970s. With the experience gained from these test sections, ADOT used both open-graded and gap-graded mixtures over existing rigid and flexible pavements. Since 1989, over 40 projects have been placed using rubber modified mixtures, and as a result, ADOT has observed a dramatic decrease in their pavement cracking.

California (CalDOT or Caltrans) has experimented with both wet and dry rubber processes for HMA since the 70s, but stopped using the dry process due to erratic pavement performance. Cook, et al. (2005), utilized Superpave tests, as well as, the Hamburg wheel tracking device to evaluate the fatigue and rutting performance of rubber modified mixtures in 2005. They concluded that asphalt rubber modified mixtures performed at least as well as, if not better than, the conventional dense-graded asphalt mixtures; therefore, they recommended the use of CRM mixtures.

The Florida Department of Transportation (FDOT) started using rubber in asphalt mixtures in 1988 and fully implementing its use in 1994. They used an asphalt rubber binder (ARB-5) in dense graded friction courses 25 mm thick to improve the resistance to shoving and rutting, particularly at intersections. On Interstate high truck volume highways, they placed a thin 15 mm open graded friction course (using ARB-12) to improve their durability.

Polymers Used as Asphalt Binder Modifier

Polymers are characterized as thermoplastic rubbers or elastomers and examples of these include: Styrene Butadiene Rubber (SBR or SB), Styrene Butadiene Styrene (SBS), Styrene Isoprene Styrene (SIS), Polybutadiene, and Polyisoprene. (NCAT, 1996) These elastomers have an important effect on the temperature susceptibility and stiffness of the asphalt binder. Due to their chemical structure, polymers are generally less susceptible to changes in temperature than standard asphalt binders; therefore, polymer modified asphalt binders (PMAs) offer a great reduction in their temperature susceptibility. A small sampling of PMA experiences is presented here:

Kentucky Transportation Center and Kentucky Department of Transportation (KDOT) tests showed that polymer modified binders can improve the rutting (using

wheel tracking tests) and the cracking resistance of asphalt mixtures (Fleckenstein, et al., 1992).

The Oregon Department of Transportation (ODOT) validates that polymers are a practical way to reduce the temperature susceptibility of asphalt pavements. They also found that polymerized asphalt mixtures are more resistant to freeze-thaw damage (Rogge, et al., 1992).

At the University of Florida, Kim (2003) showed that SBS modified mixtures generally have a lower m-value than the same unmodified mixture; indicating a reduced rate of damage in the mixture.

Development of Hybrid Binders in Recent Years

The hybrid binder composed of SBS, rubber and asphalt was a relatively new approach at the beginning of this study. Therefore, there were very few research papers on these materials. Essentially, there is little to no knowledge of the engineering performance of hybrid binder.

An FHWA evaluation of modified binders included lab as well as accelerated loading of test sections. The rutting performance of Section 5 Terminal Blend Crumb Rubber (a hybrid binder) performed as well as SBS polymer modified binders (Tia, 2002).

According to the “SBS Polymer Supply Outlook” (by Association of Modified Asphalt Producers, 2008), there was a shortage of SBS for the asphalt industry and the price of SBS was increasing, which could happen again. Because of this background, hybrid binder provides an attractive alternative.

Most research studies have focused on SBS modified binder or Asphalt Rubber Binder separately. A summary of research is presented below on the fracture resistance of these two systems.

As for the SBS modified binder and Asphalt Rubber Binder, most researchers have primarily used traditional test methods including Dynamic Shear Rheometer, Bending Beam Rheometer, Penetration, Brookfield Viscosity, Elastic Recovery, Ductility, Softening Point, thin layer chromatography, etc. Comparisons have generally been based on the traditional test properties such as the complex shear modulus G*, phase angle δ and other Superpave indices. Some researchers have developed other parameters to evaluate performance of different modified binders. For example, Gilberto, et al. (2006) used the Binder Aging Ratio (BAR) calculated from G* to differentiate binders, and found that Asphalt Rubber can decrease BAR 40%-50% compared with unmodified asphalt, but its aging level is similar to Polymer Modified Binders. Other researchers used traditional test devices such as the Dynamic Shear Rheometer to evaluate the creep behavior of binders (e.g., Felice, et al, 2006).

Some researchers noticed the limitations of traditional Superpave indices. For example, Bahia, et al (2008) found that G*sinδ only reflects linear viscoelastic behavior, but neglects the nonlinear viscoelastic behavior that may be more indicative of resistance to fracture and rutting. As an alternative, he performed time sweep tests based on the Dynamic Shear Rheometer. He found that both Yield Energy and strain at maximum stress obtained from these tests correlated well with field performance. Bahia, et al., (2008) also evaluated the Elastic Recovery and Multiple Stress Creep Recovery tests for modified binders, and found that Elastic Recovery is a good tool to identify

Polymer Modified Binders, and Jnr from Multiple Stress Creep Recovery tests characterizes nonlinear behavior.

In addition, some new test devices have been developed. For instance, the Asphalt Binder Cracking Device (ABCD) was used to evaluate the Low Temperature Thermal Cracking (Sang-Soo Kim, 2008). When temperature drops, asphalt shrinks 100 times or more than the ABCD invar ring, so the asphalt compresses the ring, and an Electrical Strain Gauge measures this compression at cracking, which is related to the tensile fracture resistance of the binders. This device was also found to be able to characterize Polymer Modified Binders but only at low temperatures.

Methodologies of Evaluating Asphalt Mixtures Healing

Fatigue cracking in asphalt concrete pavement is considered one of the four types of distresses, as well as rutting, low-temperature cracking and moisture damage. Both theoretical and empirical models have been proposed which tried to predict the fatigue life of the pavement, but the reality is most of these models developed in the laboratory have underestimated the fatigue life in the field. While one of the reasons may be contributed to the difference of rest periods between laboratory test and the real road way traffic, healing during the rest periods has been observed and verified by many researchers.

Pseudo Stiffness Method

Throughout the '80s and '90s, Lytton, Little, Kelleher and their followers from Texas Transportation Institute (TTI) have been dedicated to studying the fracture healing of asphalt concretes.

Using Schapery (1984) correspondence principle, which states that constitutive equations for certain viscoelastic media are identical to those for the elastic cases, but

stresses and strains are not necessarily physical quantities in the viscoelastic body, Lytton, Little, et al. (1997) developed the dissipated pseudo-strain energy method to evaluate the fatigue life and healing for asphalt concretes.

Since asphalt concrete is a nonlinear viscoelastic material, a non linear reference modulus is introduced to eliminate the nonlinearity of the material in order to simplify the relationship between linear viscoelastic stress and pseudo strain (straight line).

$$E_R(t) = E_R\psi(t) = E_R\frac{\sigma_c^u(t)}{\sigma_m^u(t)}$$

Where:

E_R = linear reference modulus (constant for linear viscoelasticity);

$\psi(t)$ = nonlinear reference modulus correction factor;

$\sigma_c^u(t)$ = calculated linear viscoelastic stress for undamaged nonlinear viscoelastic asphalt concrete;

$\sigma_m^u(t)$ = measured stress for undamaged nonlinear viscoelastic asphalt concrete.

Therefore, the pseudo strain for nonlinear viscoelastic asphalt concrete (damaged condition) can be calculated in the following equation:

$$\varepsilon_R^d(t) = \frac{\sigma_c^d(t)}{E_R(t)}$$

Where $\sigma_c^d(t)$ is the calculated linear viscoelastic stress in the damaged specimen.

After application of the correspondence principle using the non-linear correction reference modulus, the corrected typical pseudo-hysteresis loop can be plotted and the slope of the linear regression of the pseudo-hysteresis loop is defined as pseudo stiffness, which is an unambiguous indicator of damage and the effect of rest periods on

microcracking and healing. A typical pseudo stiffness recovery due to rest period is shown in Fig. 2-1.

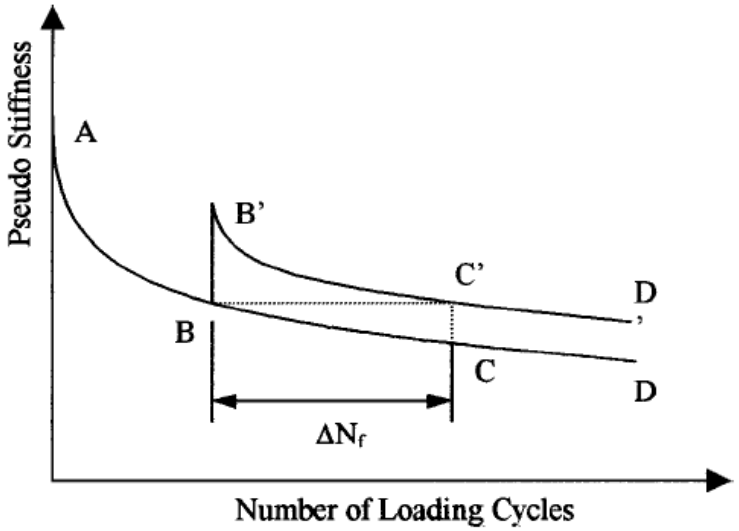

Figure 2-1. Typical effect of healing due to rest period

A healing index was introduced to describe asphalt mixture healing properties:

$$HI = \frac{\phi_{after} - \phi_{before}}{\phi_{before}}$$

Where:

HI =healing index;

ϕ_{before} =pseudo stiffness before rest period;

ϕ_{after} =pseudo stiffness after rest period.

Ratio of Dissipated Energy Change (RDEC) Method

Carpenter (2006) stated that when sustaining cyclic fatigue loading, the viscoelastic HMA material traces different paths for the unloading and loading cycles and creates a hysteresis loops. The area inside of the loop is called dissipated energy. The difference between these loops during the fatigue test indicates the amount of the dissipated energy that is producing damage.

By definition, RDEC is the ratio of dissipated energy change between two loading cycles divided by the number between the two cycles, that is, the average ratio of dissipated energy change per loading cycle. In practical usage, the RDEC value at the 50% stiffness reduction point is defined as plateau value, PV. According to the findings by Shen and Carpenter (2005), there is a unique relationship between PV and Nf_{50} (fatigue life at 50% stiffness reduction point) for different mixtures, loading modes, loading levels, and testing conditions (frequency, rest periods, etc.). The PV is a comprehensive damage index that contains the effect of both material property and loading conditions.

$$RDEC_a = \frac{DE_a - DE_b}{DE_a (b-a)}$$

Where:

$RDEC_a$ is the average ratio of dissipated energy change at cycle a, comparing to next cycle b;

a, b = load cycle a and b, respectively, The typical cycle count between cycle a and b for RDEC calculation is 100, i.e., b-a=100;

DE_a, DE_b = the dissipated energy produced in load cycle a, and b, respectively.

And:

$$PV = \frac{1 - \left(1 + \frac{100}{Nf_{50}}\right)^f}{100}$$

The PV recovery per second of rest period is an indication of healing capacity. At normal damage levels, it can require a very long rest time to fully recover damage. This is why the healing effect is not observed in normal laboratory testing. Testing results

indicate the healing/recovery rate of the polymer modified binders is significantly greater than the neat binder tested, which may account for their extended fatigue life observed in the field.

Carpenter (2006) stated that healing is a continuous physical-chemical reaction that may occur continuously as applied load damage develops, not just between load applications. Considering the energy behavior of the viscoelastic HMA material, the actual fatigue behavior can be explained as energy equilibrium between surface energy and dissipated energy, generally expressed as (Freund, et al. 2003):

Chemical potential (healing potential) = Surface energy – Dissipated energy

If surface energy is smaller than the dissipated energy, the chemical potential (healing potential) is negative, thus the material has the tendency to increase surface energy through creating more surfaces. This is the process of crack initiation and propagation (damage). On the other hand, if the dissipated energy is at a very low level and the healing potential is positive, the energy equilibrium leads to a decrease of surface energy, that is, some open crack surfaces will close through a healing process.

Dissipated Creep Strain Energy (DCSE) Method

A fundamental crack growth law was developed at the University of Florida that allows for the prediction of crack initiation and crack growth in asphalt mixture subjected to any specified loading history. This law, which is based on the principles of viscoelastic fracture mechanics, was incorporated into a cracking model which is called the HMA Fracture Mechanics Model (Roque 2002). The HMA Fracture Mechanics Model is driven by the fact that asphalt mixture has been determined to have fundamental dissipated creep strain energy (DCSE) threshold above which cracking will

initiate, or propagate, if the crack is already present. This threshold has been found to be independent of loading mode or loading history.

DCSE is calculated based on a particular tensile stress level with a haversine load of 0.1s followed by 0.9s rest period, which is commonly used to represent an applied wheel load. Therefore

$$DCSE/cycle = \int_0^{0.1} \sigma_{AVE} \sin(10\pi t)\, \dot{\varepsilon}_{P\max} \sin(10\pi t)\, dt$$

Since $\dot{\varepsilon}_{P\max} = \sigma_{AVE} \frac{dD(t)}{dt} = \sigma_{AVE} \frac{d\left(D_0 + D_1 t^m\right)}{dt} = \sigma_{AVE} m D_1 t^{m-1} = \sigma_{AVE} m D_1 (1000)^{m-1}$

So $DCSE/cycle = \sigma^2{}_{AVE}\, m D_1 (1000)^{m-1} \int_0^{0.1} \sin(10\pi t)^2\, dt = \frac{1}{20} \sigma^2{}_{AVE}\, m D_1 (1000)^{m-1}$

Where:

σ_{AVE} is the average stress within the portion of the asphalt mixture in interest;

D_1 and m are the creep compliance power law parameters.

Based on the above calculations, Kim (2003) found relationship between DCSE recovery and time. Fig. 2-2 gives a clear evidence of healing by the continuous reduction in DCSE. Regression analysis was performed on these curves and logarithmic functions were the best-fit. Healing rate was defined as the slope of the logarithmic functions and was used to evaluate the healing property of asphalt mixtures.

Also a normalized damage parameter ($DCSE/DCSE_{applied}$) was defined to evaluate the healing property independent of the amount of damage incurred in the asphalt mixture (Fig. 2-3).

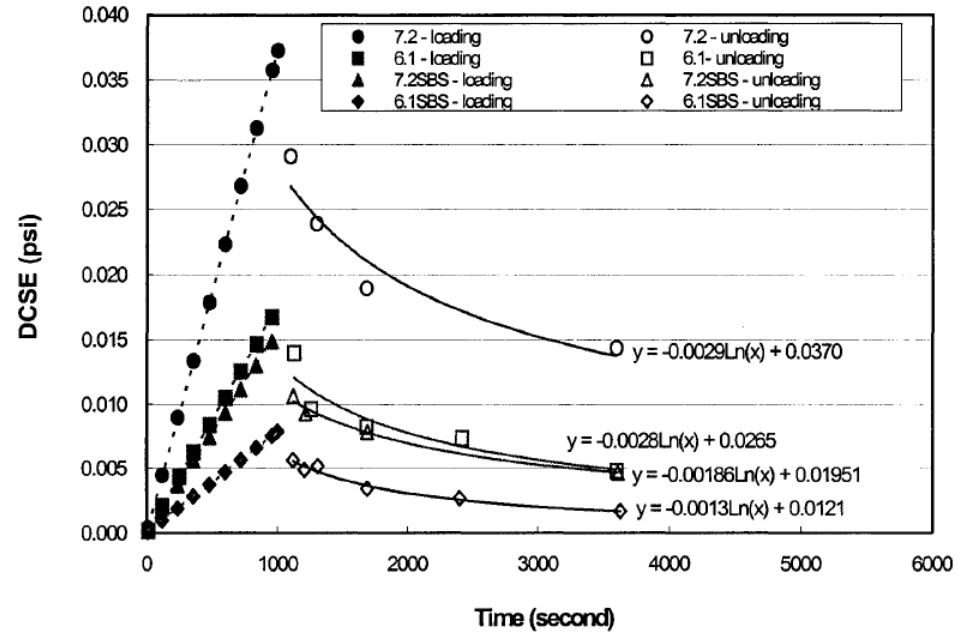

Figure 2-2. Healing test results (1,000 cycles, 75 psi, 15 °C)

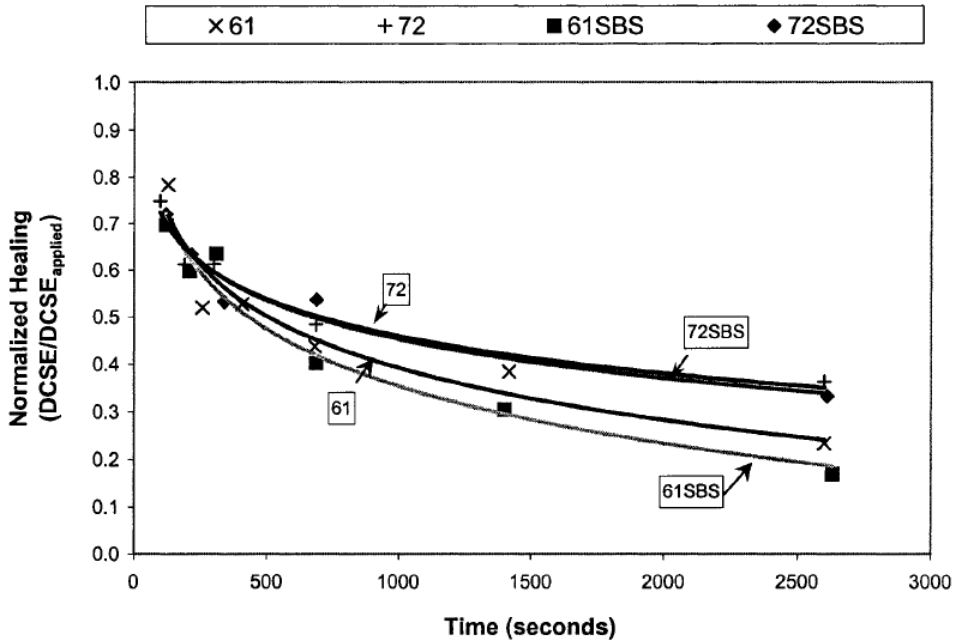

Figure 2-3. Normalized healing (after 1000 cycles, 75 psi, 15 °C)

Elastic Deformation and Strain Recovery

Chowdary, et al. (2005) from Indian Institute Technology (I.I.T.) carried out repeated triaxial tests on sand asphalt mixtures with varied confinement conditions and rest periods to quantify healing in the laboratory.

35 mm diameter and 70 mm height cylindrical cored samples with 8% and 10% air voids from Mrshall sized samples were prepared for triaxial test.

Repeated triaxial tests were carried out on san asphalt mixtures with varied confinement conditions. All tests were conducted in load controlled mode. Two loading/unloading cycles of 7 and 14 seconds were conducted. Two sets of lateral pressure/ vertical pressure (0.5kg/cm^2 / 2.5 kg/cm^2 ; 0.875kg/cm^2 / 4.375 kg/cm^2) corresponding to a ratio of 1:5 were applied for each specimen. One of the main considerations for choosing this specific ratio is related to subjecting the specimen to load levels that will engender deformation capable of healing during the rest periods and yet not physically deform the specimen.

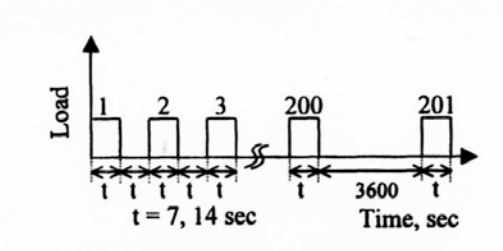

Figure 2-4. Load controlled cyclic loading and rest periods

The material was allowed to rest for one hour and the same loading and rest cycles of equal duration were applied again to observe the deformation response. The deformation of the material with time during loading and rest periods was measured.

Two parameters were selected for characterizing the healing of sand asphalt mixtures investigated in this study. The first parameter corresponds to the change in the instantaneous elastic deformation at time t=0. For the same load application, a reduction in the instantaneous elastic deformation after rest period signifies improved material property (the material modulus value increases resulting in decreased elastic deformation). Results showed this parameter depends on the magnitude of rest period.

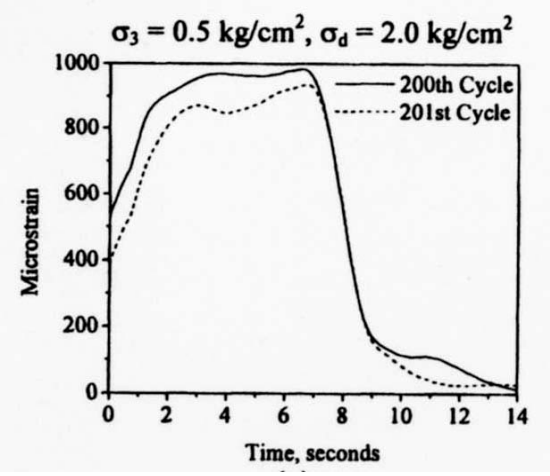

Figure 2-5. A sample plot of the strain versus time during the loading/rest period

The second parameter chosen to characterize healing is related to improved strain recovery or “springiness” resulting due to the rest period. The percentage of strain recovered at the end of three seconds after load removal when compared with the strain at the end of the loading cycle was selected as the second parameter. This parameter depends on the loading and rest period.

Summary

Generally speaking, it has been found that traditional Superpave tests and indices cannot clearly differentiate between modified binders. Also, although the Multiple Stress Creep Recovery, Elastic Recovery and Force Ductility test are able to identify polymer-like behavior to some extent, they may not differentiate between different modified binders: SBS, hybrid binder and rubber modified binder. These and other limitations with the current binder test methods need to be explored to determine whether development of new test methods which can accurately reflect the different properties of various modified binders, and reflect their relative cracking or fatigue performance at ambient temperatures is needed. The goal would be to obtain as accurate as possible

stress, strain, time and fracture energy relationships and other crucial properties, so reliable relationship between asphalt binder and mixture properties can be established.

Different approaches have been practiced by many researchers, and all of the results have shown the existence of healing characteristics of asphalt mixtures. Among these methods, apparently the dissipated energy method is the most acceptable and convenient one to detect healing potentials of the mixtures. However, evaluation methods for healing as of today are still inadequate and not mature enough to quantify it. This is because of the lack of an appropriate testing and interpreting system to measure damage recovery rates of asphalt mixtures. Therefore, there is a significant necessity to develop an appropriate and practical method for detecting and quantifying healing potentials of asphalt mixtures.

CHAPTER 3
MATERIALS AND METHODS

Since this is the first research project focused on the evaluation of hybrid binder in Florida, two commonly used aggregate types in the State were chosen (limestone and granite). Following FDOT instructions, typical gradations currently used in Florida were selected to quantify the effect of CRM and hybrid binder on mixture cracking performance.

Two mixture types frequently utilized in Florida were considered for this study: dense-graded (DG) and open-graded friction course (OGFC). DG mixtures are widely used for structural purposes; whereas OGFCs are used for their outstanding capacity for providing and maintaining good pavement frictional characteristics to reduce hydroplaning and improve safety in wet weather.

Binders

A search was conducted to gather information regarding possible sources or producers for hybrid binders as defined by this research. At first, seven vendors or companies were identified as possible participants or sources of binder for this study. When available, an assessment was made regarding the current products these companies produced and whether any of their binders would qualify for this research.

Of the original producers list, it was determined that two of them were actually working in concert and could produce a viable product, and that another company already had an existing product and had been producing it for some time. Of the remaining companies, one had extensive experience in polymer modification of asphalt and showed great interest in the research but, did not currently have a product to offer. They speculated that development of such a product would take between six months to

one year to complete. Lastly, a fourth company was developing some similar interesting product ideas but, was looking for someone to help them bring it to fruition, i.e., no product available. The remaining suppliers were either out of business, or produced a dead-end lead. Therefore, the initial search for hybrid binder producers identified only two existing viable sources for these materials.

The study was to contain three hybrid binders obtained from different producers, and this was proving to be a difficult task. After much due diligence, a third producer was identified, who produced a hybrid binder for use as a bonding agent, but had no experience using this product to produce hot mix asphalt. This was not deemed important and since it met the requirements for a hybrid binder, it was added as our third and final binder.

The research originally intended to establish guidelines for the design of the hybrid binders; controlling the amount of rubber and polymer, and the ratio between the two components. More importantly, specifying that the amount of ground tire rubber must exceed that of polymer. The least requirement to which the producers would be subject to: that their final product must be formulated to meet and pass the Superpave PG 76-22 binder specifications.

Upon further reflection, this decision would cause the research and researchers to relinquish considerable control over any aspect of the binder production, including the source of the original binder prior to modification. Therefore, it was decided to establish a baseline for the modification, that is, that all the hybrid binder producers should start with the same base binder. The three binder producers were informed of this decision and all concurred with the rationale, and agreed to modify any supplied base binder.

It was agreed to use CITGO Petroleum products, PG 67-22 and PG 76-22, as the control binders. CITGO Petroleum delivered, to each of the three hybrid binder participants, a minimum of 10 gallons of their PG 67-22 binder for modification. The University of Florida received enough PG 67-22 binder for binder testing, for mixture production, and as a base binder, to produce the rubber modified binders (ARB-5, and ARB-12) needed for the project.

Each of the hybrid binder participants was asked to disclose as much about the formulation of their product as they were willing, without infringing on proprietary products or processes. More specifically, the researchers were interested in the SBS and ground tire rubber content for comparison between producers, and for possible explanations in binder and mixture performance. In total, seven different binders were used in this project. These are outlined in the table 3-1:

Table 3-1. Asphalt binder and the constituents/formulations

Binder	Modifying Components
PG 67-22	None
PG 76-22	4.25% SBS
HB A	1% SBS (approximately 30 mesh, incorporated dry), 8% of Type B GTR, 1% hydrocarbon
HB B	3.5% crumb rubber, 2.5% SBS, 0.4%-plus Link PT-743-cross linking agent
HB C	10% rubber, 3%± 0.1% radial SBS
ARB-5	5% Type B rubber
ARB-12	12% Type B rubber

Binder testing was performed by the Florida Department of Transportation State Materials Office. The tests performed were all those required by FDOT Standard Specifications 916-1 for PG Superpave asphalt binders. In addition, DSR and creep

stiffness were performed after PAV at 110˚C, in addition to the standard 100˚C. The basic binder testing program is summarized in table 3-2.

Table 3-2. Binder tests summary

Binder Type	Number	Number of Tests*	Number of Replicates	Total Number of Binder Tests
Base	1	12	2	24
Hybrid	3	12	2	72
SBS-modified	1	12	2	24
ARB-12	1	12	2	24
ARB-5	1	12	2	24
Totals	7	12	2	168

Binder tests are as follows (FDOT Specifications 916-1; Superpave PG Asphalt Binder):

- Original Binder: Spot Test, Solubility, Smoke Point, Flash Point, Rotational Viscosity, Absolute Viscosity, Dynamic Shear Rheometer (DSR)
- Rolling Thin Film Oven Test Residue: Mass Loss, Dynamic Shear Rheometer
- Pressure Aging Vessel Residue: Dynamic Shear Rheometer (2 temperatures), Creep Stiffness

The test results were used to verify that all binders met appropriate specifications for a PG 76-22 Superpave asphalt binder. In addition, test results were evaluated to identify binder properties or parameters that may be suitable to uniquely characterize these hybrid binders and to identify potential issues associated with specifying and implementing the use of hybrid binders in Florida.

Several non-routine tests were performed on these binders: 1) binders were PAV aged at 110˚C, which may possibly be used to identify potential aging issues of concern to Florida, 2) binders were subjected to the Elastic Recovery test, which according to Bahia (2008) will identify the presence of polymer modification, 3) binders were subjected to the Multiple Stress Creep Recovery test (AASHTO TP70-08), which

according to Bahia (2008) can be used to characterize a binder's nonlinear behavior, and 4) binders were tested using the Force Ductility test, which is unique in that it loads the specimen to failure. This last test may be used to calculate energy to failure, which may be correlated to binder and possibly mixture cracking performance. This is essentially the standard ductility test with an added load cell to measure the load applied to the sample throughout its elongation.

Aggregates

Aggregates sources were chosen based on previous research work and FDOT directions; detailed information is presented in the Table 3-3. Both dense-graded (DG) and open-graded friction course (OGFC) mixtures were designed for each aggregate type (limestone and granite). The particle size distribution of DG mixes is presented in

Table 3-3. Aggregate source

Source	Type	FDOT Code	Pit No.	Producer
Nova Scotia Granite	# 7 Stone	44	NS-315	Martin Mariette Aggregates
	# 789 Stone	51	NS-315	Martin Mariette Aggregates
	Stone Screenings	22	NS-315	Martin Mariette Aggregates
South FL Limestone	S-1-A Stone	41	87-339	White Rock Quarries
	S-1-B Stone	53	87-339	White Rock Quarries
	Asphalt Screenings	22	87-339	White Rock Quarries
Georgia Granite	# 78 Stone	43	GA-553	Junction City Mining
	# 89 Stone	51	GA-553	Junction City Mining
	W-10 Screenings	20	GA-553	Junction City Mining
Rinker South FL Limestone	# 67 Stone	42	87-090	Rinker Materials Corp.
	S-1-B	55	87-090	Rinker Materials Corp.
	Med. Screenings	21	87-090	Rinker Materials Corp.
Local Sand	Local Sand	-	Starvation Hill	V. E. Whitehurst & Sons

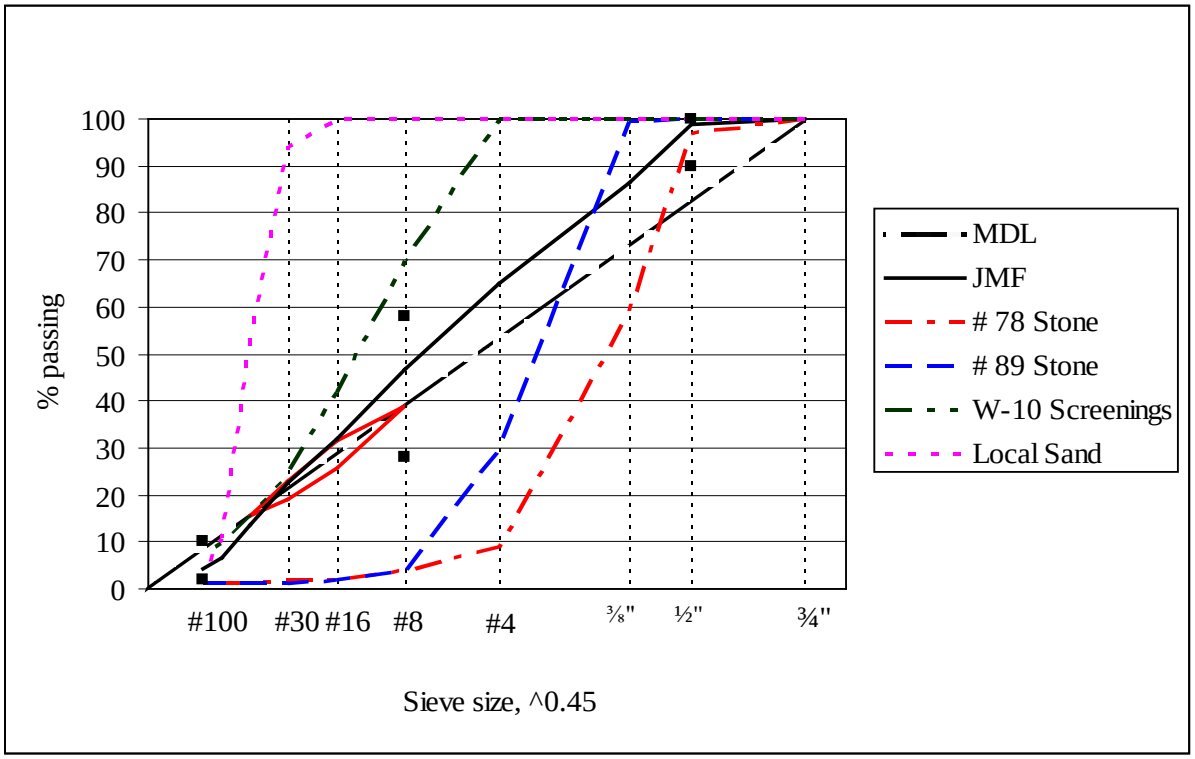

Figure 3-1. DG granite gradation

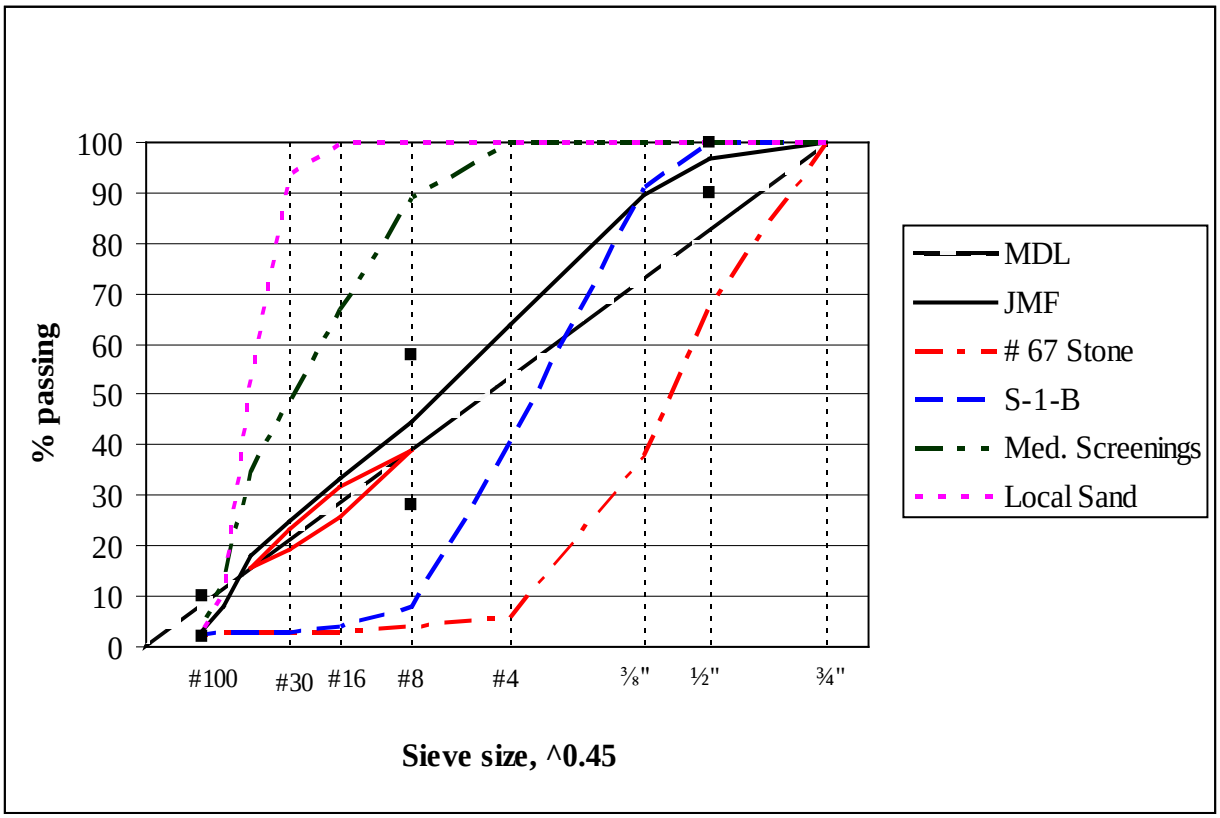

Figure 3-2. DG limestone gradation

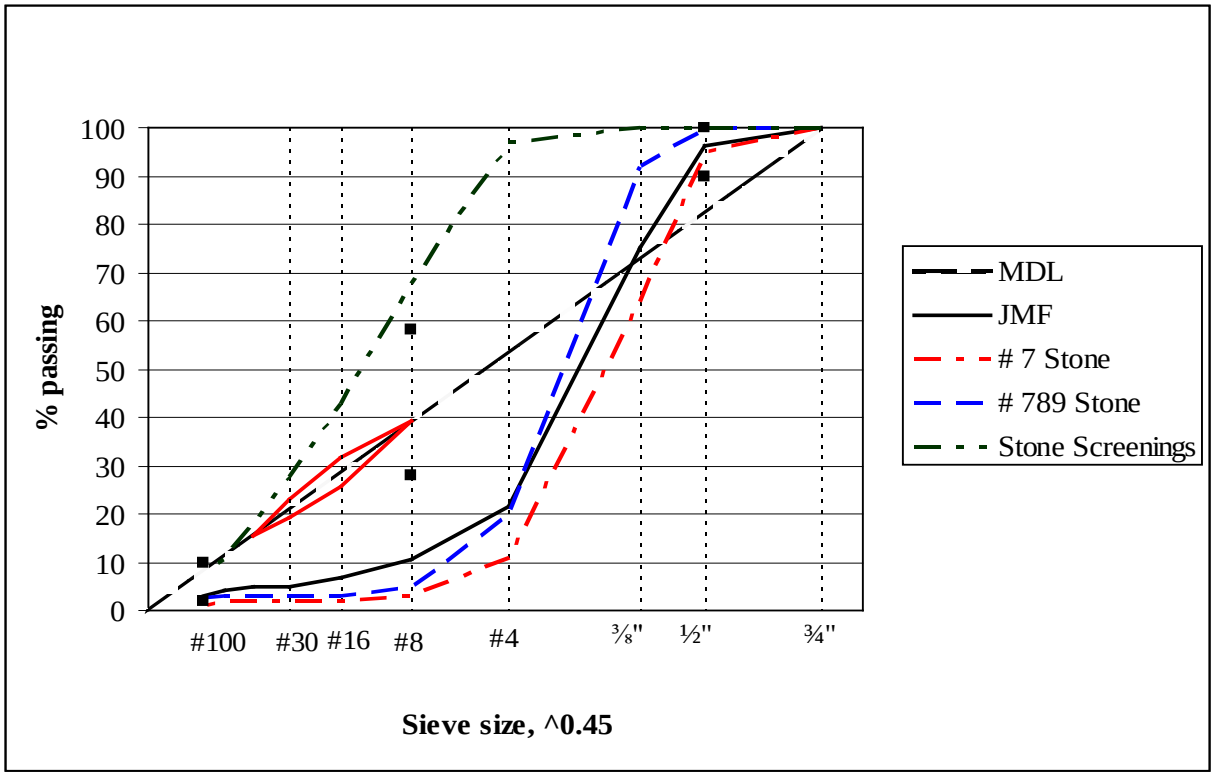

Figure 3-3. OGFC granite gradation

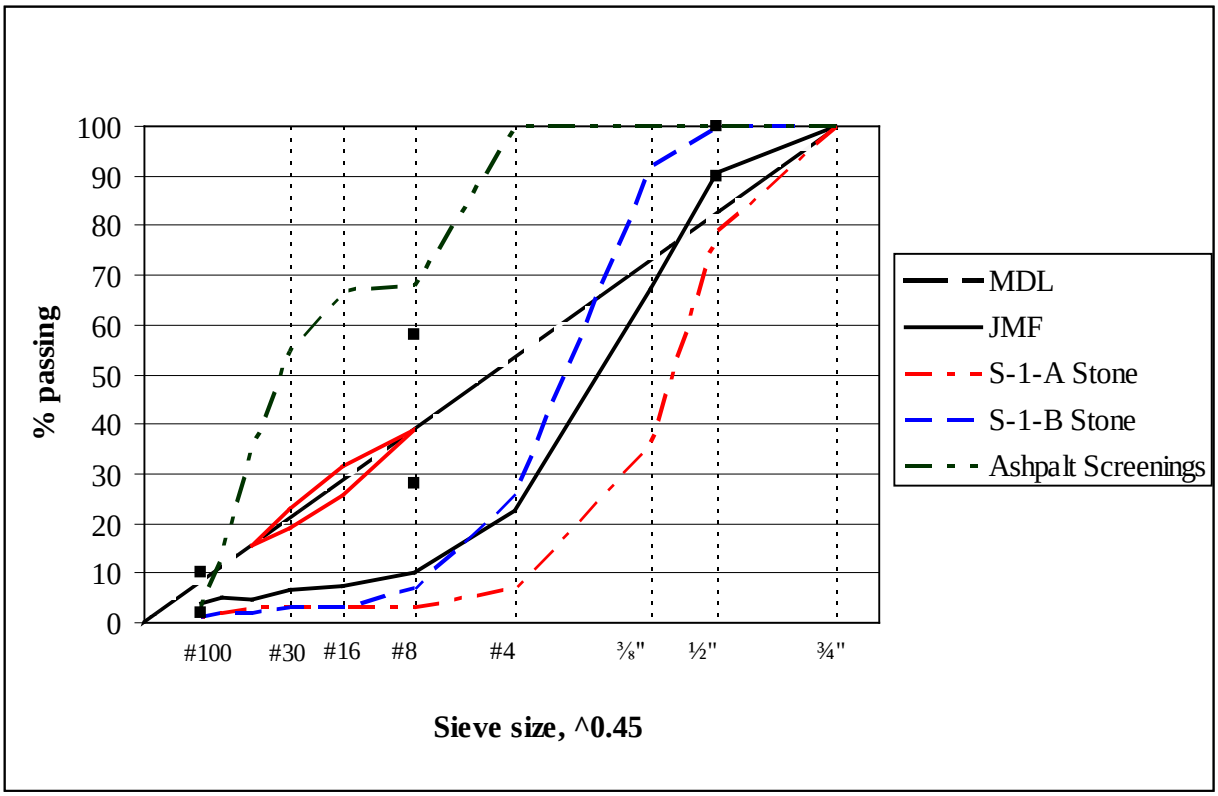

Figure 3-4. OGFC limestone gradation

the figures 3-1 and 3-2 and the OGFC gradation curves are shown in the figures 3-3 and 3-4: the granite blend was added with hydrated lime (1% by weight) to prevent stripping.

Mixtures

All dense-graded mixtures were designed to be 12.5 mm nominal maximum aggregate size mixes and to meet specification requirements for a traffic level C, which corresponds to 3 to 10 million Equivalent Single Axle Loads (ESALs) over a 20 year period. A summary of the mixture testing plan for this project is presented in the Fig. 3-5. A total of 88 gyratory specimens were prepared.

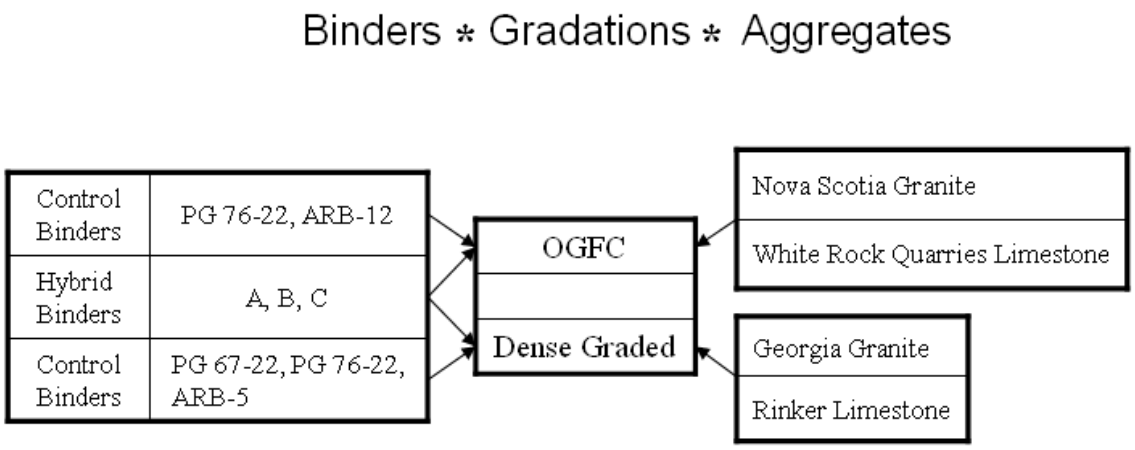

Figure 3-5. Mixture testing plan for each mixture and aggregate type

Each mixture in the test plan was designed with a particular binder type while the aggregate gradation was kept constant in order to evaluate binder effect on mixture cracking performance. In total, 12 DG (6 binders and 2 aggregate types) and 10 OGFC (5 binders and 2 aggregate types, 0.4% fiber by weight of the mix was added to granite OGFCs to prevent drain-down) mixtures were evaluated and have identifications (IDs) shown in Tables 3-4 and 3-5 (next page).

Initially, all mixtures (conventional and modified) with the same aggregate type and gradation were prepared in the laboratory with the same percentage of binder by weight. Theoretically, all mixes should have had the same effective asphalt volume, and consequently the same volumetric properties.

However, during the laboratory work, the effective asphalt volume was found to be about the same for OFGC mixtures but different for DG mixtures. Two factors were thought to have caused this difference: specific gravity of binder (G_b) and aggregate absorption. As mentioned previously, G_b was measured in the laboratory and also aggregate absorption tests conducted on the different binders indicated definite differences in absorption. Consequently, asphalt contents were adjusted to ensure that all mixtures had the same effective asphalt by volume.

Table 3-4. DG mixtures IDs for testing

Binder	PG 67-22	PG 76-22	Hybrid Binder A	Hybrid Binder B	Hybrid Binder C	ARB-5
Limestone	DLU	DLM	DLA	DLB	DLC	DLR
Granite	DGU	DGM	DGA	DGB	DGC	DGR

Table 3-5. OGFC mixtures IDs for testing

Binder	PG 76-22	Hybrid Binder A	Hybrid Binder B	Hybrid Binder C	ARB-12
Limestone	OLM	OLA	OLB	OLC	OLR
Granite	OGM	OGA	OGB	OGC	OGR

Mixture Preparation

Aggregates and binders were preheated in the oven for 3 hours before mixing; mixing temperature was set to 310 ± 5º F for unmodified and ARB-5 binder mixes and 330 ± 5º F for PMA and hybrid binder mixes. After preheating the hybrid binders, in some containers for all hybrid binders, undissolved modifiers (rubber particles) were

found accumulated on the surface of the binder resulting in about a 2 mm thick film; thus, before pouring the binder into the mixing bucket with the aggregates, a clean steel stick was used to stir the binder evenly to dissolve the film into the binder. The aggregates and binder were then mixed in a rotating bucket until the aggregates were well coated with the binder.

Before the DG and OGFC samples were compacted, they were placed in a pan and heated in an oven for about 2 hours at the mixing temperature, which is the Short Term Oven Aging (STOA). The mix was stirred after one hour of heating to obtain a more uniformly aged sample.

DG and OGFC mixtures were compacted at 310 ± 5º F and 330 ± 5º F respectively. Even though the DG mixes were designed to have 4% air void content at N_{design}, they were compacted in the Servopac Gyratory Compactor to the number of gyrations needed to get 7% air voids. The number of gyrations obtained from mix design to get 7% air voids for DG mixtures was 20 for limestone and 24 for granite mixes.

For OGFC mixtures, 50 gyrations were used to achieve compaction level similar to field after traffic consolidation (Varadhan, 2004). Specimens were allowed to cool for 30 minutes before extruding from the molds, and for at least 24 hours before cutting or preparation for testing.

LTOA is meant to represent 15 years of field aging in a Wet-No-Freeze climate and 7 years in a Dry-Freeze climate. LTOA requires a compacted sample (after STOA) be placed in a force draft oven at 185 ± 5°F for 5 days (Harrigan, et al., 1994). The same aging procedure was used for both DG and OGFC mixtures.

Because of the very coarse and open structure of OGFC; there was a possibility of these mixes falling apart at the high temperature used for LTOA. Hence, a procedure was developed to protect the pills.

A wire mesh with openings of 0.125 in and steel clamps were used. The mesh size was chosen in order to ensure that there is good air circulation within the sample for oxidation and to prevent the smaller aggregate particles from falling through the mesh. The specimen was wrapped twice with the mesh cloth and two clamps were used to contain the specimen without applying excessive pressure on it. The system is shown in the Figure 3-6.

Figure 3-6. Pill contained with mesh

After cooling the specimens at room temperature, they were cut to the required thickness for testing. The bulk specific gravity for DG mixes was determined in accordance with AASHTO T166 to ensure that the air voids of the specimens were within the required range of 7.0 ± 0.5 %. The DG mixture volumetric information is shown in Table 3-6.

For OGFC mixtures, physical parameters were obtained from the CoreLok test. The procedure is described in the Appendix D. After the sample was sealed, it was weighed in the water tank. The OGFC and DG mixture volumetric information is shown in Table 3-7.

Table 3-6. Dense graded mixture volumetric information

Mixture	DGU	DGM	DGA	DGB	DGC	DGR
P_b	4.80%	4.82%	4.90%	4.89%	4.89%	4.84%
G_{mm}	2.578	2.579	2.581	2.580	2.580	2.579
G_{mb}	2.390	2.380	2.388	2.408	2.399	2.386
Mixture	DLU	DLM	DLA	DLB	DLC	DLR
P_b	6.60%	6.49%	6.33%	6.18%	6.42%	6.60%
G_{mm}	2.319	2.316	2.312	2.309	2.314	2.319
G_{mb}	2.165	2.145	2.153	2.155	2.150	2.148

Table 3-7. OGFC mixture volumetric information

Mixture Type	Aging Condition	G_{mm}	G_{mb}	AV %
OGFC Granite	STOA	2.441	1.995	18.28
	LTOA		1.996	18.23
OGFC Limestone	STOA	2.309	1.990	13.80
	LTOA		1.978	14.33

Figure 3-7. CoreLok sample weighing equipments

CHAPTER 4
BINDER TEST RESULTS AND ANALYSIS

It is stated (NCAT, 1991) that the physical properties of asphalt measured by Superpave binder tests are directly related to field performance by engineering properties, so the binder tests were performed first and then mixtures tests (fatigue cracking and healing). Conclusions will be made on how significantly binder properties will affect their performances in mixtures.

Physical property tests including specific gravity, solubility, smoke point, flash point, rolling thin film oven mass change and spot tests were performed. A summary of test results and findings of binder tests is presented in the sections below. Additional binder test results are presented in Appendix A.

Conventional Superpave binder tests were performed using the Dynamic Shear Rheometer and Bending Beam Rheometer. The following tests, which have been specifically developed and identified to evaluate modified binders, were also performed:

- Multiple Stress Creep Recovery (AASHTO TP70-08))
- Elastic Recovery (AASHTO T301-99(2003))
- Force Ductility (AASHTO T300-00)

Binders Physical Properties

Specific Gravity of Binders

Results of specific gravity of binders based on the Standard Test Method for Density of Semi-Solid Bituminous Materials (ASTM Designation: D 70-03, Pycnometer Method) are presented in Table 4-1. As expected, all of the modified binders had a higher specific gravity than that of the base binder.

Table 4-1. Specific gravity of binders, 15.6 ºC (60 F)

Binders	Specific Gravity	Gravity (kg/m^3)
PG 67-22	1.031	1027.907
PG 76-22	1.033	1031.389
HB A	1.044	1040.918
HB B	1.036	1032.892
HB C	1.043	1040.356
ARB-5	1.036	1033.004
ARB-12	1.042	1038.824

Solubility Analysis

To determine the purity of asphalt cement, solubility test was conducted to compare modified binders and control binders. The solubility of hybrid binder A (92.76%), hybrid binder B (96.905%), ARB-5 (93.835%) and ARB-12 (88.765%) did not meet the specification requirement (minimum 99%). As illustrated in Fig. 4-1, the

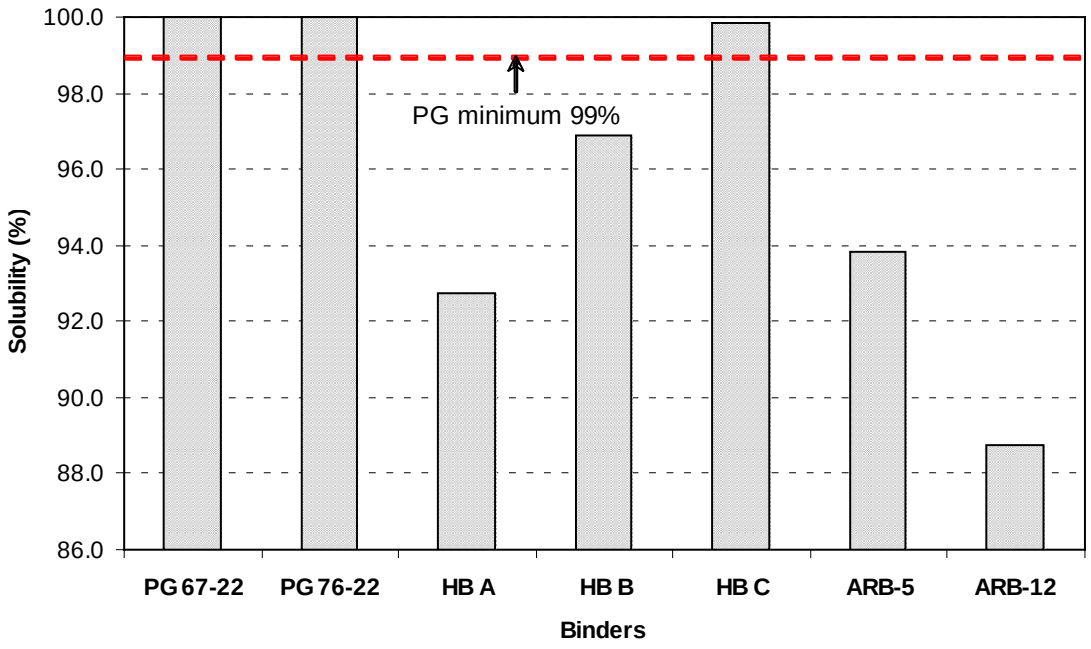

Figure 4-1. Solubility of original binders

solubility was lower for binders with higher coarse rubber content (hybrid binder A (8%), hybrid binder B (3.5%), ARB-5 (5%) and ARB-12 (12%)), indicating that the rubber may not have been fully digested in the base binder. Hybrid binder C, which was produced with finer grained rubber, did meet FDOT's solubility specification, indicating that the rubber was fully digested in the base binder, thereby making it more suitable for DSR testing.

Based on these results, it appears that solubility may be a good way to distinguish binders that may have excessively coarse particles (e.g. undigested rubber particles) that would make them unsuitable for DSR testing. Also, results of hybrid binder C show that hybrid binder can meet the solubility requirement. Therefore, solubility appears to be a good way to distinguish hybrid binder from asphalt rubber binder.

Mass of Volatiles Loss Analysis

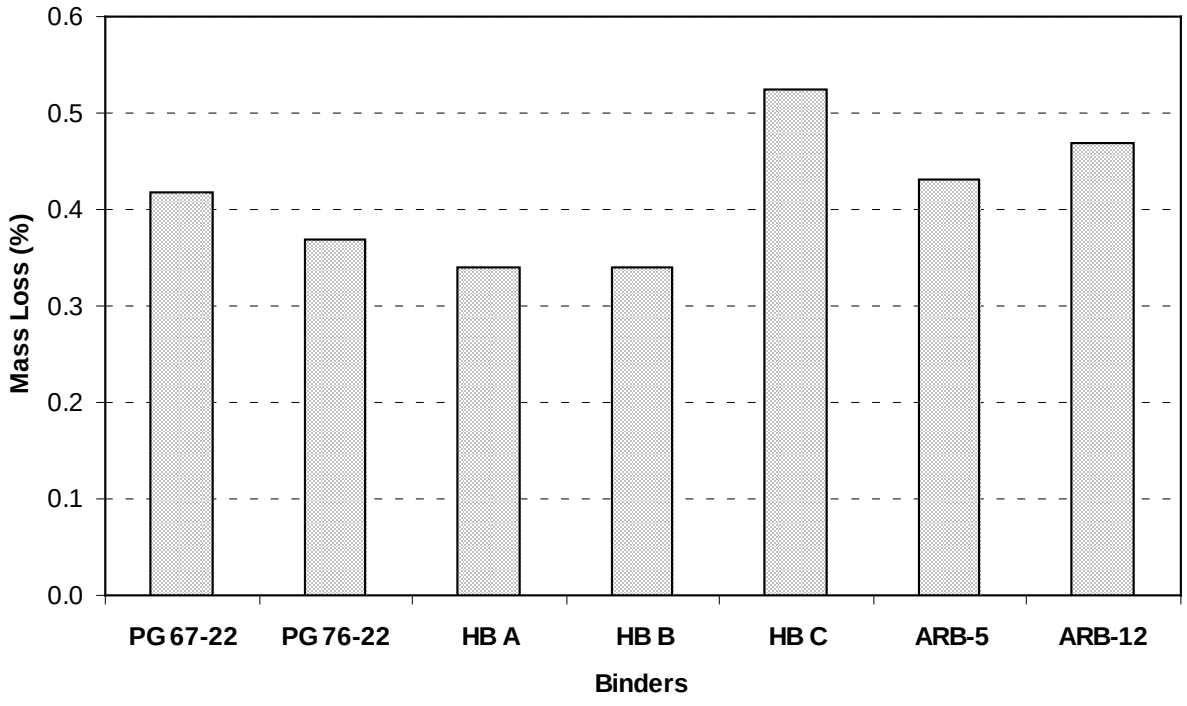

Figure 4-2. RTFOT, mass loss at 163 ºC (325.4 F)

The RTFOT allows the determination of the mass of volatiles lost from the binder during the test. The amount of volatiles lost indicates the amount of aging that may occur during HMA production and construction.

As indicated in Fig. 4-2, all binders except hybrid binder C, which had a Mass Loss of -0.524%, met the specification requirement for Mass Loss after RTFOT (±0.5%). The Mass Loss of hybrid binder A, B was the smallest.

Binders Rheological Properties

Dynamic Shear Rheometer (DSR) and Bending Beam Rheometer (BBR) tests were performed and analyzed at different testing temperatures, i.e. DSR at high (76 ºC, 168.8 F) and intermediate temperatures (25ºC, 77 F), and BBR at low temperature (-12ºC, 10.4 F).

DSR Test Results Analysis

The DSR is used to characterize the viscous and elastic behavior of asphalt binders at high and intermediate service temperatures. It measures the complex shear modulus G* and phase angle δ at the desired temperature and frequency of loading. According to NCAT, original and RTFOT aged binder samples were tested at high temperature to determine the binder's ability to resist rutting, while PAV aged samples were tested at the intermediate temperature to determine binder's ability to resist fatigue cracking. G* and δ results with 5% testing error range at high temperature were shown through Fig. 4-3 and Fig. 4-4. Fig. 4-5 and Fig. 4-6 show the results at low temperature.

As indicated in Fig. 4-3, all modified binders resulted in an increase in G*/sinδ (indicator of rutting resistance) relative to the base binder. Also, G*/sinδ of all modified binders was above the minimum requirements for PG 76-22 binder. A significant difference was observed in the magnitude of G*/sinδ for the different modified binders in

both original and RTFOT conditions. The largest values of G*/sinδ were observed for binders with the highest concentration of coarse rubber (hybrid binder A, hybrid binder B and ARB-12) and may be suspect.

Fig. 4.4 illustrates that all modified binders exhibited a lower phase angle (δ) than the base binder. The SBS modified binder and hybrid binder A and B resulted in the greatest reduction. Lower phase angle is associated with lower energy loss or more elastic behavior, which would indicate better rutting and cracking resistance.

Solubility results indicated that the coarser rubber in hybrid binder A and B as well as the ARB binders were not fully digested in the base binder made the test results from DSR suspect because the presence of particulates in the binder is well known to affect DSR results. The binders produced with the coarser grained rubber met, and even far exceeded requirements for PG76-22 binder, resulting in binder performance parameters that indicated better performance characteristics than all other binders evaluated, including the SBS polymer modified binder. These results were not consistent with relative cracking performance characteristics determined from mixture tests.

Conversely, solubility results indicated that the finer rubber in Hybrid binder C was fully digested in the base binder, which made it suitable for DSR testing. This binder also met requirements for PG76-22 binder with the exception of the maximum phase angle (which is an FDOT requirement).

Fig. 4-5 shows that all binders, including the base binder, meet the specification requirement for a maximum G*sin δ of 5000 kPa for both the 100 ^{o}C and 110 ^{o}C PAV residue. All modified binders, except hybrid binder C, exhibited lower G*sinδ than the base binder. G*sinδ was intended to be an indicator of resistance to fatigue cracking

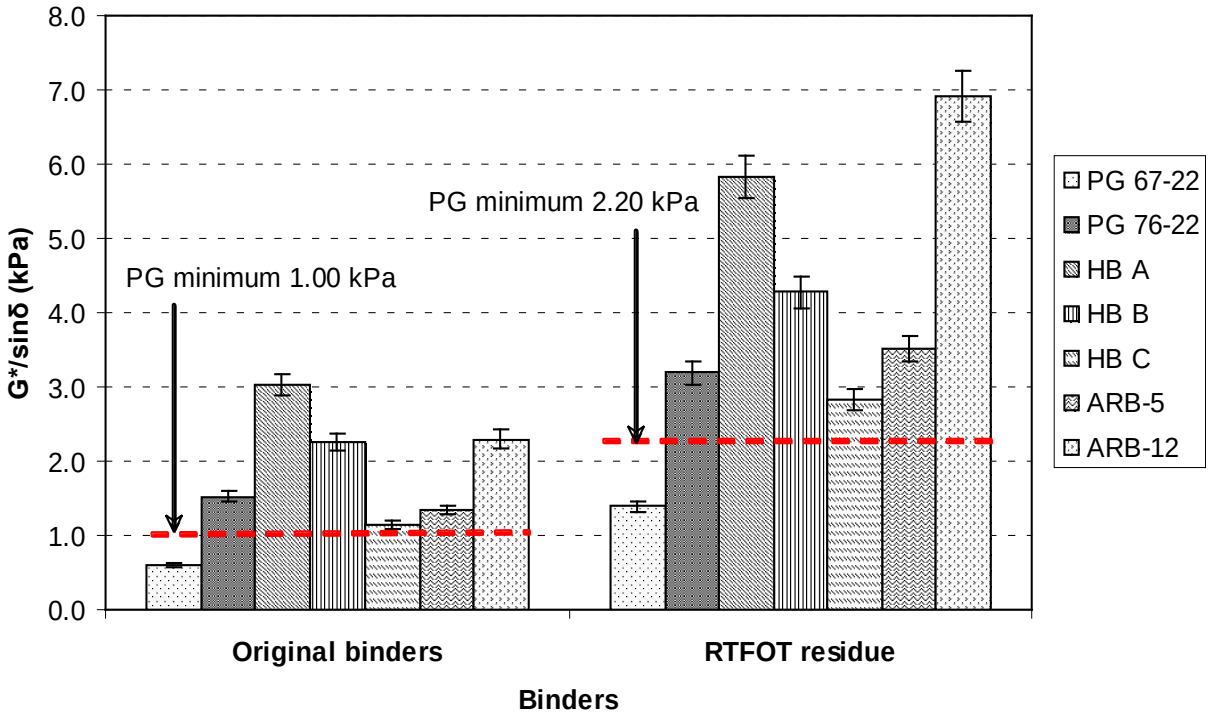

Figure 4-3. G*/sinδ, 76 ºC (168.8 F) @ 10 rad/s

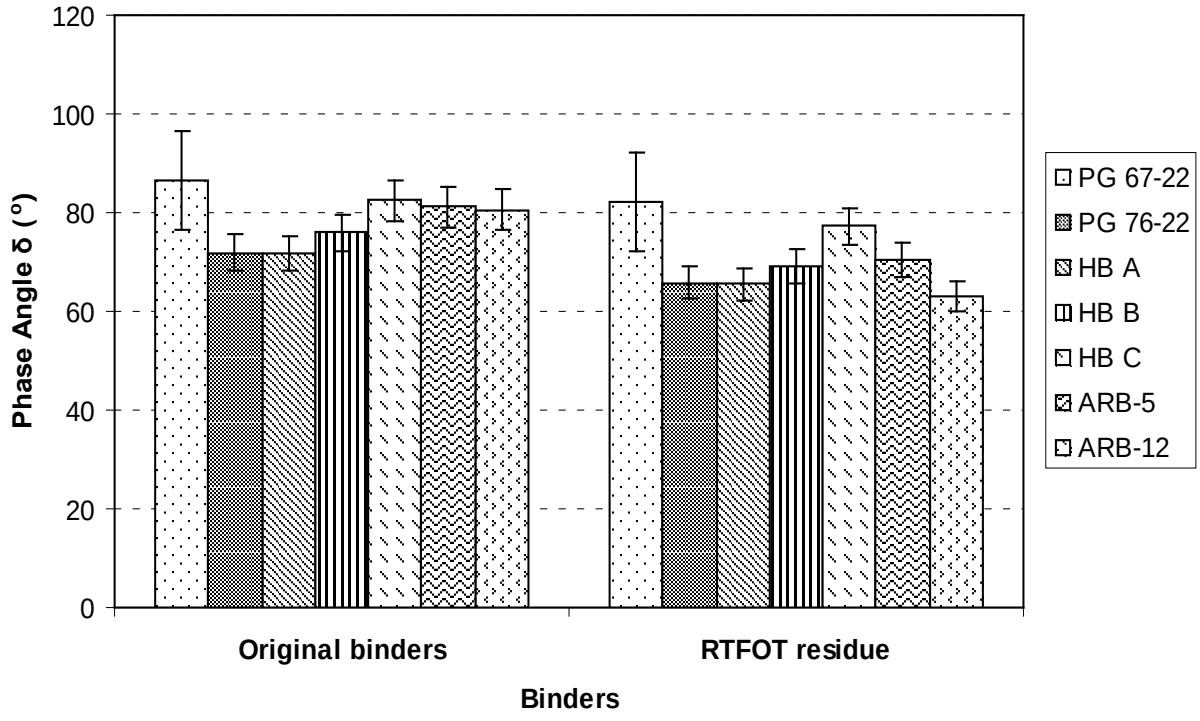

Figure 4-4. Phase angle δ, 76 ºC (168.8 F) @ 10 rad/s

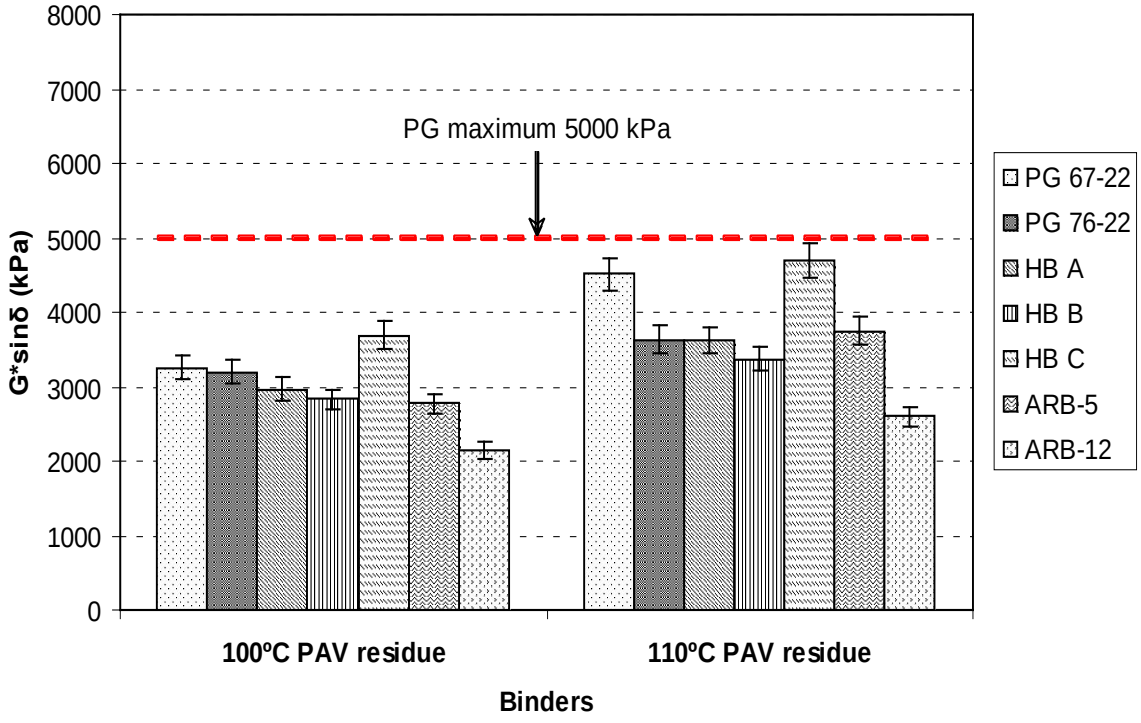

Figure 4-5. G*sinδ, 25 ºC (77 F) @ 10 rad/s

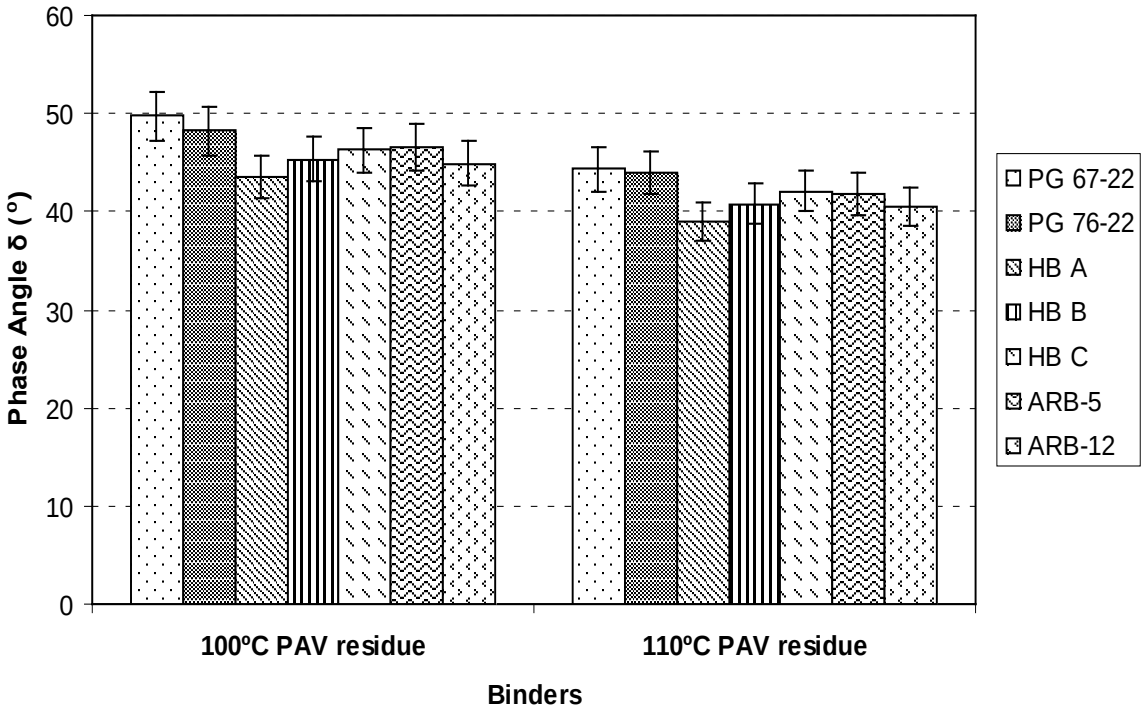

Figure 4-6. Phase angle δ, 25 ºC (77 F) @ 10 rad/s

because it represents a measure of energy loss (higher G*sinδ, higher energy loss). However, post-SHRP research has revealed that this parameter may not relate very well to fatigue cracking resistance because a large part of the energy loss associated with G*sinδ is not related to damage.

Fig. 4-6 shows that all modified binders result in phase angles lower than the base binder. Lower phase angles imply lower energy loss, but as with G*sinδ, the energy loss associated with lower δ is not necessarily related to damage.

BBR Test Results Analysis

The BBR tests asphalt binders at low pavement service temperatures to determine the binder's propensity to thermal cracking. Thermal cracking of HMA pavements results when the temperature drops rapidly at cold temperatures. As the pavement contracts, stresses begin to build up within the HMA pavement layers. If the contraction occurs very rapidly the stresses can build and eventually exceed the stress relaxation ability of the HMA pavement.

The BBR uses a transient creep load, applied in the bending mode, to load an asphalt beam specimen held at a constant low temperature. The stiffness, S(t), is a measure of the thermal stresses developed in the HMA pavement as a result of thermal contraction. The slope of the stiffness curve, m, is a measure of the rate of stress relaxation by asphalt binder flow. Accordingly, the Superpave binder specification requires a maximum limit of S(t) at 60 seconds and a minimum m-value. Figure 4-7 and 4-8 show the results of S(t) and m-value with 5% testing error range for all tested binders. These two figures imply all binders meet specification requirement for both creep stiffness (S) and m-value at 60 seconds loading time.

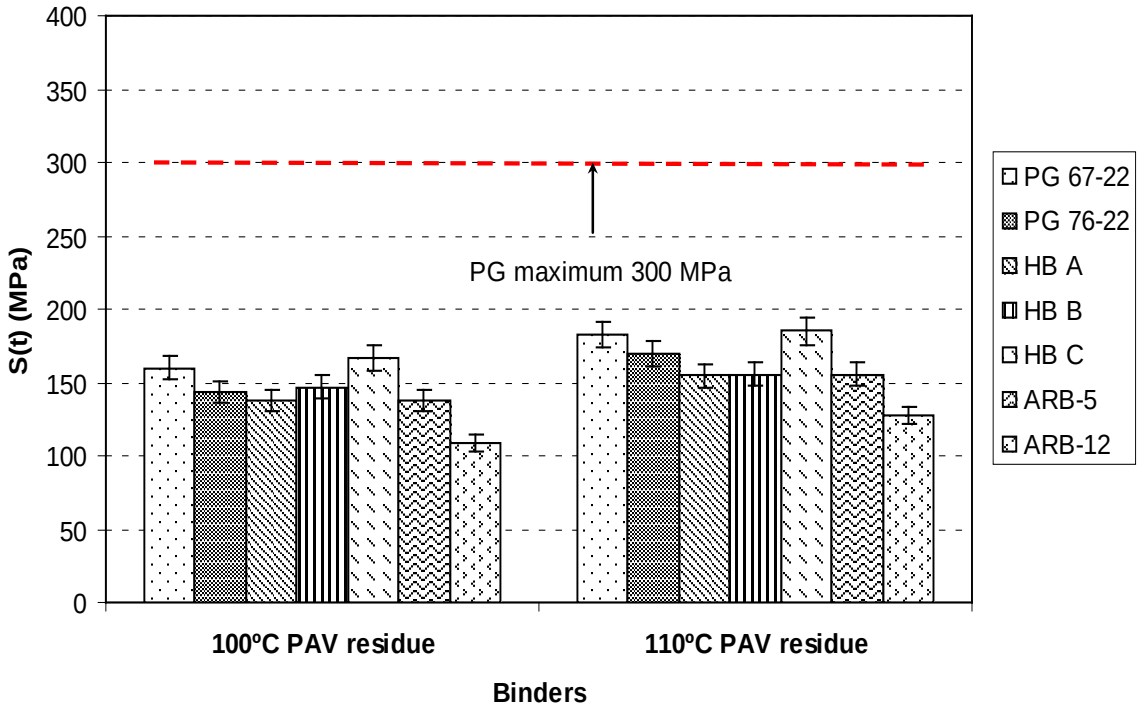

Figure 4-7. S(t), -12 ºC (10.4 F) @ 60 second

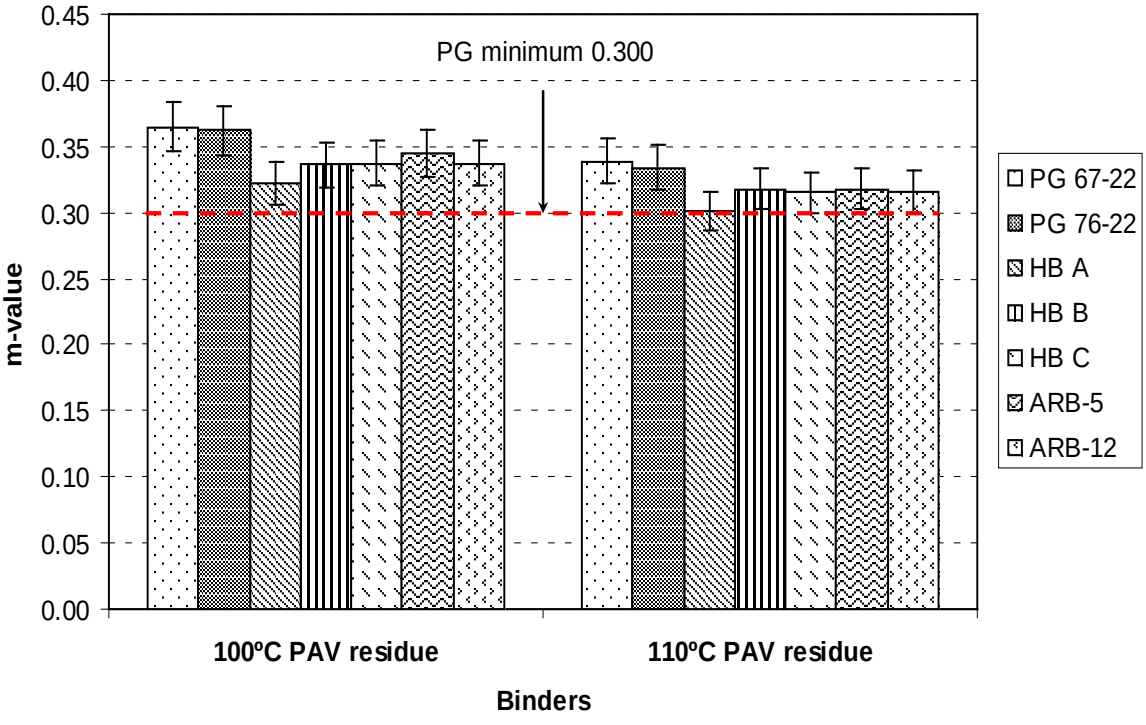

Figure 4-8. m-value, -12 ºC (10.4 F) @ 60 second

Multiple Stress Creep Recovery (MSCR)

MSCR (AASHTO TP70-07, ASTM D7405) is used to identify the presence of elastic response in a binder and the change in elastic response at two different stress levels. The percent recovery in the MSCR test of asphalt binders is affected by the type and amount of polymer used in the polymer modified asphalt binder, so it is intended to provide a means for determining if the polymer used in modification will provide an elastomeric response. Non-recoverable creep compliance (J_{nr}) has been shown to be an indicator of the resistance of an asphalt binder to permanent deformation (rutting) under repeated load. D'Angelo et al. (2009) found that reducing J_{nr} by half typically reduced rutting by half.

The following Fig. 4-9 and 4-10 show typical MSCR test results. Two parameters were calculated and evaluated: average percent recovery and non-recoverable compliance at two different stresses 100 Pa and 3200 Pa.

Percent recovery $\varepsilon_r(100, N)$ for N=1 to 10:

$$\varepsilon_r(100, N) = \frac{(\varepsilon_{10} - \varepsilon_1) * 100}{\varepsilon_1}$$

Where ε_{10} is the adjusted strain value at the end of recovery portion of each cycle.

ε_1 is the adjusted strain value at the end of creep portion of each cycle.

Non-recoverable compliance $J_{nr}(\sigma, N)$ for N=1 to 10:

$$J_{nr}(\sigma, N) = \frac{\varepsilon_{10}}{\sigma}$$

Where σ is the applied stress.

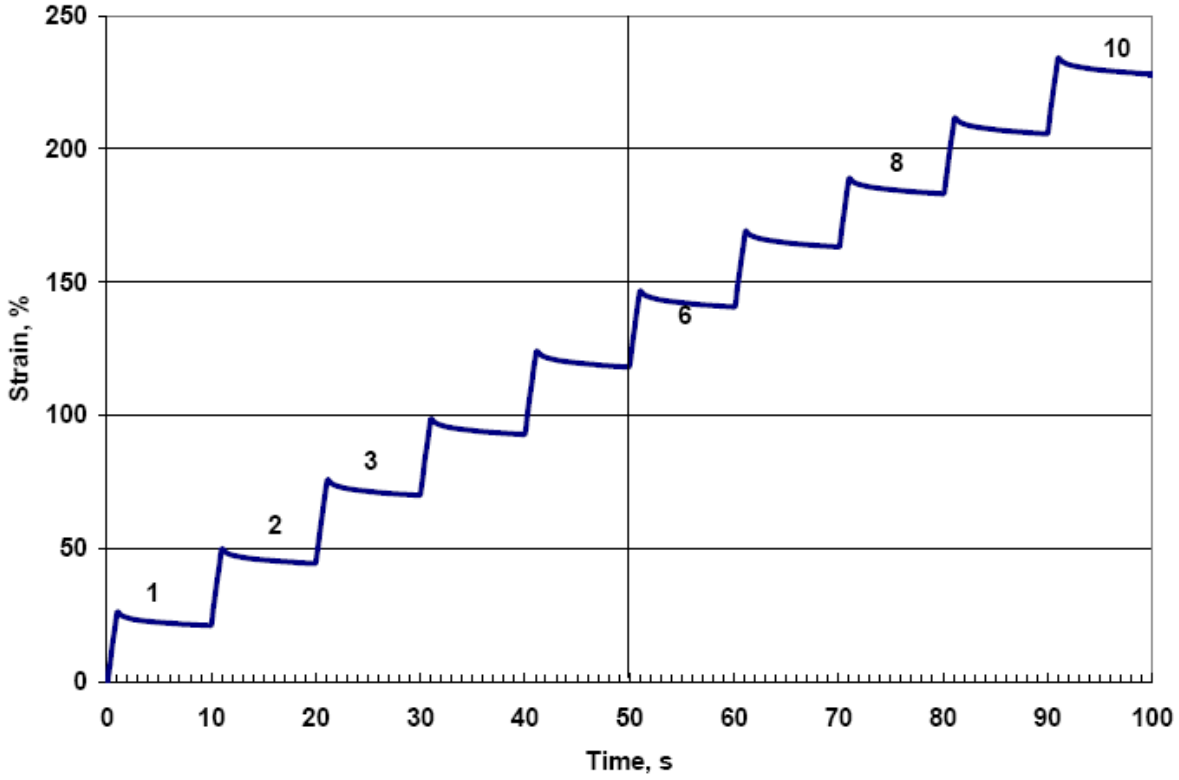

Figure 4-9. Typical ten cycles creep and recovery with creep stress of 100 Pa

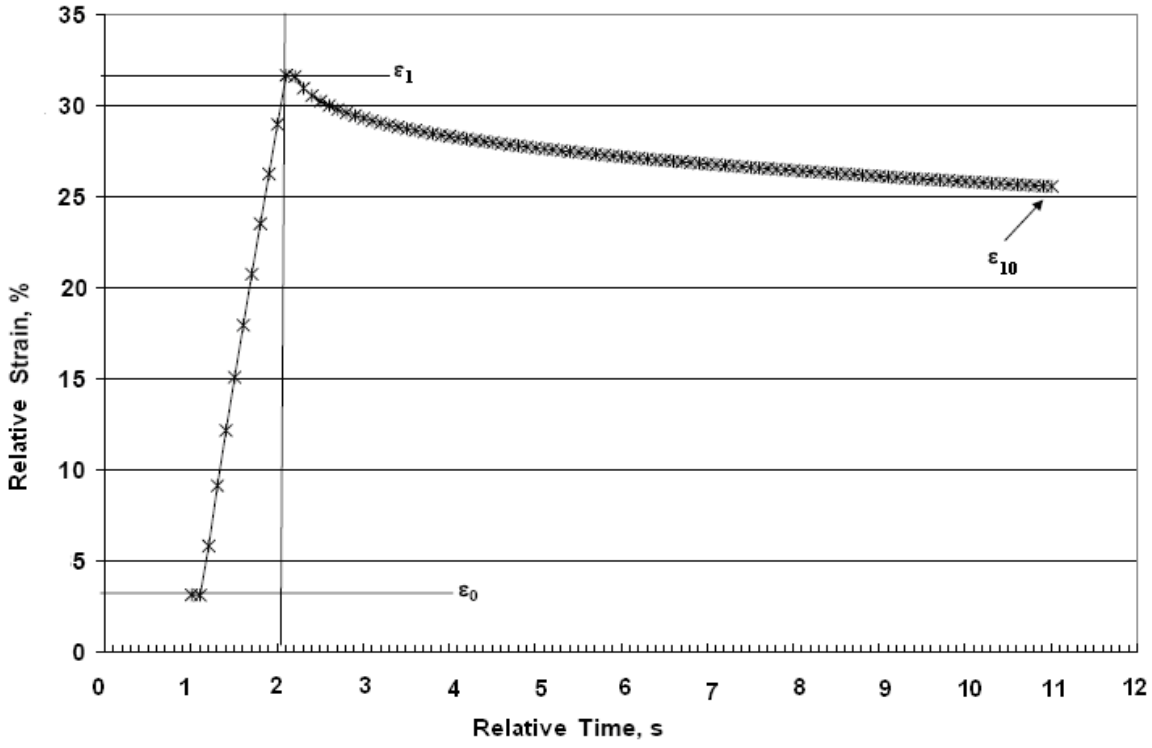

Figure 4-10. Typical creep and recovery cycle with creep stress of 100 Pa

Fig. 4-11 through 4-14 provide MSCR results with 5% testing error range in terms of percent recovery and non-recoverable compliance at different stress levels at two different test temperatures 67.0^{o} C (Fig. 4-11 and 4-12), and 76.0^{o} C (Fig. 4-13 and 4-14).

In general, modified binders' percent recovery is greater than control binder (PG 67-22) at both test temperatures. Accordingly, creep compliance is much lower for all modified binders than that of the control binder. However, among all modified binders, hybrid binder C does not appear as competitive as others. Considered percent recovery aspect, hybrid binder C exhibits even lower recovery than ARB-5. Accordingly, hybrid binder C shows higher non-recoverable compliance at both test temperatures.

Since the percent recovery reflects the elastic response of the materials, the results seem to show that PG 76-22, hybrid binder A and B and ARB-12 exhibit the best elastic response among tested binders, and they are less sensitive to stress changes. According to D'Angelo et al. (2009) and some other sources, these binders will exhibit less rutting fatigue in the field under the same loading conditions compared to other tested binders. Although it is believed that MSCR can identify the presence of polymers in asphalt binders, this is not true for hybrid binder C as shown in the results. Whether it is because the 3% radial SBS and 10% fine rubber in hybrid binder C have been completely dissolved when produced needs to be further tested and verified.

All in all, the MSCR test results are strongly related the presence and concentration of coarse rubber (hybrid binder A, hybrid binder B and ARB-12), not just SBS polymer. Parameters obtained from the MSCR test distinguished most of the SBS polymer modified binders from the control binder.

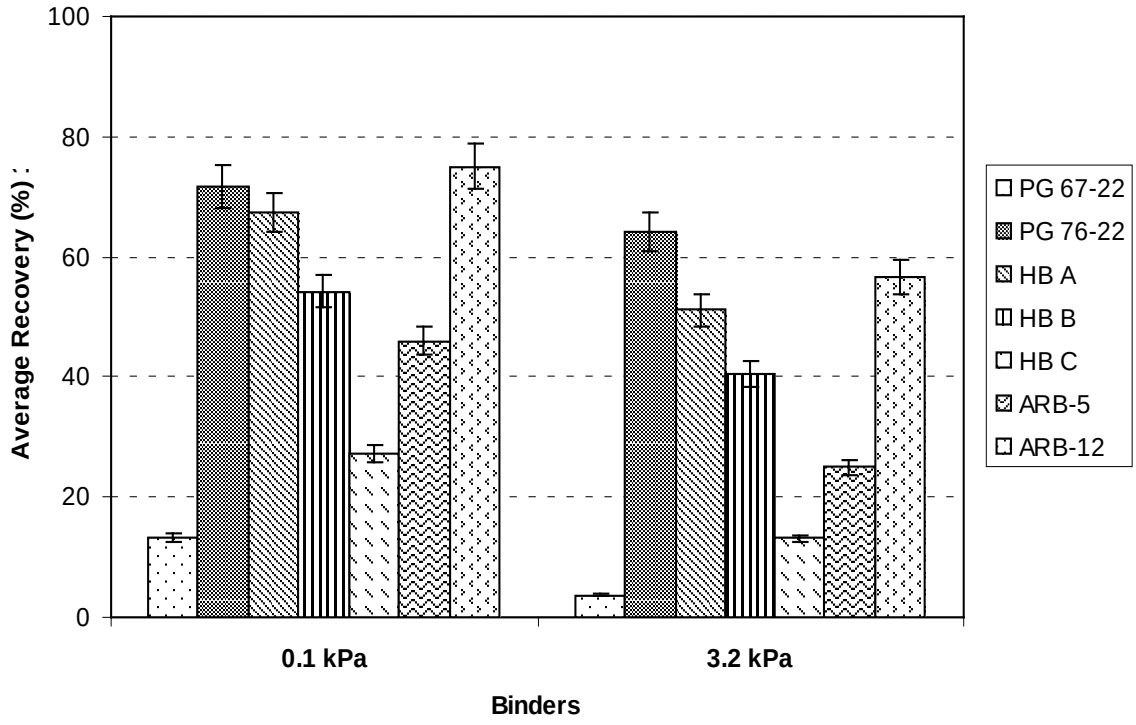

Figure 4-11. MSCR average recovery at 67.0 ºC (152.6 F) (RTFOT residue)

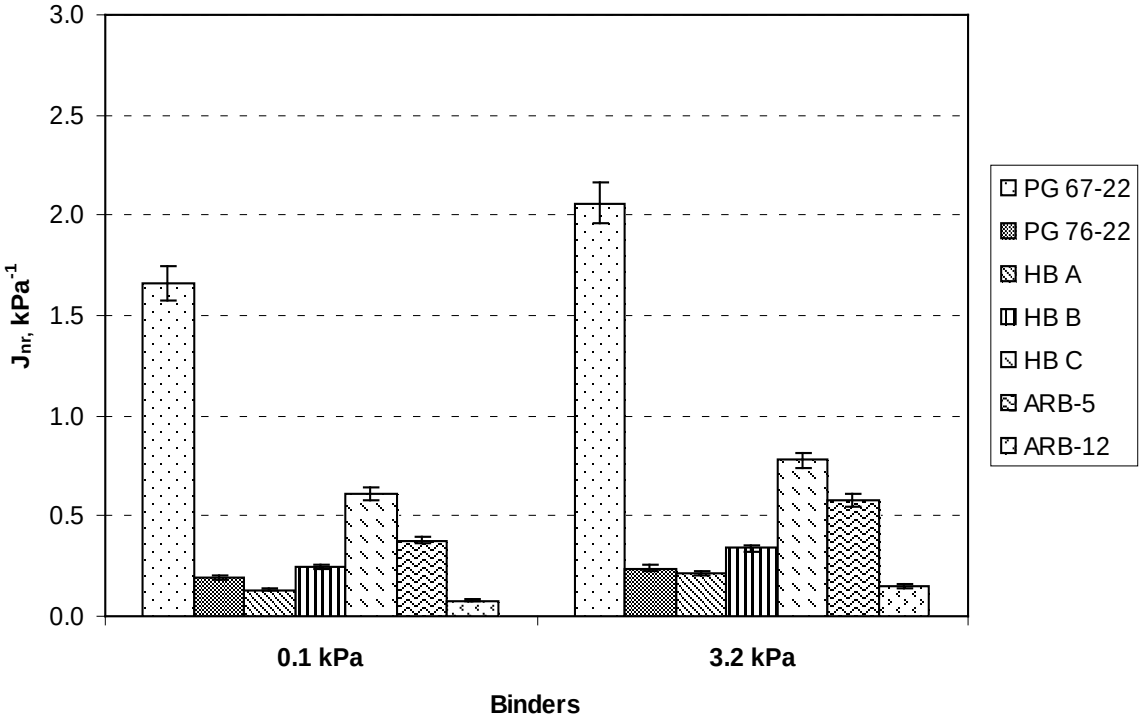

Figure 4-12. MSCR non-recoverable compliance at 67.0 ºC (152.6 F) (RTFOT residue)

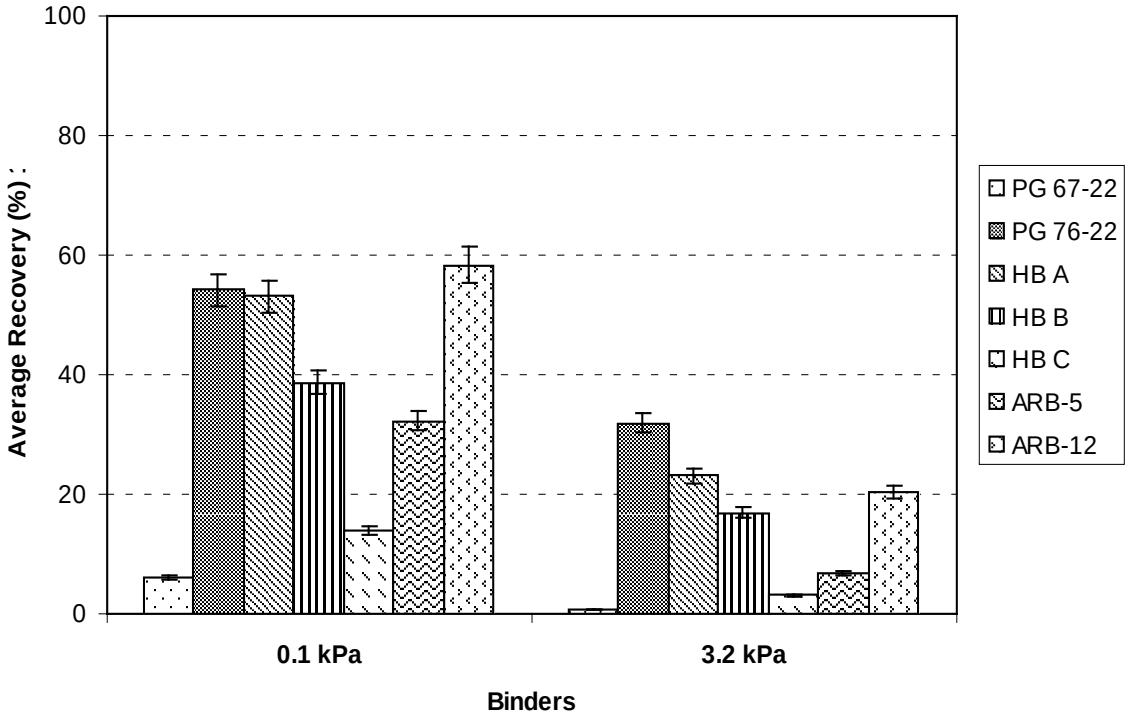

Figure 4-13. MSCR average recovery at 76 ºC (168.8 F) (RTFOT residue)

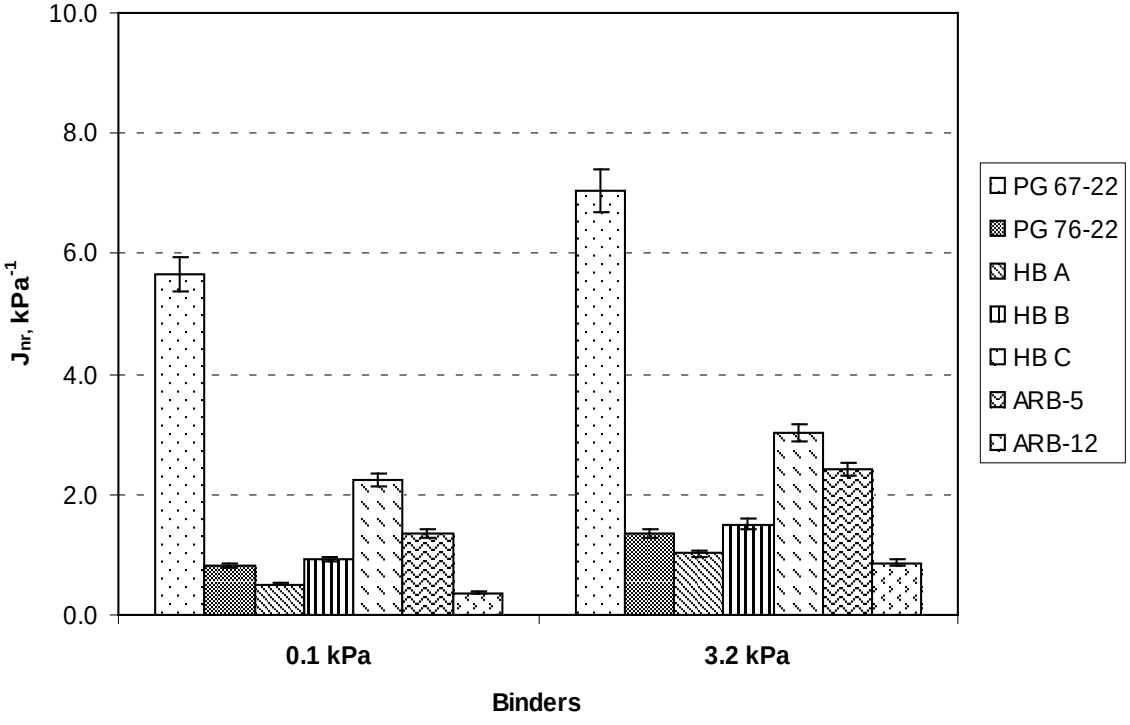

Figure 4-14. MSCR non-recoverable compliance at 76 ºC (168.8 F) (RTFOT residue)

Elastic Recovery

The elastic recovery is a measure of the tensile properties of the polymer modified asphalt cement RTFOT residue. It is measured by the percentage to which the asphalt cement residue will recover its original length after it has been elongated to a specific distance at a specified rate of speed and then cut in half.

Fig. 4-13 illustrates that the SBS modified binder and the hybrid binders exhibited greater elastic recovery at 25^{o} C than the base binder. Both rubber modified binders broke before the specified elongation of 20cm was reached, indicating that the rubber appears to make the binder more brittle at this temperature. Also, it appears that the presence of SBS made the binder less brittle (even when combined with rubber). Hybrid binder C, which used rubber with the finest gradation, did not increase the elastic recovery as much as the SBS modified binder or the other two hybrid binders.

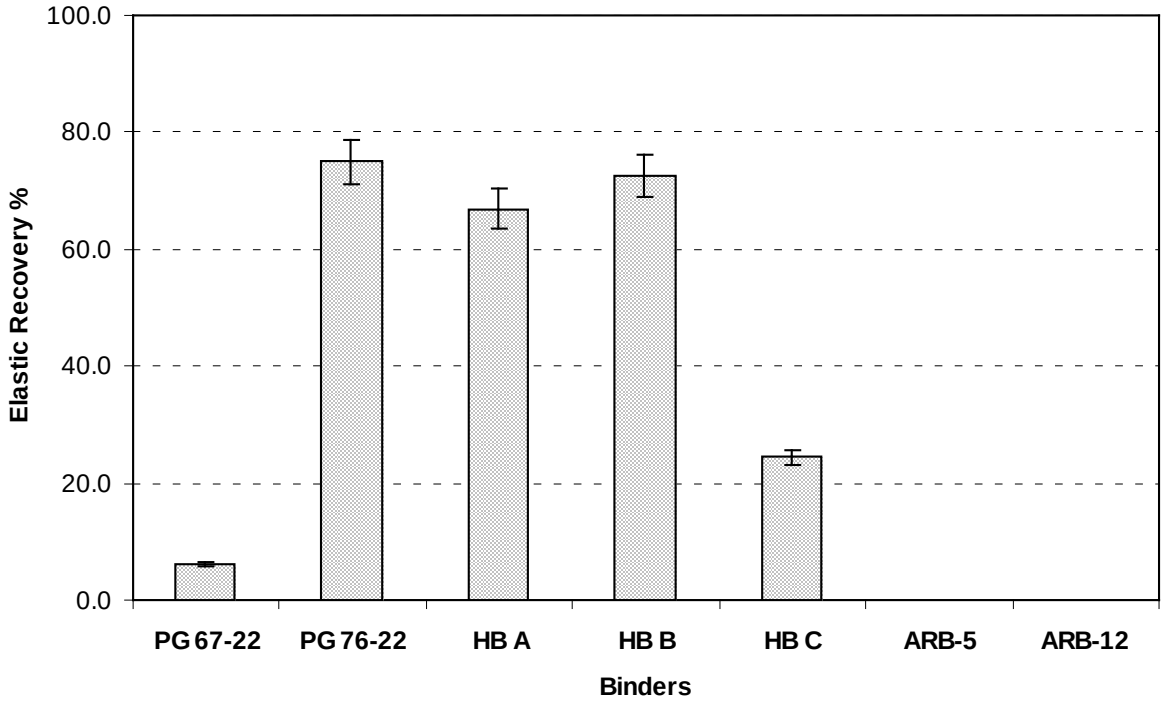

Figure 4-15. Elastic recovery at 25 ºC (77 F) (RTFOT residue)

Force Ductility Test

Force ductility test (AASHTO T 300) is used as a means of characterizing polymer modified binder. During the test, the specimen is elongated in a mold at a test temperature and loading rate, the results can be constructed as a stress and strain curve. An important parameter calculated from this test is the force ratio between first loading peak and second loading peak.

The test was performed at elongation rate of 5 cm/minute at temperature of 4ºC in water bath until the length reaches 100 cm or ruptures. Peak force ratios with 5% testing error range for all tested binders were plotted through Fig. 4-16 and Fig. 4-17. Fig. 4-16 shows that all modified binders exhibit higher ratio of residual to peak force (f_2 / f_1) than the control binder, which is similar to MSCR test results.

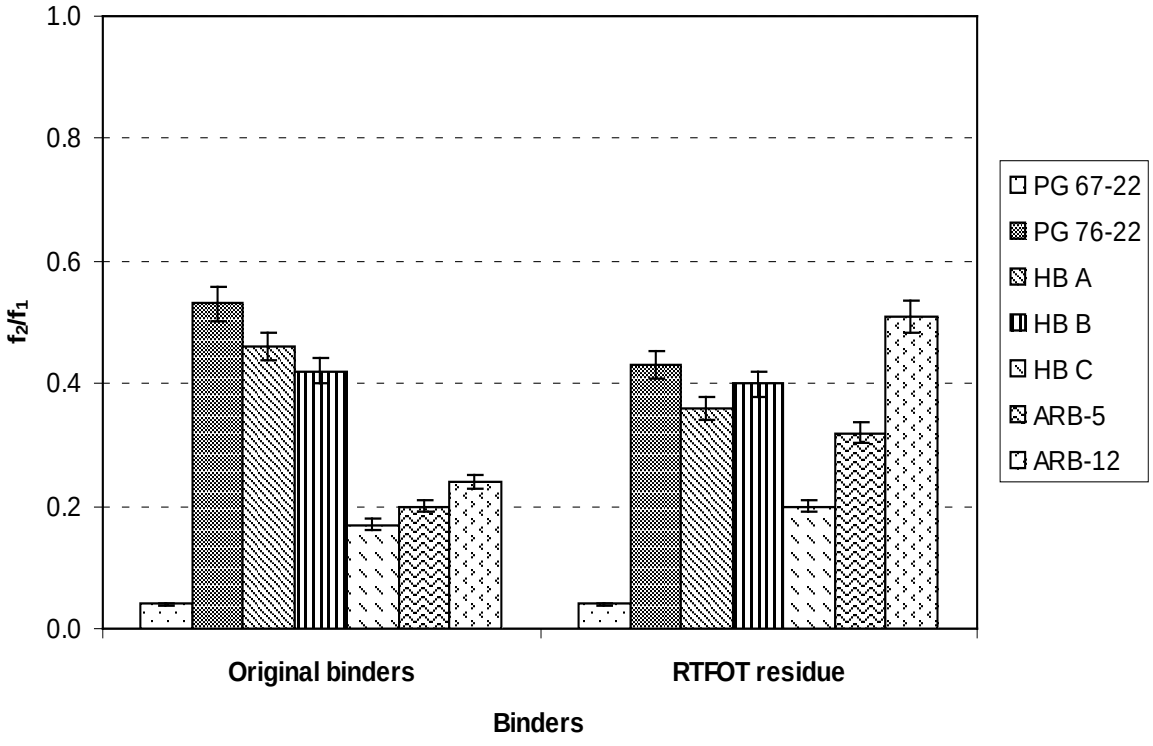

Figure 4-16. Force ductility test result, 10 ºC (50 F)

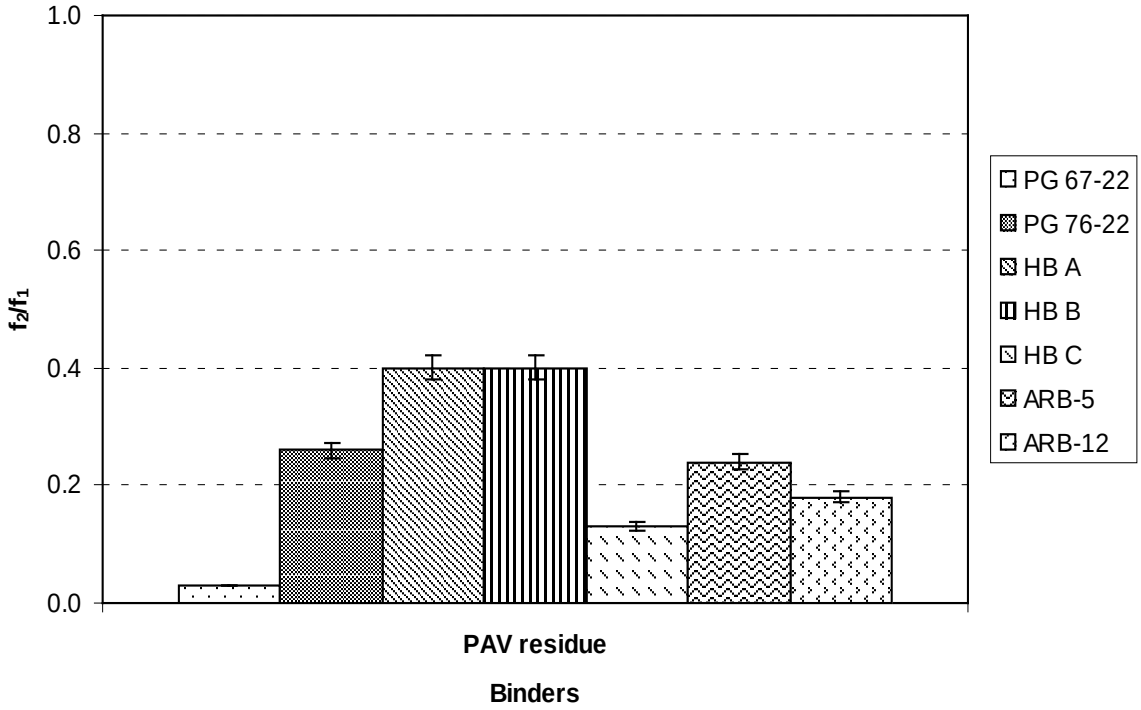

Figure 4-17. Force ductility test result, 25 ºC (77 F)

Binders performed slightly different at different test temperatures. At the test temperature 10 ºC, control binder (PG67-22) apparently shows less value than any other modified binders. However, except for binders after RTFOT, hybrid binder C along with ARB-5 and ARB-12, do not perform as good as PG 76-22, hybrid binder A and B, which is consistent with MSCR test results.

A stress-Strain curve was constructed to observe binders responses to loading. The strain may be calculated as follows:

$$\varepsilon_t = \int_{L_0}^{L} \frac{dL}{L} = \ln \frac{L}{L_0} = \ln \frac{A_0}{A}$$

Where,

L_0 — Original length of specimen

L — Length of specimen after elongation

A_0 — Original cross-sectional area of specimen

A —Cross-sectional area of specimen after elongation

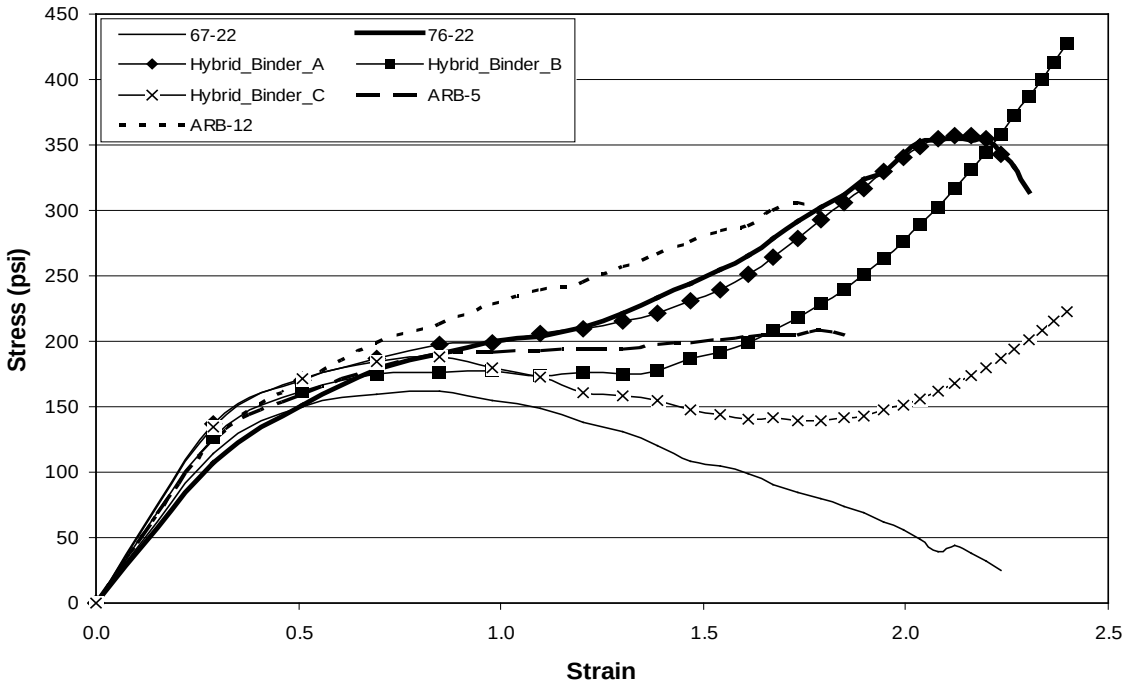

Figure 4-18. Stress-strain diagram of RTFOT residue at 10 ºC (50 F)

Fig. 4-18 shows two characteristic primary and secondary loading regions. From this figure it can be seen that both modified binders and control binder appear similar left half stress-strain curve, or “asphalt modulus”. However, as unloading occurs after peak stress, control binder continues to unload to approximately zero stress, following the modified binders unloading curve to the point where modified binders demonstrates secondary loading. At this point, the curves deviate, the control binder continuing to unload while most modified binders begin to increase in load. This secondary increase in load phenomenon can be regarded as an indicator of the presence of modifiers in binders, and the modifier, at this point is thought to begin carrying the load. Apparently there is some difference for different modifiers in “carrying secondary load” capability.

ARB-5 and ARB-12 broke they reach certain strains while hybrid binders and PG 76-22 keep increasing secondary half until reach either higher stress or higher strain, which can be attributed to the either the presence of SBS polymers or the cross-link interaction between crumb rubber and SBS polymer.

In a word, force ductility parameters f_2/f_1 is helpful to differentiate most SBS polymer modified binders from control binder. In addition, the stress-strain curve constructed from force ductility test, especially the secondary half, seems to be a good indicator of the presence of SBS polymers and the cross-link of SBS polymer and crumb rubbers.

Summary

The physical property results reveal the information that control binders (PG 76-22) can be differentiated from polymer and rubber modified asphalt, but purely polymer modified binder PG 76-22 can not be clearly distinguished from hybrid binders or sometimes even ARB-12 simply by these physical properties. The solubility test results show that some coarse crumb rubber particles were not completely digested in asphalt, which affected binders' rheology test results. Since the DSR test requires asphalt specimen with specific shape, the DSR results were influenced the most by the undigested particles in the binder. Therefore, DSR test results provide little meaningful information with respect to binders' ability to resist rutting or cracking.

Combined with Elastic Recovery test and Force Ductility test, MSCR test can not only distinguish modified binders from control binders, but differentiate crumb rubber modified binders ARB-5 and ARB-12 from hybrid binders: ARB-5 and ARB-12 broke at some strain level where PG 76-22 and hybrid binders still exhibited smooth extension. It

is believed that it is the cross-link of CRM and SBS polymer which improved binders' ductility.

Although test results showed the hybrid binder A and B behave as well as PG 76-22, hybrid binder C did not exhibit the same competency in some properties such as the elastic recovery and non-recoverable compliance. Why this is the case implies further binder test needs to be developed to verify the existence of polymers in binders. Also, whether it is true that binders showing improved performance in binder test will exhibit the same in mixture test needs to be verified in the following mixture tests.

CHAPTER 5
MIXTURE IDT TEST RESULTS AND ANALYSIS

Mixture Test Results

In accordance with AASHTO T 322, standard Superpave Indirect Tension Test (IDT) was performed at 10°C on all mixtures to determine resilient modulus (M_r), creep compliance (m-value and D_1), tensile strength (S_t), failure strain (ε_f), fracture energy (FE) and dissipated creep strain energy (DCSE) (Roque, 1997) to failure. Results were combined and analyzed using Hot-Mix-Asphalt (HMA) Fracture Mechanics Model (Zhang, 2001) and Energy Ratio Theories (Roque, 2004), to evaluate the mixtures' resistance to cracking.

The number of specimens and testing cycles are listed in Table 5-1. A total number of 132 IDT specimens were tested for this project. For each specific type of mixture, three specimens were tested and the variability of the specimens was considered and treated by using a trimmed mean approach.

Table 5-1. Summary of total mixture tests

Mixture Type	Aggregate Type	Conditions	Types of Binders	Number of Replicates	Total No. of Mixture Tests
OGFC	Limestone	LTOA/STOA	5	3	90
	Granite	LTOA/STOA	5	3	90
Superpave Dense	Limestone	LTOA/STOA	6	3	108
	Granite	LTOA/STOA	6	3	108
Totals	4	2	7	132	396

All test results and calculated parameters are listed in Table 5-2 through Table 5-7.

Table 5-2. DG mixtures creep and damage test results

Aggregate	Binder Type	Aging Conditions	m-value	D_1 (1/psi)	D(1000 sec) (1/GPa)	d(D)/ dt(1000 sec)
Granite	PG 67-22	STOA	0.668	4.77E-07	7.055	3.20E-08
		LTOA	0.532	4.48E-07	2.619	9.43E-09
	PG 76-22	STOA	0.534	7.54E-07	4.414	1.61E-08
		LTOA	0.413	5.43E-07	1.414	3.88E-09
	HB A	STOA	0.446	5.93E-07	1.926	5.76E-09
		LTOA	0.411	4.35E-07	1.128	3.05E-09
	HB B	STOA	0.455	9.17E-07	3.110	9.64E-09
		LTOA	0.438	5.18E-07	1.584	4.66E-09
	HB C	STOA	0.521	7.52E-07	4.074	1.43E-08
		LTOA	0.402	6.73E-07	1.602	4.33E-09
	ARB-5	STOA	0.600	3.841E-07	3.575	1.45E-08
		LTOA	0.576	3.05E-07	2.444	9.44E-09
Limestone	PG 67-22	STOA	0.477	5.42E-07	2.176	6.99E-09
		LTOA	0.385	4.892E-07	1.062	2.69E-09
	PG 76-22	STOA	0.436	5.44E-07	1.665	4.83E-09
		LTOA	0.308	6.60E-07	0.83	1.70E-09
	HB A	STOA	0.376	6.24E-07	1.291	3.15E-09
		LTOA	0.327	4.12E-07	0.628	1.29E-09
	HB B	STOA	0.386	4.26E-07	0.948	2.38E-09
		LTOA	0.300	5.30E-07	0.652	1.27E-09
	HB C	STOA	0.406	5.38E-07	1.353	3.63E-09
		LTOA	0.348	3.44E-07	0.592	1.32E-09
	ARB-5	STOA	0.506	6.08E-07	3.019	1.02E-08
		LTOA	0.392	4.72E-07	1.069	2.78E-09

Table 5-3. DG mixtures strength and fracture test results

Aggregate	Binder Type	Aging Conditions	S_t (MPa)	M_R (GPa)	e_f (micro)	$N_{initiation}$	$N_{propagation}$ (2in)	FE (kJ/m^3)	$DCSE_{HMA}$ (kJ/m^3)
Granite	PG 67-22	STOA	2.14	10.85	2566.05	1.63E+04	5.58E+03	4.2	4.0
		LTOA	2.25	11.99	1336.78	2.02E+04	6.92E+03	2.2	2.0
	PG 76-22	STOA	2.23	10.55	3326.20	3.15E+04	1.08E+04	5.5	5.3
		LTOA	2.59	11.37	1824.64	6.01E+04	2.06E+04	3.5	3.2
	HB A	STOA	1.90	11.55	1272.15	2.24E+04	7.68E+03	1.8	1.6
		LTOA	2.26	14.13	940.13	3.14E+04	1.07E+04	1.5	1.3
	HB B	STOA	1.92	10.12	2426.19	2.84E+04	9.73E+03	3.6	3.4
		LTOA	2.08	11.96	1537.91	3.51E+04	1.20E+04	2.3	2.1
	HB C	STOA	2.02	11.35	2285.38	2.17E+04	7.42E+03	3.5	3.3
		LTOA	2.44	13.23	1423.10	3.73E+04	1.28E+04	2.5	2.3
	ARB-5	STOA	2.12	13.26	1470.04	1.64E+04	5.62E+03	2.3	2.1
		LTOA	2.12	13.85	1100.17	1.62E+04	5.53E+03	1.6	1.4
Limestone	PG 67-22	STOA	2.17	11.88	1167.65	1.69E+04	5.80E+03	1.6	1.4
		LTOA	2.2	13.62	1066.45	1.69E+04	5.80E+03	1.5	1.3
	PG 76-22	STOA	2.41	11.36	1431.47	3.25E+04	1.11E+04	2.3	2.0
		LTOA	2.71	11.97	1294.71	7.37E+04	2.52E+04	2.5	2.2
	HB A	STOA	2.04	11.16	1000.95	2.57E+04	8.81E+03	1.4	1.2
		LTOA	2.02	12.00	707.20	3.38E+04	1.16E+04	0.9	0.7
	HB B	STOA	2.40	11.87	1116.24	4.49E+04	1.54E+04	1.8	1.6
		LTOA	2.33	11.94	864.94	4.76E+04	1.63E+04	1.3	1.1
	HB C	STOA	2.32	12.56	1116.28	3.14E+04	1.07E+04	1.8	1.6
		LTOA	2.62	12.88	962.87	6.80E+04	2.33E+04	1.7	1.4
	ARB-5	STOA	1.9	10.81	1185.45	1.18E+04	4.05E+03	1.5	1.3
		LTOA	2.38	13.53	999.93	3.48E+04	1.19E+04	1.6	1.4

Table 5-4. DG mixtures energy ratio results

Aggregate	Binder Type	Aging Conditions	$DCSE_{MIN}$, (kJ/m^3)	ER@ stress, 150 psi
Granite	PG 67-22	STOA	2.971	1.34
		LTOA	1.440	1.38
	PG 76-22	STOA	2.440	2.16
		LTOA	0.852	3.76
	HB A	STOA	1.081	1.52
		LTOA	0.646	2.04
	HB B	STOA	1.773	1.93
		LTOA	0.910	2.33
	HB C	STOA	2.206	1.51
		LTOA	0.956	2.38
	ARB-5	STOA	1.738	1.23
		LTOA	1.226	1.17
Limestone	PG 67-22	STOA	1.247	1.12
		LTOA	0.595	2.22
	PG 76-22	STOA	0.984	2.08
		LTOA	0.438	5.01
	HB A	STOA	0.695	1.75
		LTOA	0.302	2.42
	HB B	STOA	0.537	2.90
		LTOA	0.312	3.43
	HB C	STOA	0.781	2.03
		LTOA	0.325	4.41
	ARB-5	STOA	1.617	0.82
		LTOA	0.619	2.25

Table 5-5. OGFC mixtures creep and damage test results

Aggregate	Binder Type	Aging Conditions	m-value	D_1 (1/psi)	D(1000 sec) (1/GPa)	d(D)/dt(1000 sec)
Granite	PG 76-22	STOA	0.599	1.49E-06	13.601	5.59E-08
		LTOA	0.577	8.68E-07	6.851	2.70E-08
	HB A	STOA	0.487	1.15E-06	4.929	1.63E-08
		LTOA	0.459	6.88E-07	2.496	7.52E-09
	HB B	STOA	0.478	1.64E-06	6.491	2.13E-08
		LTOA	0.439	1.65E-06	5.035	1.50E-08
	HB C	STOA	0.537	1.31E-06	7.932	2.87E-08
		LTOA	0.570	6.29E-07	4.804	1.84E-08
	ARB-12	STOA	0.557	8.38E-07	5.828	2.19E-08
		LTOA	0.555	7.47E-07	5.118	1.91E-08
Limestone	PG 76-22	STOA	0.434	8.83E-07	2.657	7.65E-09
		LTOA	0.365	9.02E-07	1.741	4.11E-09
	HB A	STOA	0.458	6.35E-07	2.254	6.86E-09
		LTOA	0.366	5.12E-07	0.994	2.36E-09
	Hybrid Binder B	STOA	0.451	9.50E-07	3.199	9.62E-09
		LTOA	0.416	4.89E-07	1.310	3.61E-09
	Hybrid Binder C	STOA	0.521	6.53E-07	3.522	1.24E-08
		LTOA	0.408	9.95E-07	2.484	6.80E-09
	ARB-12	STOA	0.533	5.87E-07	3.500	1.25E-08
		LTOA	0.427	6.26E-07	1.824	5.13E-09

Table 5-6. OGFC mixtures strength and fracture test results

Aggregate	Binder Type	Aging Conditions	S_t (MPa)	M_R (Gpa)	e_f (micro)	$N_{initiation}$	$N_{propagation}$ (2in)	FE (kJ/m^3)	$DCSE_{HMA}$ (kJ/m^3)
Granite	PG 76-22	STOA	1.61	5.29	3601.16	2.14E+04	7.33E+03	4.5	4.3
		LTOA	1.44	6.46	1454.68	1.39E+04	4.77E+03	1.5	1.3
	Hybrid Binder A	STOA	1.35	6.13	1538.19	2.51E+04	8.58E+03	1.6	1.5
		LTOA	1.38	8.92	674.36	1.84E+04	6.31E+03	0.6	0.5
	Hybrid Binder B	STOA	1.33	5.47	1966.58	2.43E+04	8.33E+03	2.0	1.8
		LTOA	1.54	4.92	2638.98	5.35E+04	1.83E+04	3.1	2.9
	Hybrid Binder C	STOA	1.07	5.81	1018.97	5.91E+03	2.02E+03	0.7	0.6
		LTOA	1.43	6.59	1136.02	1.60E+04	5.46E+03	1.2	1.0
	ARB-12	STOA	1.17	6.93	1499.10	1.54E+04	5.28E+03	1.3	1.2
		LTOA	1.27	7.29	1215.67	1.46E+04	4.98E+03	1.1	1.0
Limestone	PG 76-22	STOA	1.58	7.83	1107.59	3.83E+04	1.31E+04	1.2	1.0
		LTOA	1.50	8.53	732.86	3.89E+04	1.33E+04	0.7	0.6
	Hybrid Binder A	STOA	1.59	7.42	1175.16	5.04E+04	1.73E+04	1.4	1.2
		LTOA	1.82	9.71	916.91	1.11E+05	3.80E+04	1.1	0.9
	Hybrid Binder B	STOA	1.64	7.28	1211.57	3.55E+04	1.22E+04	1.4	1.2
		LTOA	1.77	8.23	1220.33	1.02E+05	3.49E+04	1.5	1.3
	Hybrid Binder C	STOA	1.56	7.99	1073.92	2.15E+04	7.34E+03	1.1	0.9
		LTOA	1.62	7.03	975.14	3.78E+04	1.29E+04	1.1	0.9
	ARB-12	STOA	1.45	9.10	1058.80	2.45E+04	8.38E+03	1.2	1.1
		LTOA	1.57	10.16	1013.60	5.37E+04	1.84E+04	1.1	1.0

Table 5-7. OGFC mixtures energy ratio results

Aggregate	Binder Type	Aging Conditions	$DCSE_{MIN}$ (kJ/m^3)	ER @ stress 150 psi
Granite	PG 76-22	STOA	6.326	0.7
		LTOA	3.246	0.41
	Hybrid Binder A	STOA	2.578	0.56
		LTOA	1.290	0.38
	Hybrid Binder B	STOA	3.449	0.53
		LTOA	2.758	1.04
	Hybrid Binder C	STOA	3.793	0.16
		LTOA	2.265	0.46
	ARB-12	STOA	2.740	0.44
		LTOA	2.436	0.41
Limestone	PG 76-22	STOA	1.427	0.73
		LTOA	0.868	0.65
	Hybrid Binder A	STOA	1.208	1.02
		LTOA	0.515	1.80
	Hybrid Binder B	STOA	1.735	0.70
		LTOA	0.715	1.83
	Hybrid Binder C	STOA	1.821	0.52
		LTOA	1.348	0.68
	ARB-12	STOA	1.735	0.62
		LTOA	0.969	1.01

Analysis of IDT Test Results

Since currently there is no single mixture property or characteristic that can reliably predict top-down cracking performance of HMA (Roque, 2004), a number of mixture parameters obtained from the IDT were evaluated by using HMA fracture mechanics and DCSE theory to determine the mixtures' potential to cracking. In addition, some observations regarding mixture preparation were cited as they helped to explain some of the findings. Since the relative cracking performance was different in the two types of mixtures evaluated, the analysis was categorized into two parts: dense-graded (DG) mixtures and open-graded friction course (OGFC) mixtures.

DG Mixtures

The number of loading cycles for crack initiation ($N_{initiation}$) and to 5-mm of propagation ($N_{propagation}$) were calculated from Dissipated Creep Strain Energy to failure ($DCSE_f$) and the DCSE/cycle concepts based on resilient modulus, creep test and tensile strength test results (Appendix B and C). Energy Ratio, defined as the dissipated creep strain energy threshold of the mixture divided by the minimum dissipated creep strain energy required, is a criterion recently developed by Roque, et al.(2004) to evaluate top-down cracking performance of mixtures. These three parameters: $N_{initiation}$, $N_{propagation}$ and ER were used as the principal basis to evaluate the mixtures cracking performance in this research.

Fig. 5-1 through 5-6 show that hybrid binder mixtures generally performed better than both PG 67-22 and ARB-5 mixtures regardless of aggregate types and aging conditions. These figures also show that SBS polymer modified binder mixtures exhibited superior performance among all mixtures regardless of aggregate type or aging condition.

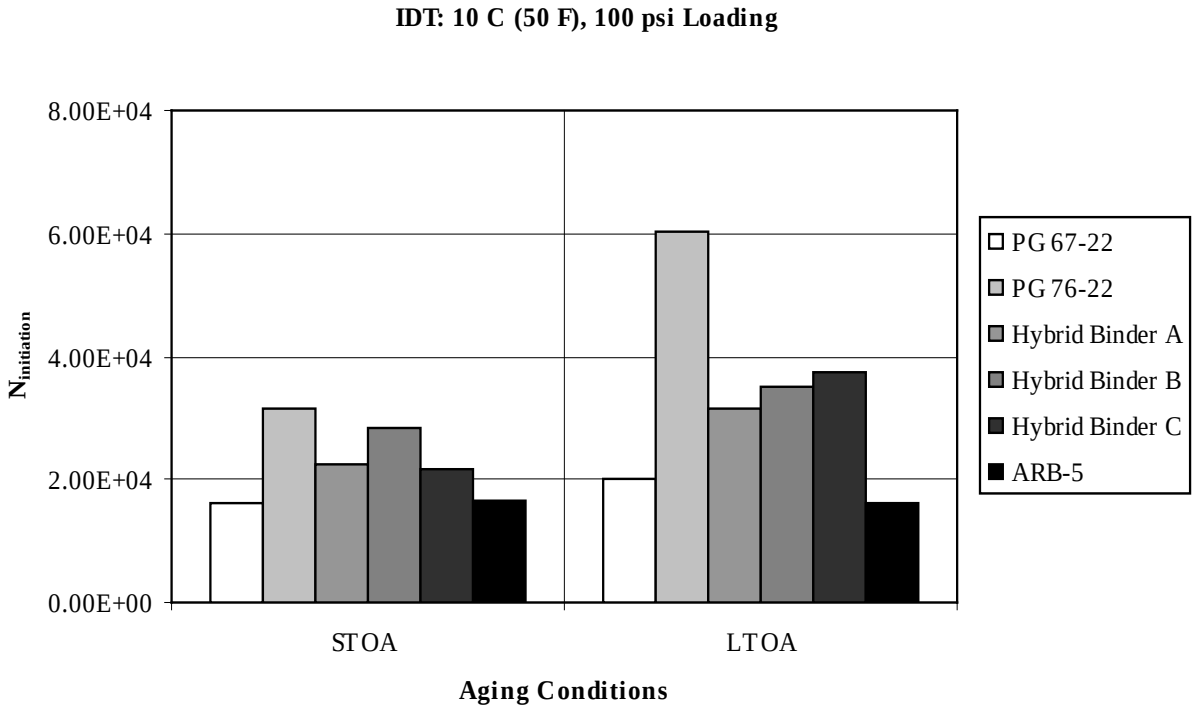

Figure 5-1. $N_{initiation}$ for DG granite mixtures

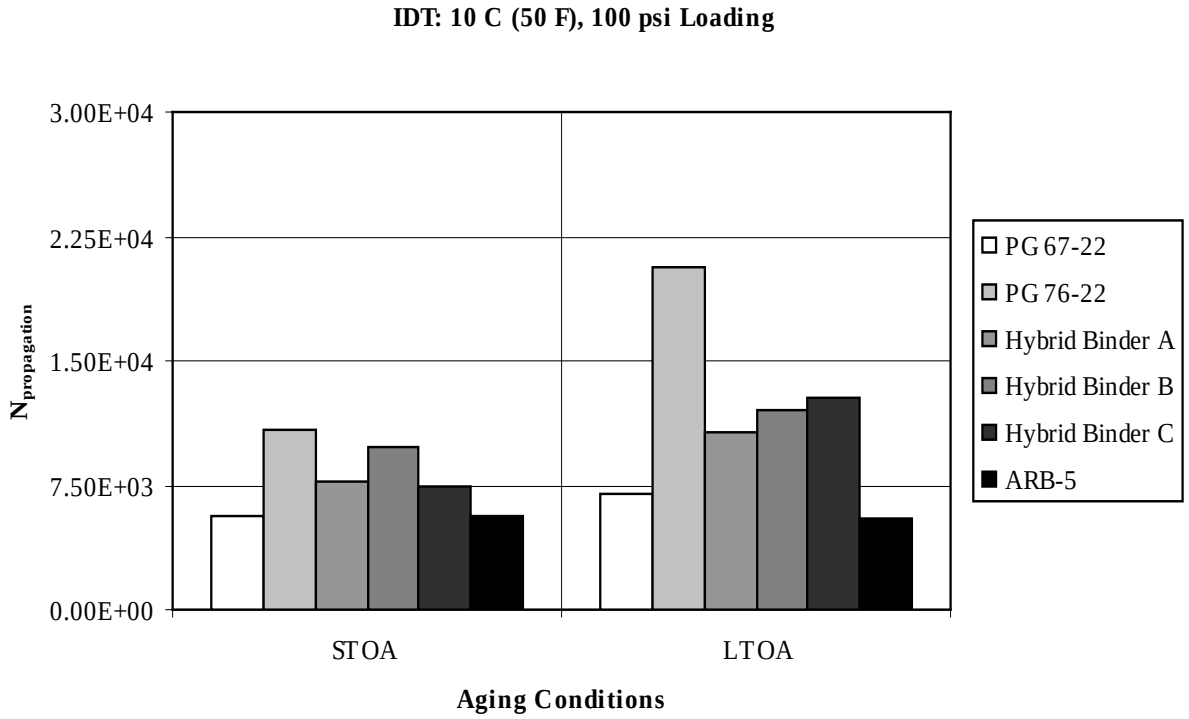

Figure 5-2. $N_{propagation}$ for DG granite mixtures

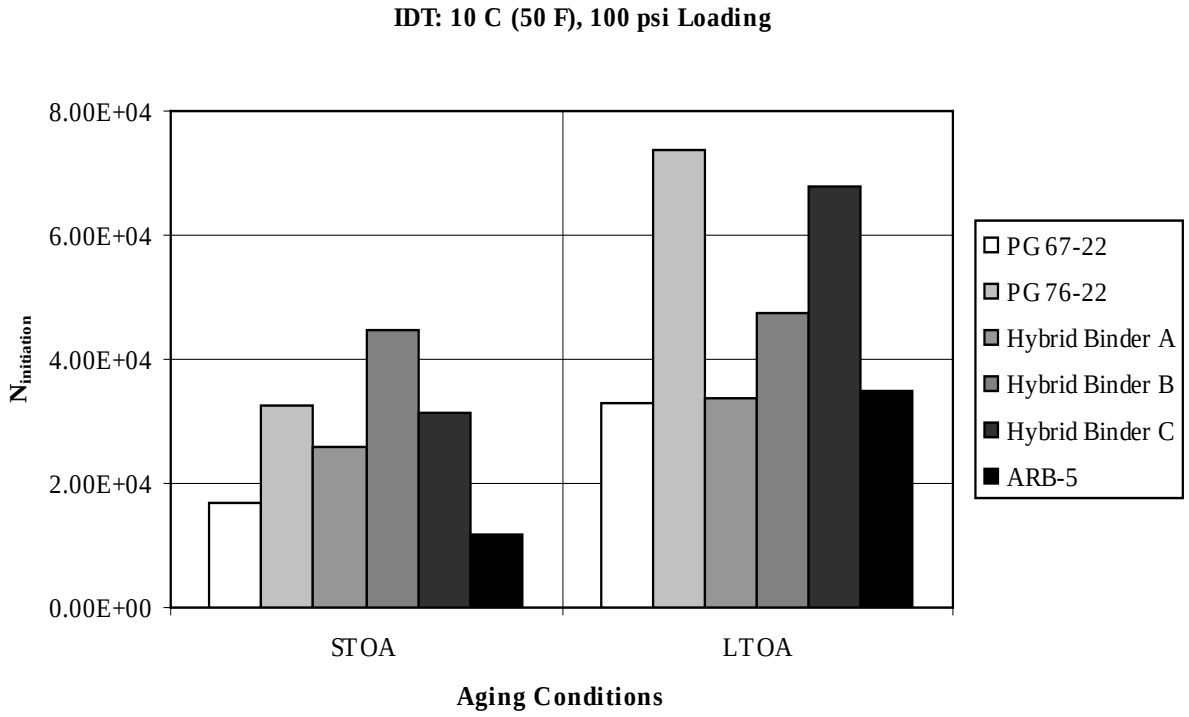

Figure 5-3. $N_{initiation}$ for DG limestone mixtures

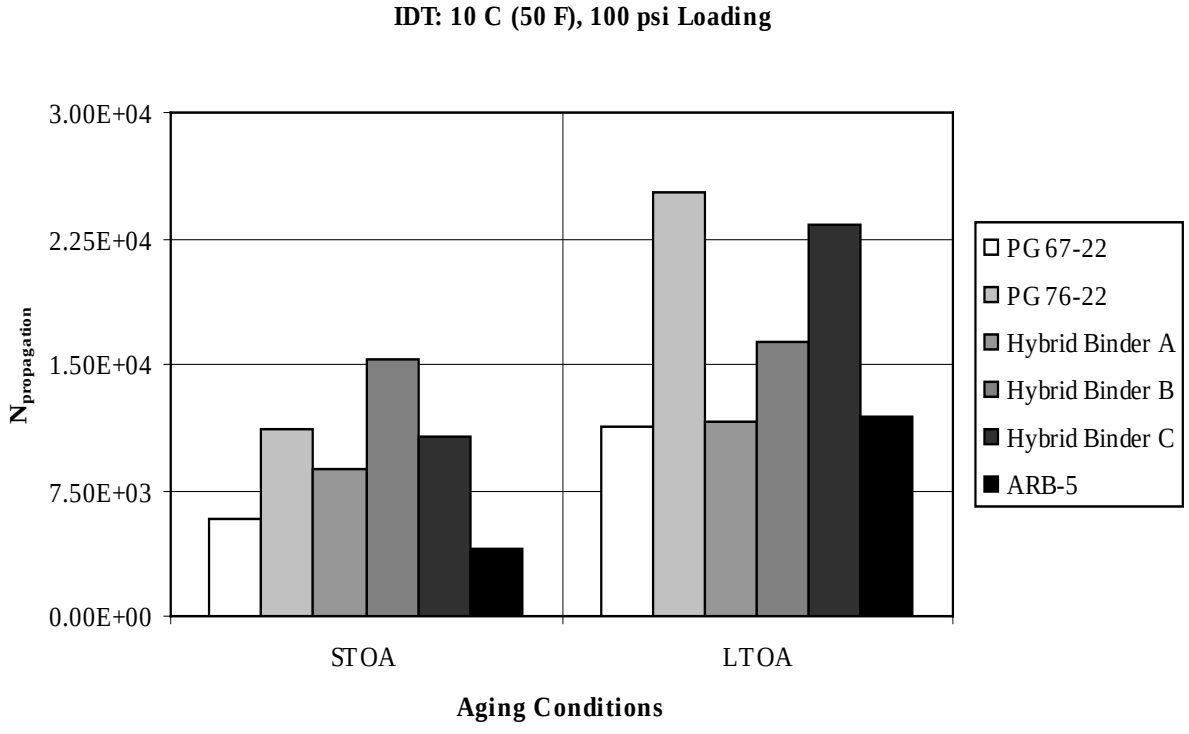

Figure 5-4. $N_{propagation}$ for DG limestone mixtures

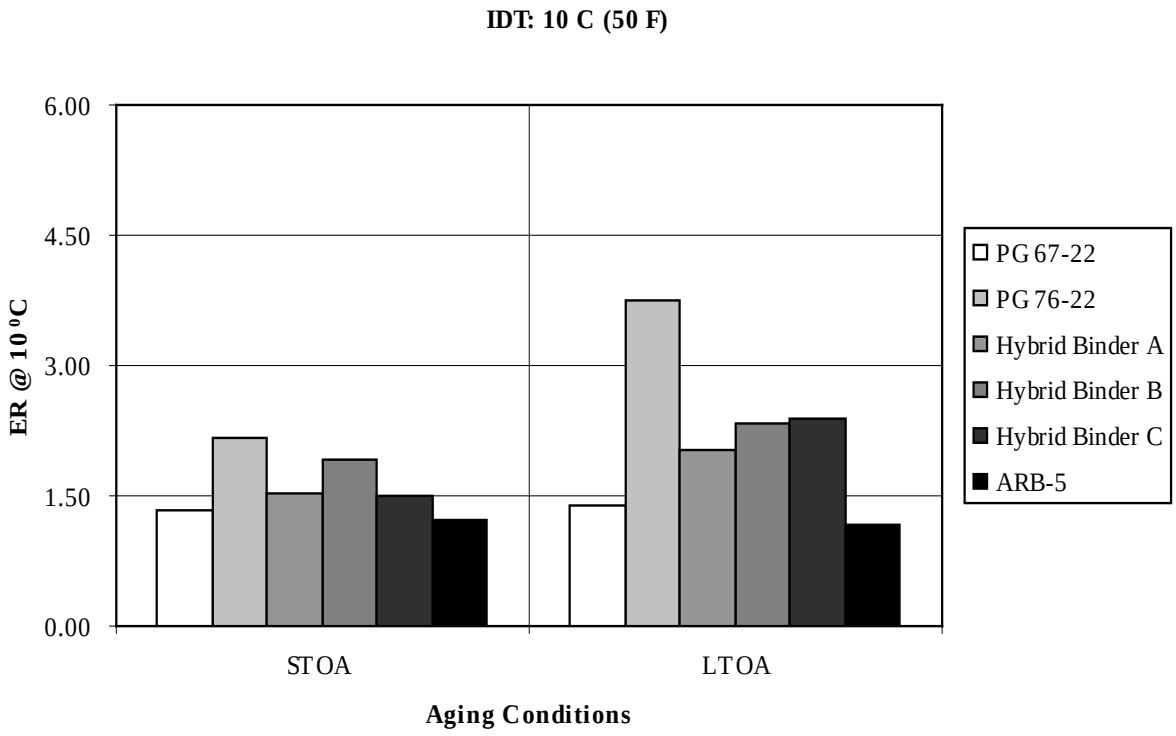

Figure 5-5. ER for DG granite mixtures

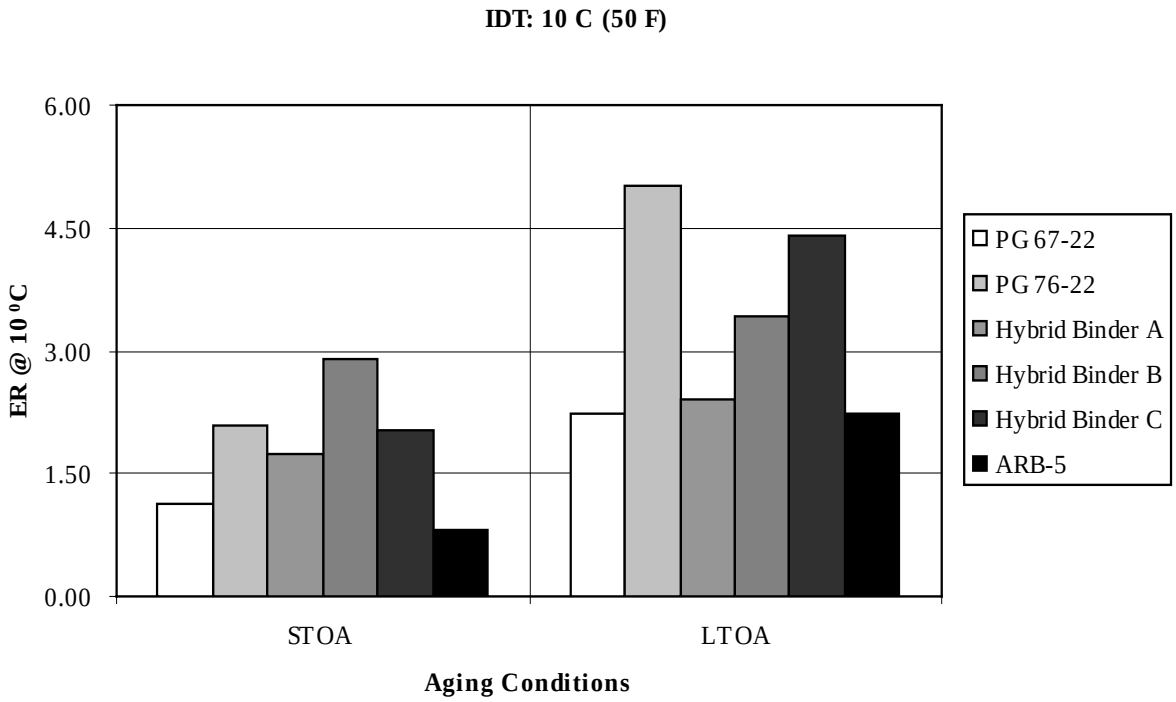

Figure 5-6. ER for DG limestone mixtures

If considered by STOA and LTOA separately, all three hybrid binders were found exhibiting similar cracking resistance trends for both granite and limestone mixtures. However, if compared for the same mixtures with different aging conditions, different cracking performance trends were observed: the LTOA apparently increased the cracking resistance of hybrid binder mixtures. A larger increase in cracking resistance was observed for limestone mixtures, which could be explained by the fact that limestone has a much rougher surface texture and greater absorption than granite. Therefore, it is hypothesized that laboratory aging at 85ºC (LTOA) results in more binder being absorbed by the limestone, which in these mixtures appeared to increase resistance to damage with little or no reduction in fracture energy limit.

The ARB-5 mixtures did not exhibit improvements in cracking resistance to the PG 67-22 mixtures. This result is consistent with previous research which indicated that rubber alone did not improve cracking resistance of mixtures.

As for the other mixtures, aging effects were found to be particularly acute in the limestone mixtures. Once again it is hypothesized that these effects may be somewhat artificially caused by increased absorption in these aggregates during LTOA.

OGFC Mixtures

Although the relative performance of hybrid binders in OGFC mixtures was somewhat different from that observed in DG mixtures, Fig. 5-7 through 5-12 show that hybrid binders exhibited similar or better cracking resistance than both SBS polymer modified binder and ARB-12 in OGFC mixtures, except for one special case (hybrid binder C, STOA in granite mixture). This result was true for all parameters evaluated ($N_{initiation}$, $N_{propagation}$ and ER) for both aggregate types and aging levels. Hybrid binders A and B resulted in OGFC mixtures with particularly high resistance to cracking,

especially for the LTOA condition and limestone aggregate. These effects are likely responsible: the coarse rubber binders may be more resistant to age-hardening and the limestone aggregate absorbs more asphalt during LTOA, therefore making the mixture more resistant to damage. It is interesting to note that the hybrid binders exhibited greater cracking resistance than ARB-12, indicating that the addition of SBS polymer provided an added benefit.

The relatively low fracture resistance exhibited by hybrid binder C with the fine rubber, and granite aggregate was probably a result of binder redistribution (partial draindown), rather than the quality of the binder itself. The smoother texture and lower absorption of the granite, combined with the lower viscosity of the finer rubber binder provide an explanation for this phenomenon. These factors may have contributed to the binder's inability to maintain a uniform distribution within the granite OGFC, therefore creating areas of relative weakness within the mixture. This effect was minimized or eliminated where the rougher, more absorptive limestone aggregate was used.

In summary, it appears that the hybrid binders evaluated in this study can be used as a substitute for either SBS modified (PG 76-22) or ARB-12 in OGFC mixtures. However, there may be a need to check on draindown potential of hybrid binder produced with finer rubber when used in smooth textured, non-absorptive aggregate OGFC mixtures.

Summary

In general, the IDT test results showed that all mixtures with hybrid binders, regardless of aggregate types and aging conditions, performed comparatively better than PG 67-22 and ARB-5 mixtures in terms of cracking resistance. Better cracking

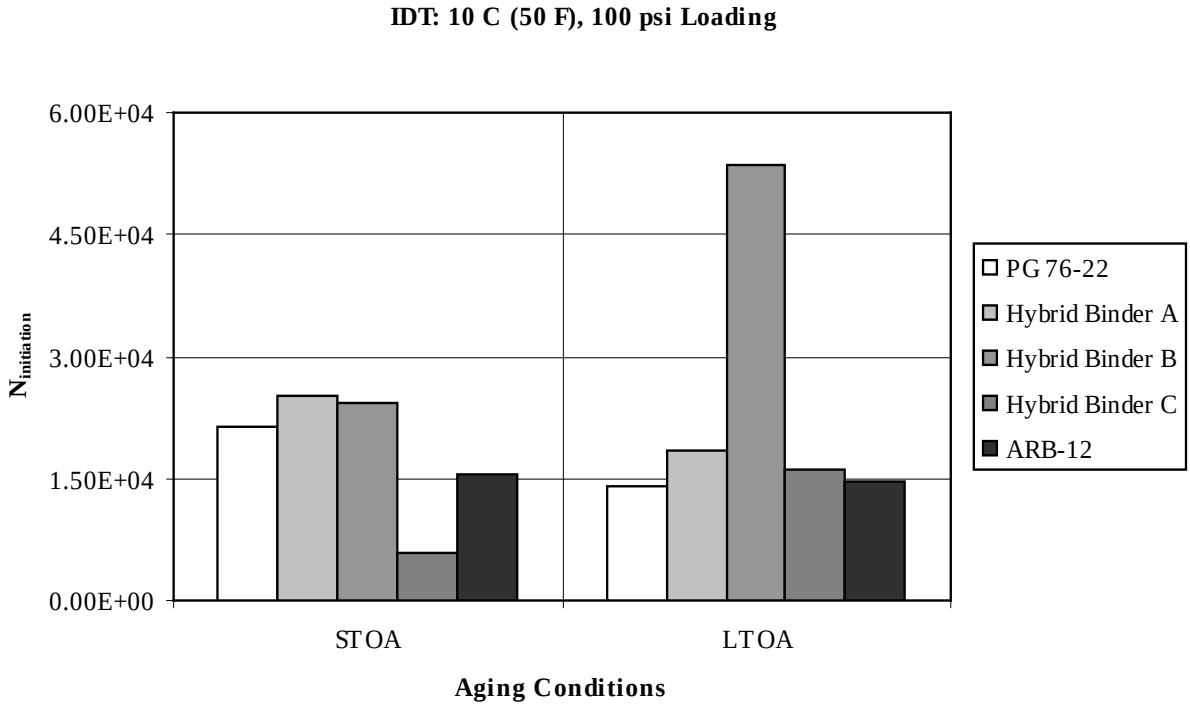

Figure 5-7. $N_{initiation}$ for OGFC granite mixtures

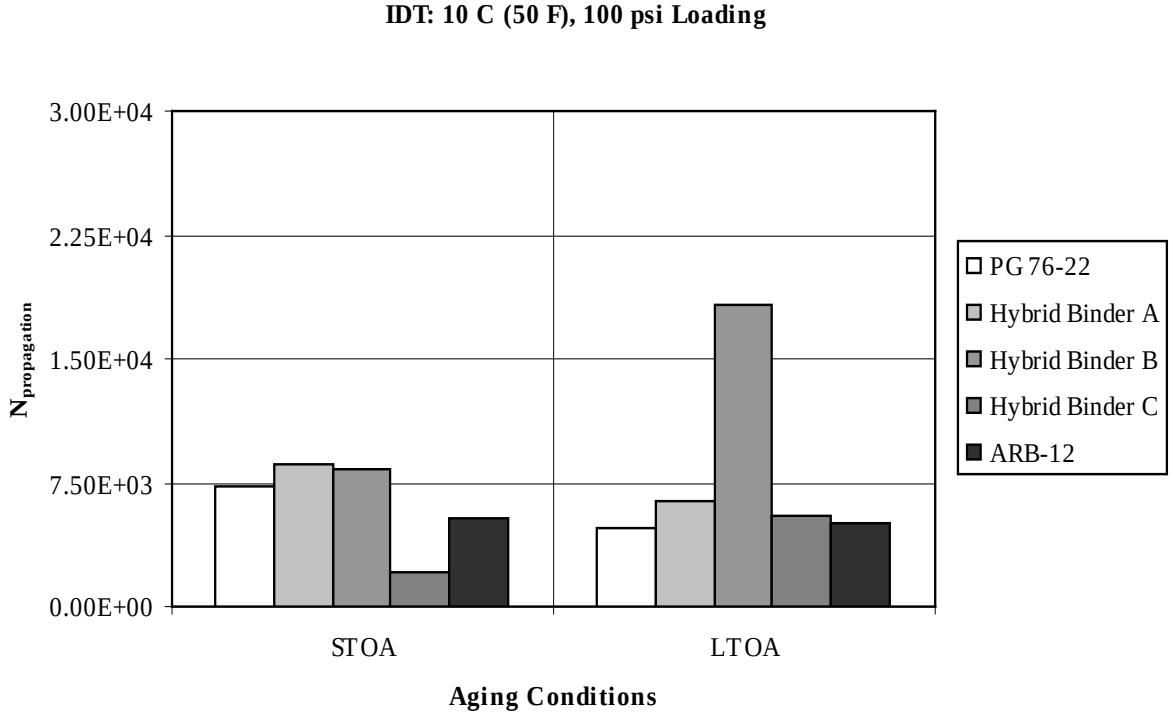

Figure 5-8. $N_{propagation}$ for OGFC granite mixtures

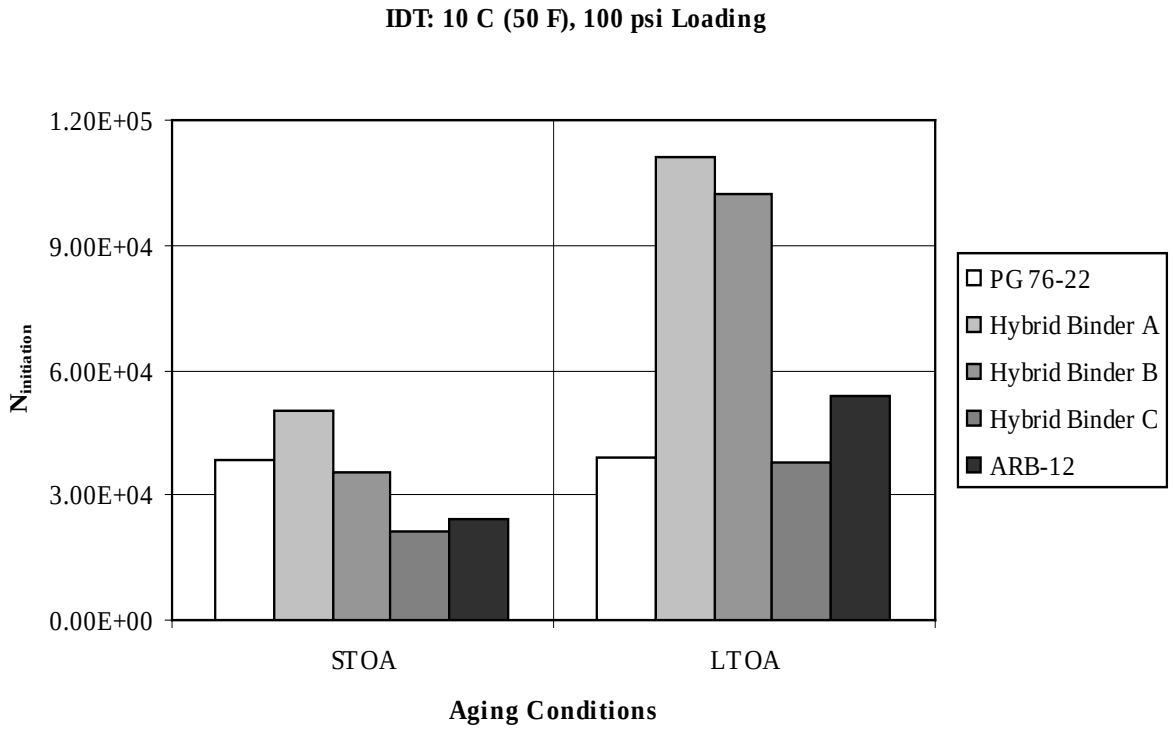

Figure 5-9. $N_{initiation}$ for OGFC limestone mixtures

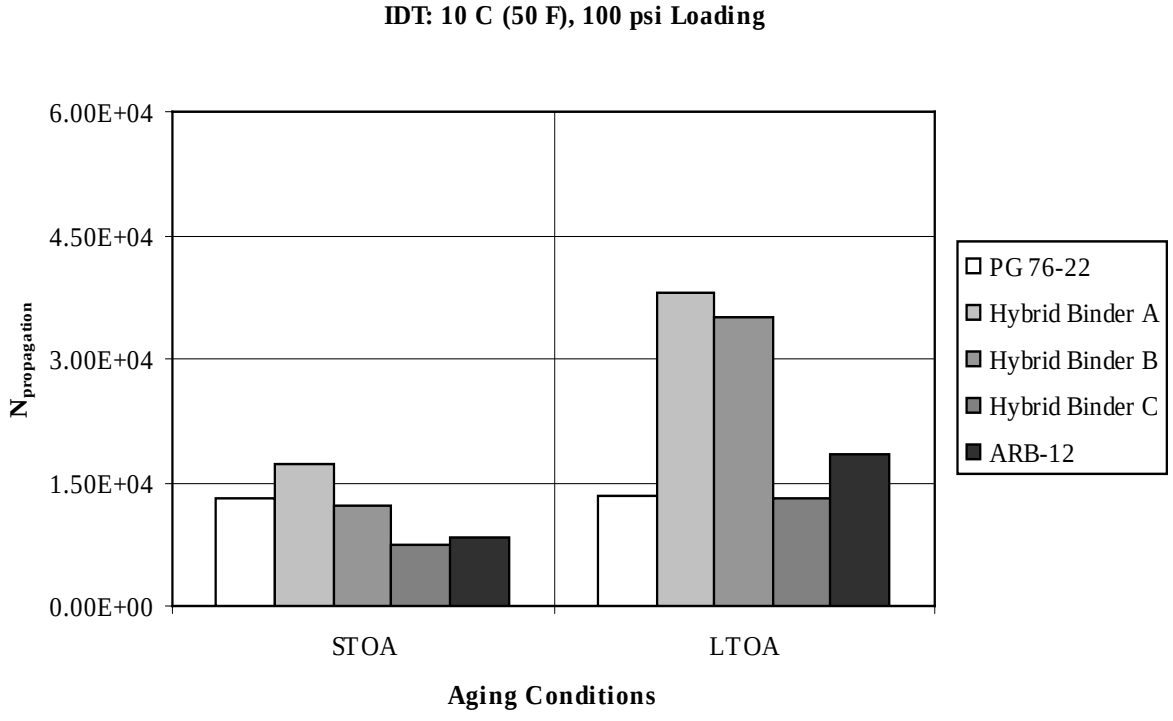

Figure 5-10. $N_{propagation}$ for OGFC limestone mixtures

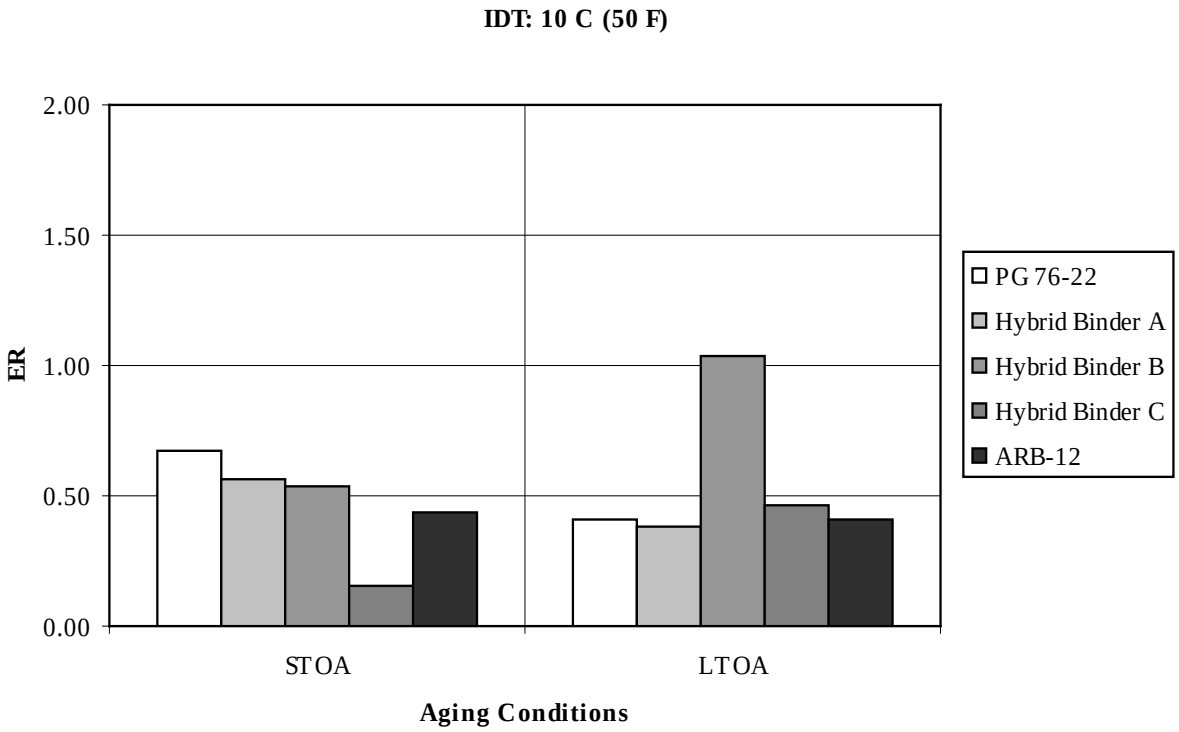

Figure 5-11. ER for OGFC granite mixtures

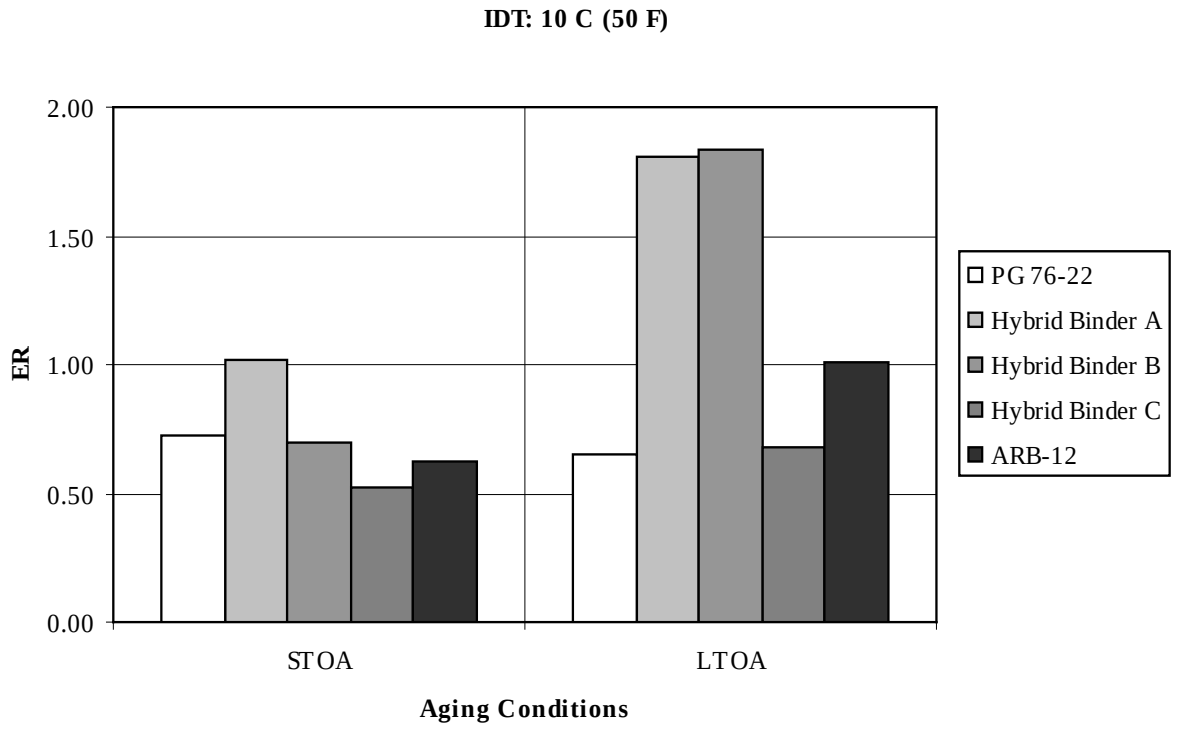

Figure 5-12. ER for OGFC limestone mixtures

response observed in hybrid binder mixtures compared to both unmodified and asphalt rubber modified binders offer the promise of using tire rubber while providing similar performance benefit as polymer modified asphalts.

If STOA and LTOA were considered separately, all three hybrid binders exhibited similar cracking resistance trends for both granite and limestone mixtures. However, the same mixtures showed different cracking performance trends at different aging conditions: the LTOA apparently increased the cracking resistance of hybrid binder mixtures. A larger increase in cracking resistance was observed for limestone mixtures, which could be explained by the fact that limestone has a much rougher surface texture and greater absorption than granite.

In summary, it appears that the hybrid binders evaluated in this study can be used as a substitute for either SBS modified (PG 76-22) or ARB-12 in OGFC mixtures. However, there maybe a need to check the draindown potential of hybrid binder produced with finer rubber when used in smooth textured, non-absorptive aggregate OGFC mixtures.

CHAPTER 6
DEVELOPMENT AND EVALUATION OF HEALING TEST

Experimental and Theoretical Background of Healing Test

As stated in Chapter 2, healing properties of HMA mixtures have been regarded as an important parameter to predict HMA pavement life. This chapter explains about developing IDT programs to evaluate the healing potentials of dense graded granite mixtures with different binder types. The healing test basically comprises of two parts: damage phase and healing phase. Results were analyzed and compared to show how hybrid binders behave differently from control binders (PG 67-22, ARB-5) and SBS modified binders with respect to damage and healing.

Fatigue Test with Static and Cyclic Loading

Typically, there are two different types of loading modes to test fatigue life of IDT specimens, static loading with constant loading rate or displacement rate and cyclic loading with rest period or without rest period. The first loading condition is usually used to obtain the tensile strength of the HMA IDT samples while the second one is to simulate the real traffic loading conditions on the road.

During the standard Superpave IDT strength test, gyratory compressed samples with 7% air voids were loaded at a constant displacement rate. For OGFC samples, the rate is set as 100 mm/min, whereas for DG mixtures, 50 mm/min. The reason for using these loading rates during the strength test is to allow little or no time for stress relaxation or creep to develop prior the specimen failure. This characteristic of static loading mode makes itself impractical for healing, as we know the purpose of healing test is trying to measure how much damage will be recovered after loading is removed from the material. If the static loading were used to evaluate the damage phase, it would

be almost impossible to differentiate delayed elasticity recovery or stress relaxation from damage recovery. Therefore, static loading mode will not be considered to damage the material for healing test.

If cyclic loading mode were decided for the damage phase of healing test, three other aspects need to be considered: loading shape, loading amplitude and rest period. The relationship between static loading and cyclic loading only is discussed, whereas more discussion can be found in the following subchapter,

IDT strength test results, obtained under static loading mode, should be analyzed as a reference to cyclic loading. It is believed that if the HMA specimen subjected to loading less than certain amplitude in a relatively short period (0.1 second, for example), it behaves as an elastic material, which means the stress and strain relationship will be linear. Therefore it is necessary to know in advance in what loading amplitude range the HMA material will behave as an elastic material. A typical horizontal stress-strain curve from IDT strength test for dense graded granite mixture is shown in Fig. 6-1. From Fig. 6-1, it can be seen that the stress-strain relationship could be regarded as linear at the beginning of loading curve (for loading value less than 150 psi). Since the resilient modulus is computed as the tangent of this linear relationship, it can be regarded as a constant parameter during instant loading period (0.1 second). Also loading magnitude which will be used in healing test should be in this linear range (less than 150 psi). Based on this point of view, IDT strength test results for DG mixtures will be used as a reference to decide loading magnitude for the cyclic loading during healing test.

If the IDT sample experienced cyclic loading with certain amplitude, it will deteriorate and fail after a certain number of N cycles and the fatigue life can be

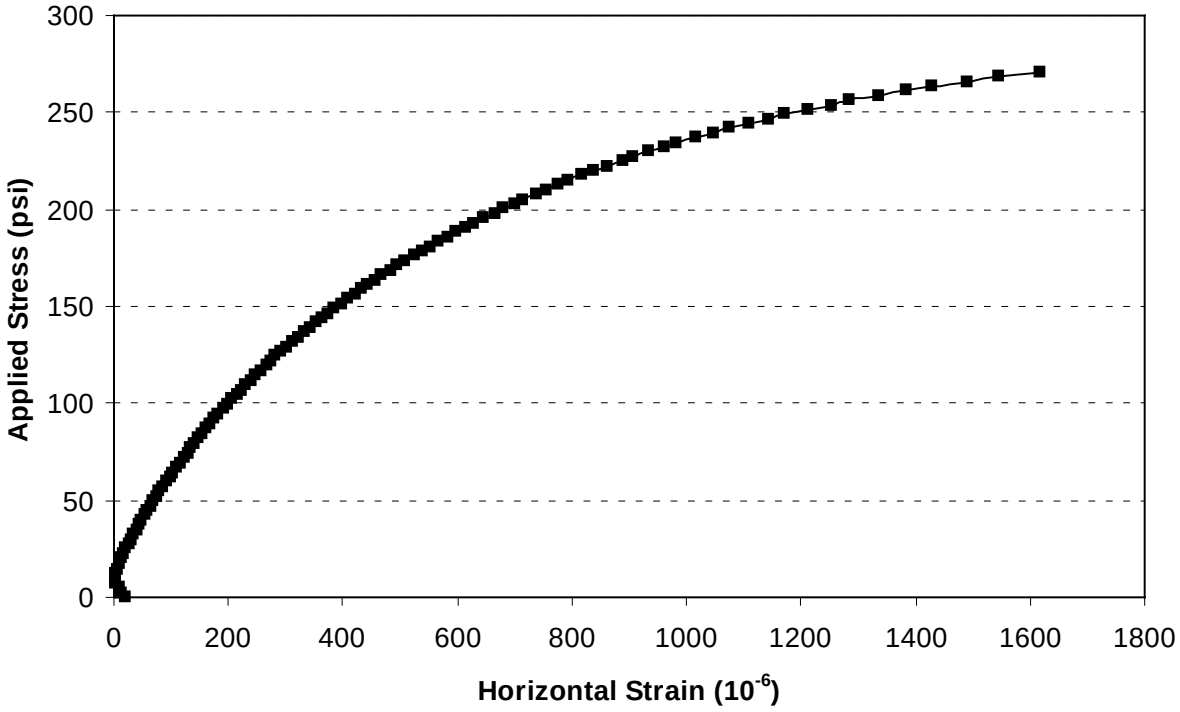

Figure 6-1. Typical strength test result for DG mixtures, STOA, 10 ºC

obtained through the stress and strain curve. The typical loading waves used in IDT test is the haversine wave with 0.1 second loading followed by 0.9 second rest period. However, loading period and rest period may change for different testing purposes, which will be discussed in the following subchapters.

Damage and Healing

In this research, there will be two different ways to describe damages made to HMA materials: dissipated energy and resilient modulus reduction. The dissipated energy can be obtained through work from cyclic loading, whereas modulus reduction needs to be measured through resilient deformation changes. Because for the same material in the same testing environment, resilient deformation is inverse to resilient modulus of the tested HMA material, the fatigue curve could be expressed by $1/M_R$ versus loading cycles as shown in Fig. 6-2. The fatigue process could be divided into

three parts: at the beginning, the mixture experienced microdamage, heating and reversal of steric hardening. After that, the mixture will experience a steady-state damage process, where $1/M_R$ is linear to number of loading cycles. After a certain amount of loading cycles, the rate of DCSE-loading curve rapidly increases with loading cycles, at which point macrocrack occurs.

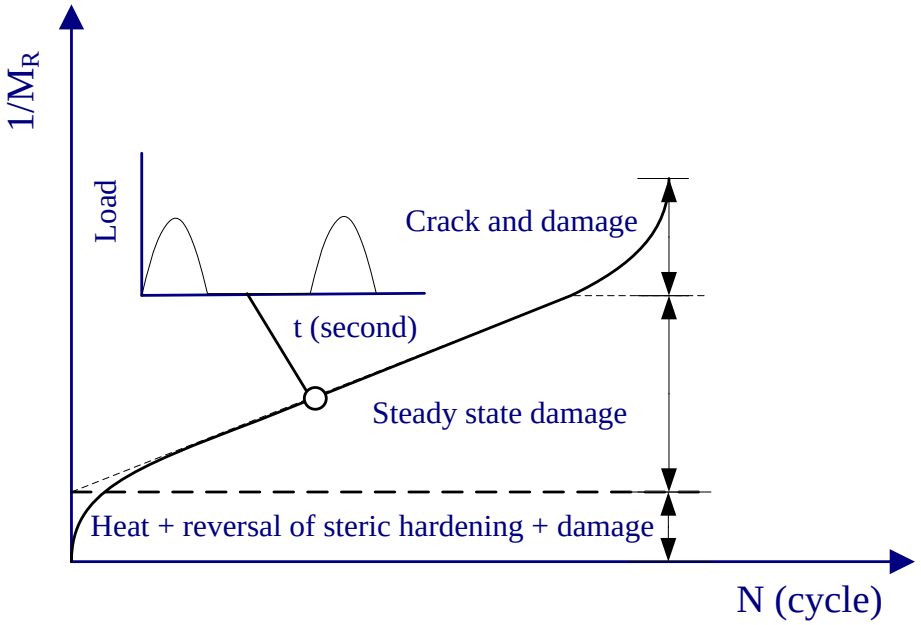

Figure 6-2. HMA material fatigue curve under cyclic loading

As shown in Fig. 6-2, the HMA material will experience a steady state damage period before it cracks under cyclic loading. Once cracks occur in the material, it is no longer considered healable. Therefore, in order to observe healing potentials of HMA materials, the accumulated damage should be controlled in such a manner that it won't cause any macrocracks in the material. If the reduction of resilient modulus is considered as a parameter to describe damage and healing, the total resilient modulus should decrease with loading. As soon as the cyclic loading removed, healing starts in the HMA material.

What is happening to the asphalt mixture after loading was removed is a complicated process: the mixture is not only experiencing healing, but also cooling and long term steric hardening as shown in Fig. 6-3. However, the steric hardening and cooling have such little effects on resilient modulus recovery, they were considered negligible. Therefore, the resilient deformation measured in this healing test will not count in cooling and steric hardening effects. The healing procedure itself also consists of reconstruction of chemical bonds in asphalt and particle flow in microscopic scale (Little et al. 1997). Fig. 6-3 shows the sketch of the damage recovery process.

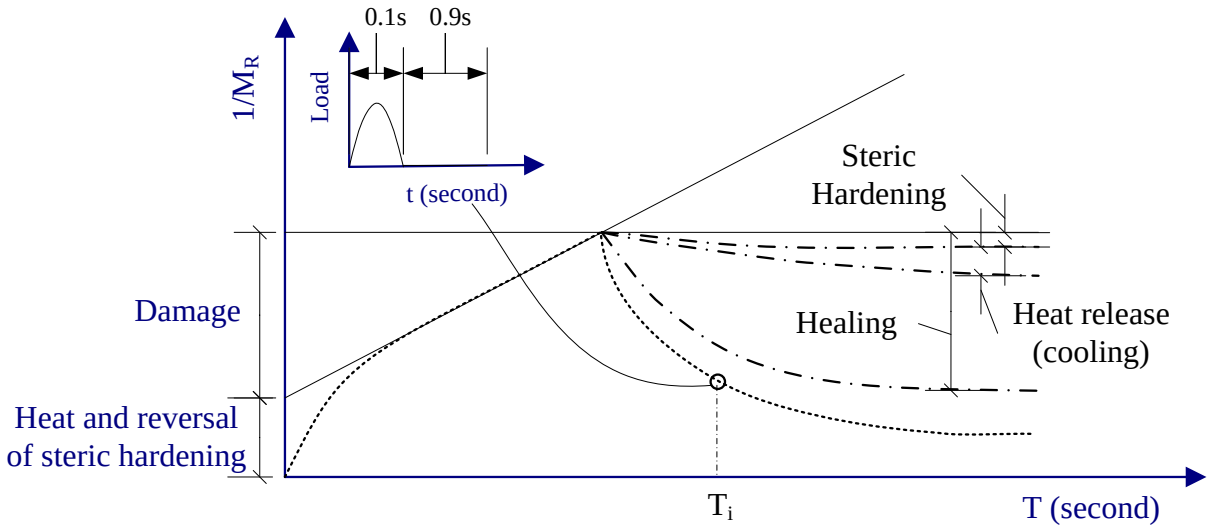

Figure 6-3. Damage recovery curve

Healing Test Development

Cyclic Damage Loading (CDL) Mode

There are three most important elements need to be considered when choosing CDL mode: loading amplitude, shape and rest period. Among these three elements, loading amplitude and shape is directly related to damage applied to the material, whereas rest period determines how much delayed elasticity could be recovered. In this

section, only loading shape and rest periods were discussed, whereas loading amplitude will be discussed in the following section.

Major concerns about loading shapes are maneuverability and side effects. Because of the limitation of available testing equipments, only haversine and square shapes of loading were analyzed.

Compared to haversine loading, it is more difficult to control square loading in MTS machine which applies loading by hydraulic transmission. As we know square loading is applied by adjusting frequencies and amplitude of harmonic loading, it is always hard to minimize the harmonic loading effects at the edge of square loading, which causes work instability to the tested specimen. Another issue need to be addressed about square loading is that upon the command of loading removal from the control program, loading in the MTS machine can not be instantaneously removed, which causes additional damage to the tested specimen and it is almost impossible to measure that. In contrast, haversine wave loading does not have this problem and it is convenient to compute dissipated energy per loading cycle. In addition to the problems stated above,

- Haversine load assures longer rest period for delayed elasticity;
- Square load may need much longer time than haversine load to assure delayed elasticity resumption.

Therefore, haversine wave loading shape was considered for the damage phase during healing test. As long as the loading shape was decided, rest period needs to be studied because various rest periods may cause vast difference in results if not chosen reasonably. The main effects that rest period may cause are summarized in the following:

- Effect on healing
- Delayed elastic recovery

- Effect on measured M_R

Figure 6-4. Haversine loading waves

In order to study how different rest periods affect the material responses to loading, several rest periods: 0.1, 0.2, 0.4 and 0.9 second (Fig. 6-4), following 0.1 second haversine wave loading were tried during damage phase. Since it is believed that healing will occur as soon as loading is removed from the specimen, the major consideration of different rest periods should be minimization of healing during the rest period while allowing delayed elasticity fully recovered. All four tests were applied on the same IDT specimen and the final resilient deformations were normalized for a direct comparison of the results.

The ever first cycle of loading curves obtained during fatigue test was picked and trimmed. Results were plotted in Fig. 6-5. From Fig. 6-5 it can be seen that if the material experienced only 0.1 second rest period, 10.4% of resilient deformation would be missed compared to 0.9 second rest period. This would definitely result in overestimation of resilient modulus of the material. Another effect should be addressed here is that cyclic loading with 0.1 second rest period will lead to large permanent deformation in a relatively short loading time, which will result in an earlier specimen failure. The same problem will happen to loading with 0.2 second rest period as well.

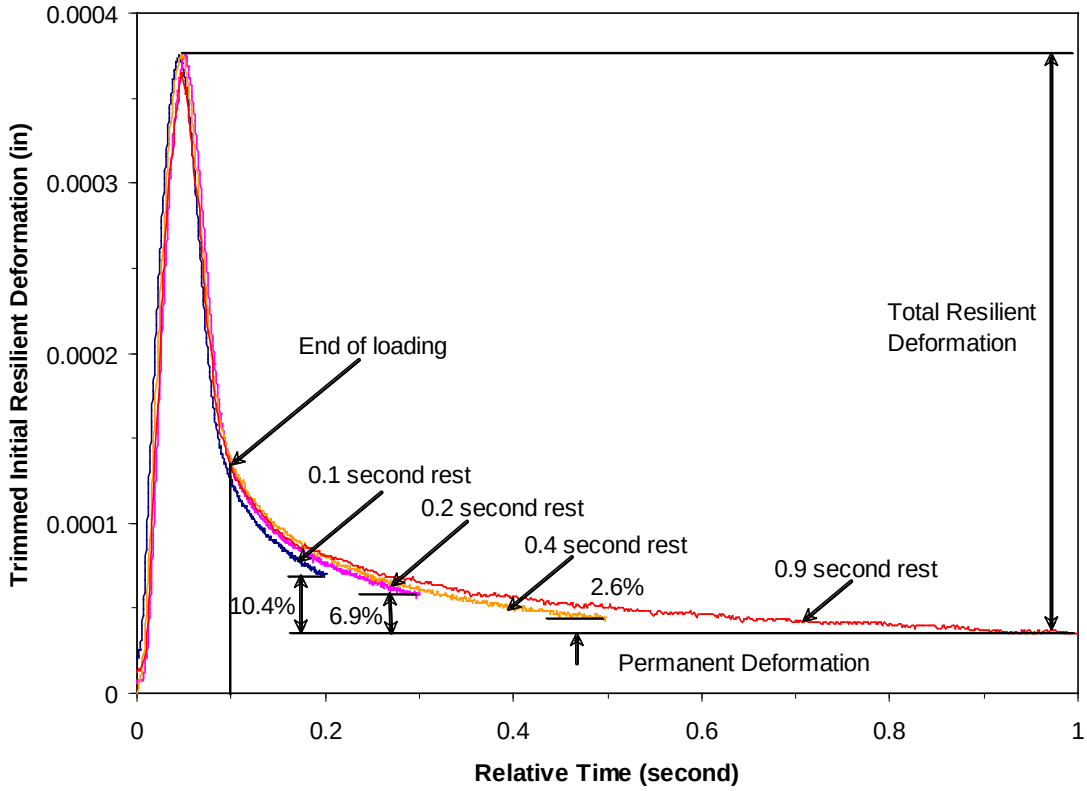

Figure 6-5. Initial resilient deformation with different rest periods, 10 ºC

Further time of loading was performed to evaluate rest period's effects on materials resilient deformation. Fig. 6-6 shows the normalized resilient deformation of the dense graded granite IDT specimen which was loaded with the same loading amplitude of1755 lbs for 0.1 second per cycle, but with different rest periods. From Fig. 6-6 it can be seen that rest period has a significant influence on HMA material resilient deformation changes. Since short term rest period allows less time for delayed elasticity recovery, the tested material deforms in a much faster rate compared to long term rest periods. However, short term rest period shows some advantages that long term rest periods can not compete with: certain amount of damage to the material could be reached at a relatively short time. As shown in Fig. 6-6, 10 minutes loading could result in up to 50% reduction in resilient modulus. The shortage of short term rest period is not

allowing enough time for full delayed elasticity recovery, which is practically difficult to be differentiated from healing at the end of damage phase during healing test. Consequently, it is not convenient to evaluate the healing potentials of the material if short term rest period was applied to cyclic loading.

Moreover, Fig. 6-6 discloses another piece of important information: resilient deformation almost remains the same during the whole damage phase for 0.9 second rest period loading. This result implies that 0.9 second rest period allows enough time not only for delayed elasticity recovery, but also for complete healing in the material. Compared to other short term rest periods, 0.9 second rest is such a long term period that microdamage in the HMA material has been fully healed. A further proof of this conclusion is shown in Fig. 6-7. From Fig. 6-7 it can be seen that even if the loading amplitude has been almost doubled (1100 lbs to 1974 lbs), the reduction in resilient deformation did not show any significant difference. If Fig 6-7 was interpreted by dissipated energy, the DCSE/cycle of loading 1974 lbs is about 4 times of that of loading 1100 lbs. However, Fig. 6-7 shows that all damage has been fully recovered in 0.9 second rest period.

In Fig. 6-6, results from 0.2 and 0.4 second rest period during damage phase have shown that there is an ideal rest period which not only allows enough time for the material to fully recover delayed elasticity, but also limit the time for healing. For 0.2 second rest period loading case in Fig. 6-6, most of the damage occurred during the initial 2 minutes. As it is known that during the initial minutes of damage phase, most of the deformation is due to materials heating and reverse of steric hardening. Apparently the 0.2 second rest period loading curve has shown that most of the damage has

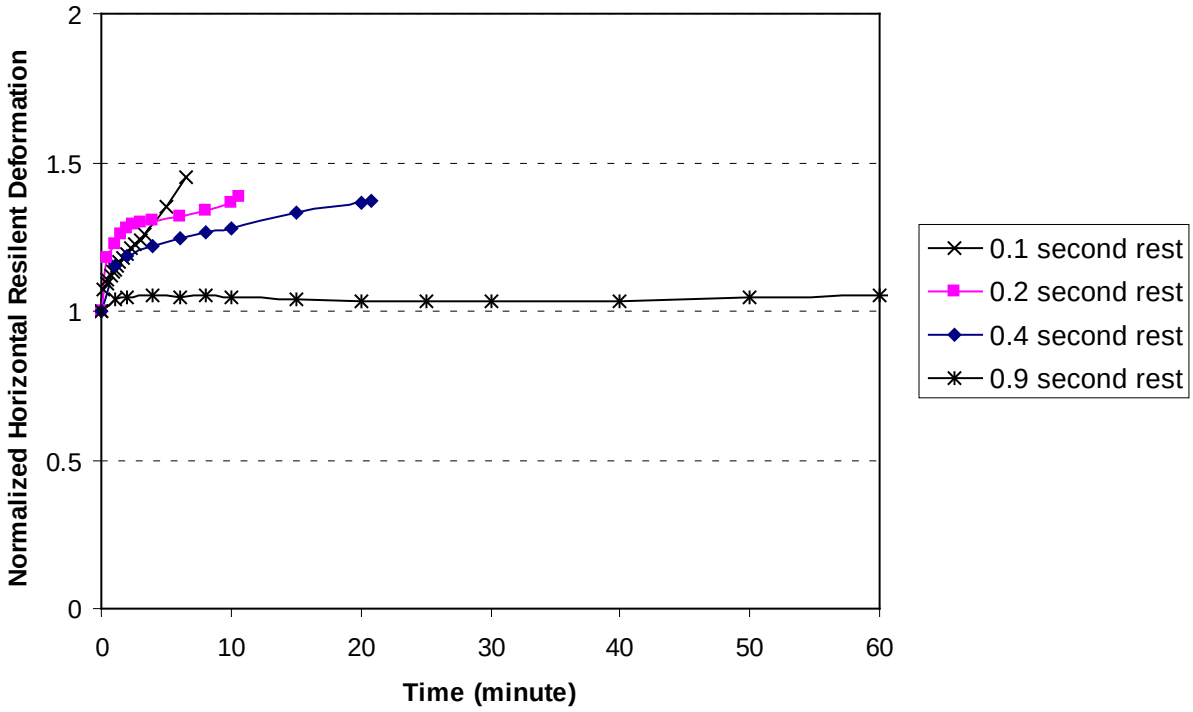

Figure 6-6. Rest period effects on resilient deformation, 1755 lbs, 10 ºC

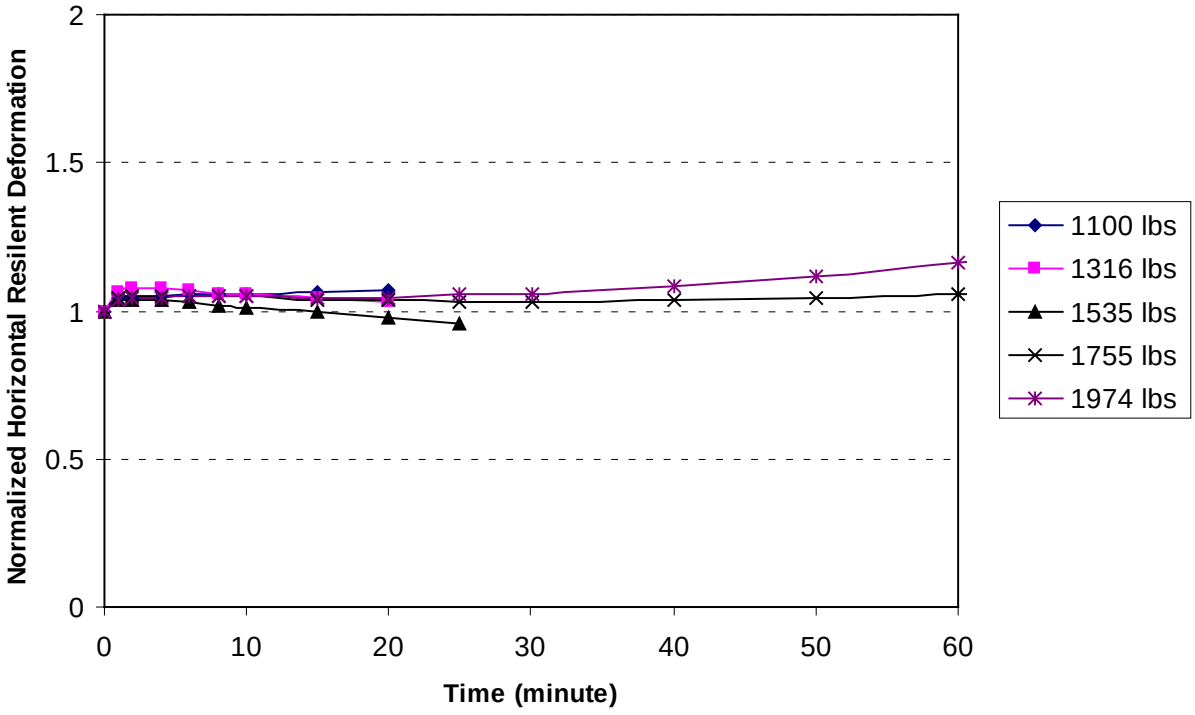

Figure 6-7. CDL test results, 0.9 second rest, 10 ºC

occurred in the beginning minutes, which makes it impossible to separate heat and reverse of steric hardening from damages. However, the 0.4 second rest period loading curve didn't show this problem. The 0.4 second rest period could be considered as a balance between delayed elasticity and damage healing. Therefore, 0.4 second rest period was chosen for the damage phase during healing test.

Loading Amplitude Verification

After the rest period was decided, loading amplitude for CDL needs to be finalized. There are three issues need to be considered for loading amplitude: first, the amplitude should be in such a range that the induced stress is linear to resilient deformations; second, the materials stiffness and ductility effects and third, number of CDL cycles should be in a reasonable testing period.

Although in IDT tensile strength test the HMA specimen was loaded with static loading mode, results presented a clear relationship between loading stress and horizontal resilient deformation for STOA dense graded mixtures. As shown in Fig. 6-8, at the beginning of loading (load amplitude less than 2000 lbs), the applied force could be regarded as linear to horizontal deformation. This would be true especially when the material undergoes 0.1 second quick loading. The linear relationship guarantees that if material is loaded within this range, the error of resultant resilient modulus calculated through stress-strain relationship can be negligible. And this is true for all dense graded granite mixtures with all types of binders.

Another problem with loading more than 2000 lbs is that it causes more temperature changes and reversal of steric hardening at the beginning of damage phase. Also because of the IDT specimen dimension, high level loading can cause stress concentration at the loading edge, which results in bulging problems at an early

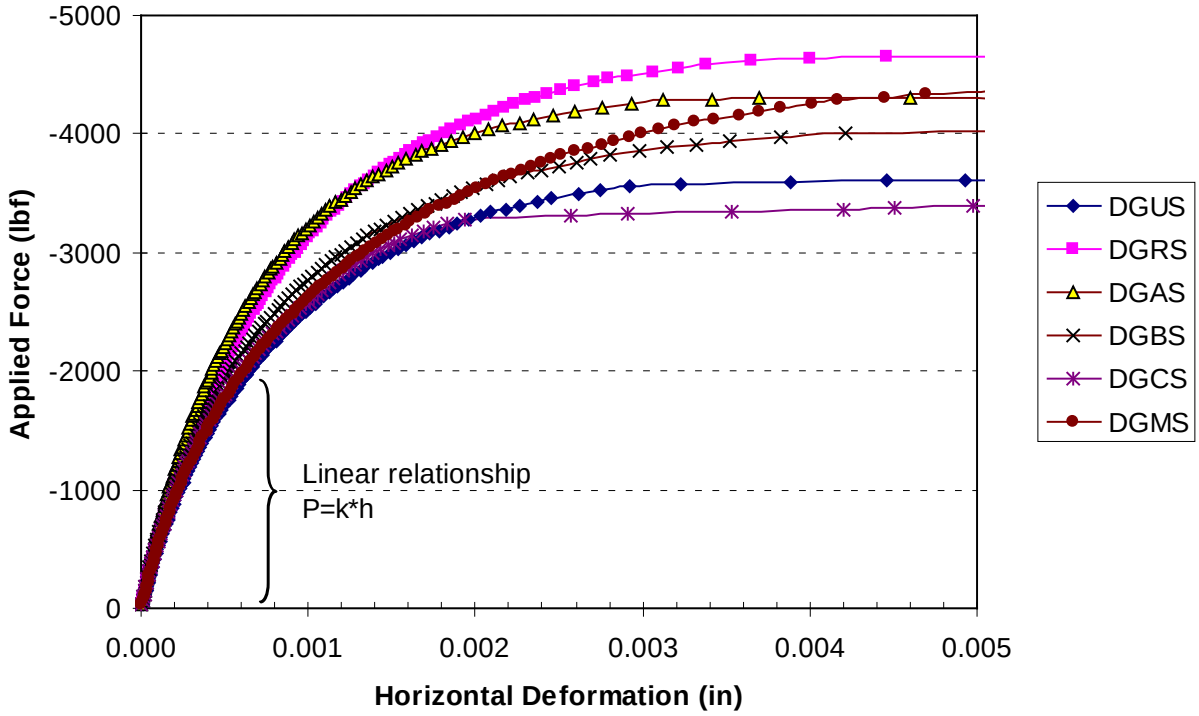

Figure 6-8. DG mixtures IDT strength test, 10 ºC

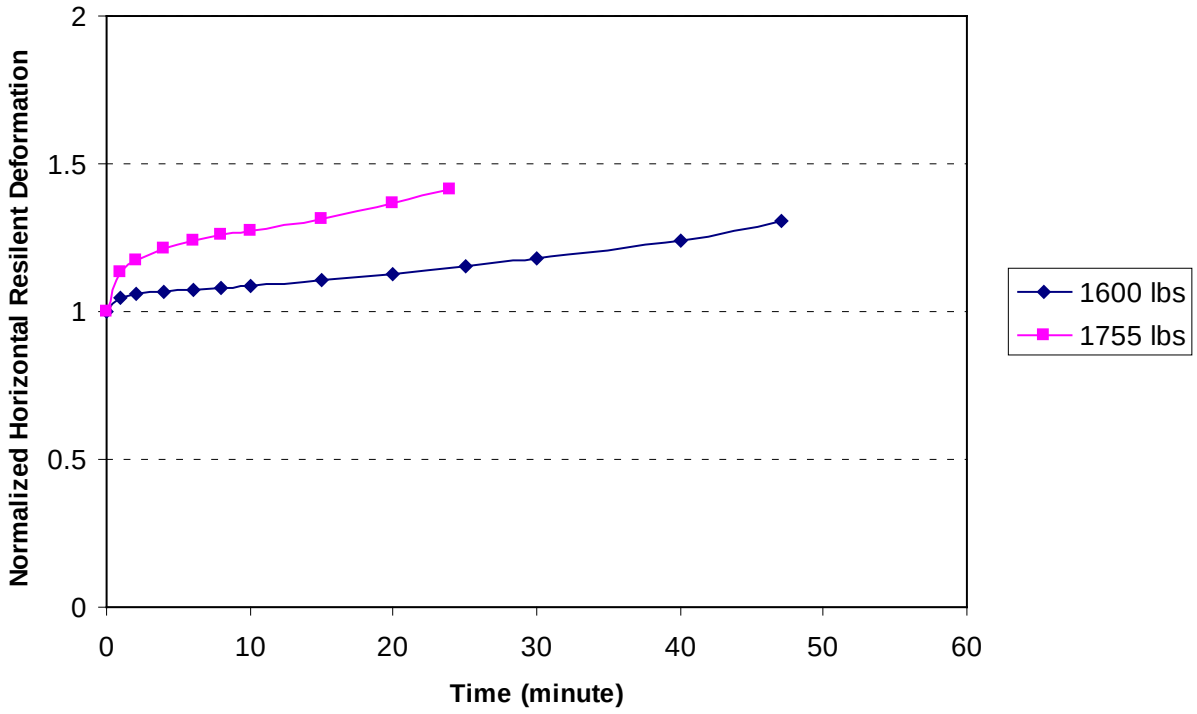

Figure 6-9. DGUS cyclic loading test results, 0.4 second rest, 10 ºC

loading stage. Ultimately, the specimen fails at the loading edge rather than at the center of the specimen. In contrast, if the loading amplitude is too low, the temperature changes and steric hardening may not be problems any more, but it would cost too much time to finish the test, which is not desirable for this research (Fig. 6-9).

Two criteria were chosen to terminate CDL for the healing test: percentage of $DCSE_f$ (50%) (Fig. 6-10) or reduction in resilient modulus (30% reduction), which means if either of these two criteria is reached, the damage phase will be stopped and loading removed. Both of these two criteria were monitored during CDL in such a manner that the accumulated microdamage in the specimen would not lead to macrodamage which is considered not healable.

The loading amplitude also affects the amount of dissipated creep strain energy done to the specimen per loading cycle.

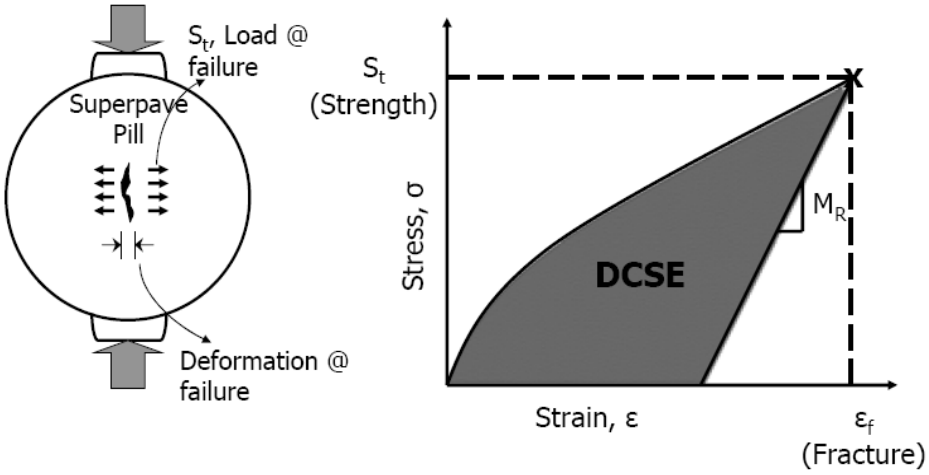

Figure 6-10. DCSE obtained from tensile strength test

The $DCSE_f$ could be obtained from regular IDT test and DCSE/cycle can be expressed as:

$$\frac{DCSE}{cycles} = \int_0^{0.1} \sigma_{AVE} \sin(10\pi t)\, \dot{\varepsilon}_{pMAX} \sin(10\pi t)\, dt$$

$$= \int_0^{0.1} \sigma^2{}_{AVE}\, \dot{D}(t) \sin^2(10\pi t)\, dt$$

$$= \sigma^2{}_{AVE}\, \dot{D}(t) \int_0^{0.1} \sin^2(10\pi t)\, dt$$

$$= \frac{1}{20} \sigma^2_{AVE} D_1 m 1000^{m-1}$$

Where D_1 and m are creep parameters and can be obtained from IDT creep test. Therefore if the stress is known, cycles needed for obtaining some percentage of $DCSE_f$ can be calculated by $cycles = \frac{\%DCSE_f}{DCSE/cycle}$.

The HMA material properties, especially stiffness and ductility play an important role in CDL amplitude decision. If the mixture is very brittle at given testing temperature, the strain at failure will be lower than less brittle materials, although the 50% of $DCSE_f$ criterion may has not been reached after a certain cycles of loading. In this case, observation of reduction in resilient modulus of mixture is very important. 10-20%

Table 6-1. Failure criteria for fatigue test

Mixture Stiffness	FE and/or $\dot{\varepsilon}_{cr}$	Reduction in M_R
Brittle	Low	10-20%
↕	Medium	50%
Ductile	High	>50%

reduction in modulus can be a substitute of 50% of $DCSE_f$ criterion. Reversely, if the resilient modulus of the mixture is very low, which means the material is ductile, more than 50% reduction in modulus may be obtained when the 50% of $DCSE_f$ criterion is

reached. A brief summary of the fatigue loading criteria to materials with different properties is listed in Table 6-1.

Healing Test Program

A program chart for running healing test was summarized in Fig. 6-11. From this chart it can be seen that before running healing test, some basic information need to be obtained from IDT test, such as resilient modulus, tensile strength, $DCSE_f$, etc. Of the IDT test results, the tensile strength is of importance because it would be referred as to decide the loading amplitude for fatigue test. Also the failure strain and fracture energy will be referred as well to estimate starting loading amplitude and cycles to end the fatigue test.

This test continues until it is manually stopped. This allows the user to test a specimen for a certain amount of time. On screen, a constantly updated graph of the deformations shows the user the current state of the gyratory specimen and a rough estimate of when macrocrack propagation begins.

Data Acquisition

The data acquisition is similar to that used for the M_R test, but different in some specific program steps. The healing test requires achieving enough microdamage in the mixture in a reasonable period (ideally about 2 hours for both loading and unloading process.

The data acquisition system was divided into two parts: damage phase and healing phase. There are some minor differences between data acquisition systems in these two phases. For the damage phase, loading amplitude is around 1800 lbs and loading frequency is 2 Hz. In order to record readings from strain gages as much

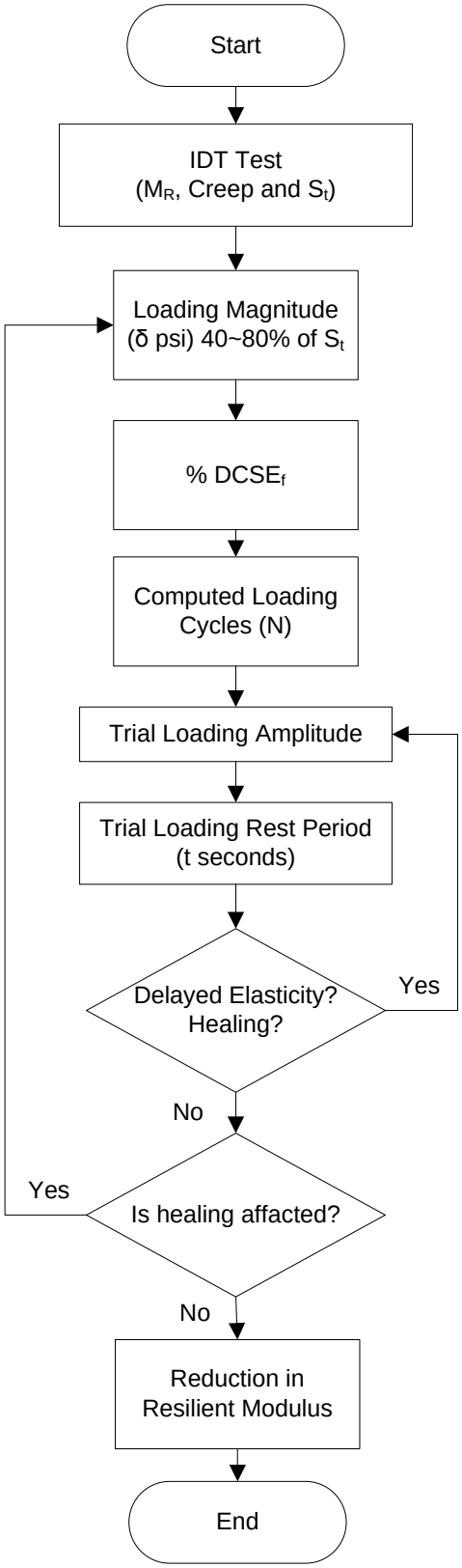

Figure 6-11. Healing test flow chart

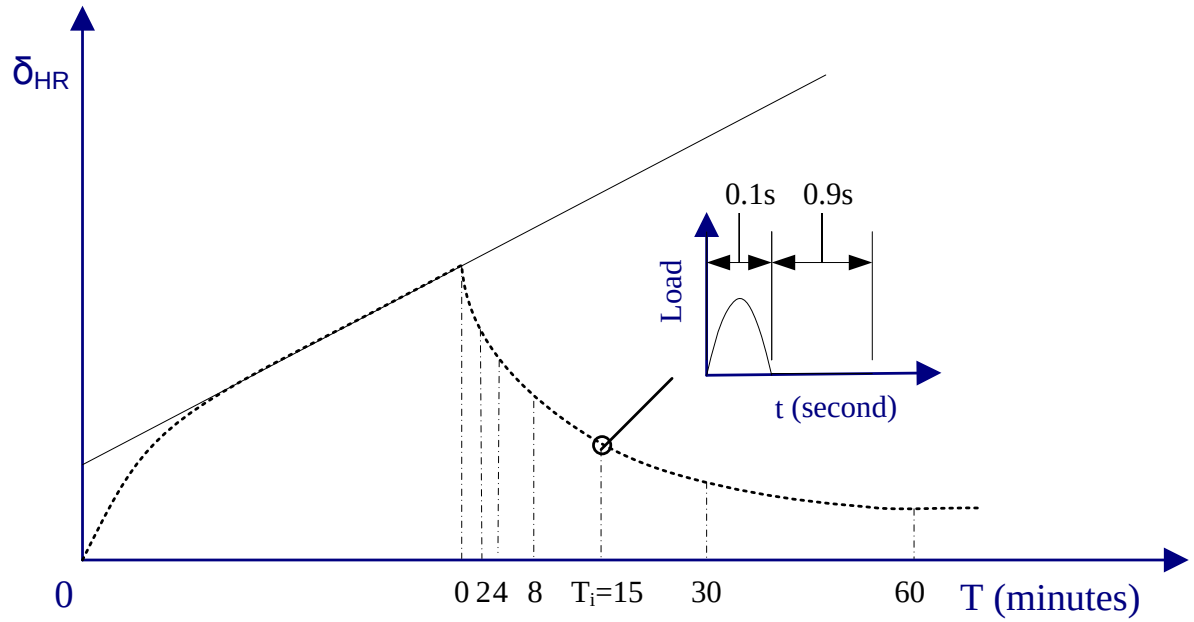

Figure 6-12. Data acquisition during healing phase

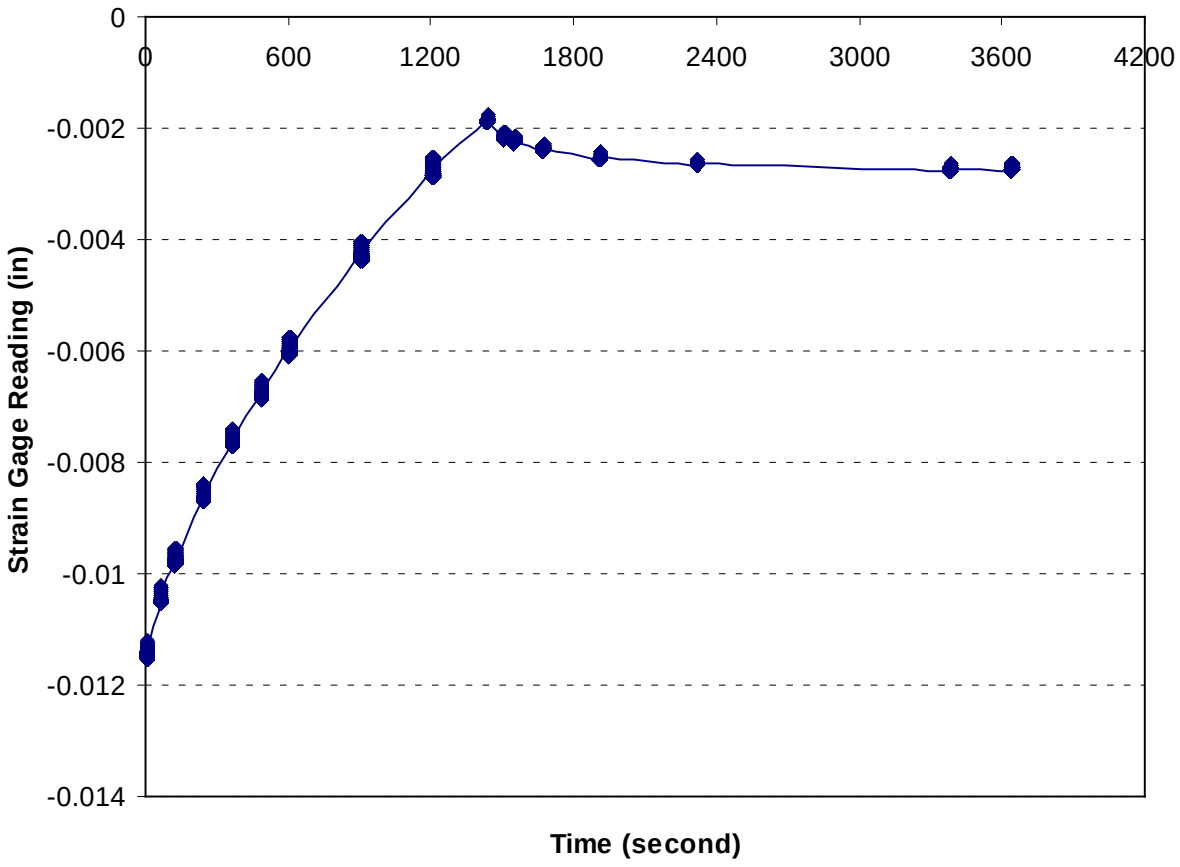

Figure 6-13. Data collection illustration

accurate as possible within the capability of computer ram, 512 sets of reading per loading cycle were saved. However, it would be redundant and unnecessary to record every single loading cycle. So the program was set to pick up to 5 cycles of data each time it was commanded to do so. These times were set as 0.1, 2, 4, 6, 8, 10, 15, 20, 25, 30, 40 minutes…… until the damage phase was manually terminated. If the required damage was observed on the program during the damage phase loading process, the operator needs to press a button manually to record the last set of data and immediately after the program finish recording the loading was removed and healing phase started.

During the healing process, the user manually controlled the data collection at the interval times (0.1, 2, 4, 8, 15, 30 and 60 minutes) (Fig. 6-12). This denser data acquisition frequency at the beginning is because based on trial healing test results, up to 80% of the healing will happen at the first several minutes of loading removal. Every time the data collection button was pushed during the test, the program takes an M_R reading over five cycles of loading at an arbitrary time. When the test was terminated, the testing and seating loads were removed from the test specimen. Fig. 6-13 shows a data acquisition sample from dense graded mixture healing test.

Materials Prepared for Healing Test

Georgia granite aggregates were prepared and batched. The batching formula, binder content and other volumetric properties could be found in chapter 3. The mixtures were gyratory compacted to 7% air voids and then processed with STOA. After the pills cooled down, they were cut to IDT specimens with about 1.5 in thickness. A summary of number of samples and tests is shown in Table. 6-8. All healing tests will be done at 10ºC in the MTS temperature controlled chamber after specimens were dehumidified up to 8 hours.

Table 6-2. Materials for healing test

Mixture Type	Aggregate Type	Conditions	Number of Binders	Number of Pills	No. of Tests/Specimen
Superpave Dense	Granite	STOA	6	12	18

Healing Test Results Analysis

Healing test results will be analyzed through damage phase and healing phase separately. For each phase, recorded data will be trimmed and interpreted via resilient modulus. After that, resilient modulus will be normalized and compared to evaluate dense graded granite mixtures damage and healing potentials. Dissipated creep strain energy will also be included in the final analysis.

Damage Analysis during CDL

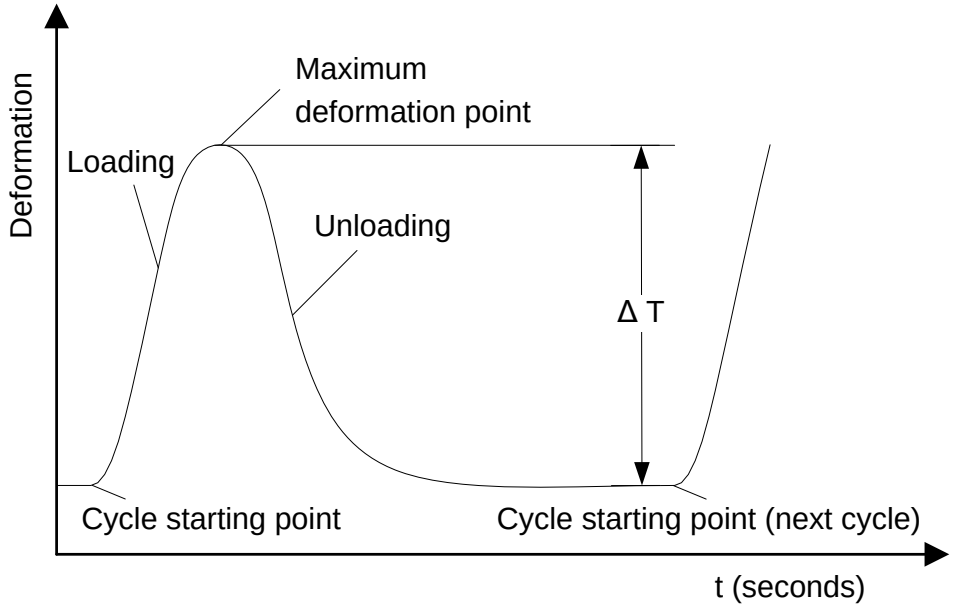

Figure 6-14. Resilient deformation

Fig. 6-14 shows an illustration of resilient deformation for one loading cycle. The resilient modulus calculation is based on the formula below:

$$M_r = \frac{\sigma_r}{\varepsilon_r}$$

Roque and Buttlar (1994, 1997) developed IDT data analysis program, of which resilient modulus calculation program was applied here to compute resilient modulus of the material during both damage and healing phases. The final equation is described below and more details could be found from Roque (1997) “Evaluation of SHRP indirect tension tester to mitigate cracking in asphalt concrete pavements and overlays” (page 108-128):

$$M_{RT\,i} = \frac{GL * P_{AVG}}{\Delta H_{TTRIM\,i} * D_{AVG} * t_{AVG} * C_{CPMLT}}$$

Where:

$M_{RT\,i}$: total resilient modulus of each cycle (i = 1~3, the number of cycle)

GL: gage length

P_{AVG}: average peak load of three replicate specimens

$\Delta H_{TTRIM\,i}$: total trimmed mean horizontal deformation array of each cycle (i = 1~3, the number of cycle)

D_{AVG}: average diameter of three replicate specimens

t_{AVG}: average thickness of three replicate specimens

C_{CPMLT}: non-dimensional factor, Roque (1994)

And

$$M_{RT} = \frac{\Sigma M_{RT\,i}}{i}$$

Another important parameter for calculating resilient modulus is the poisson's ratio:

$$v_{Ti} = -0.100 + 1.480\left(\frac{\Delta H_{TTRIM\,i}}{\Delta V_{TTRIM\,i}}\right)^2 - 0.778\left(\frac{t_{AVG}}{D_{AVG}}\right)^2\left(\frac{\Delta H_{TTRIM\,i}}{\Delta V_{TTRIM\,i}}\right)^2$$

The variables in this equation refer to the same meaning as those in resilient modulus equation.

The poisson's ratios calculated from CDL results and IDT results for all tested dense graded granite mixtures are summarized and plotted in Table 6-3 and Fig. 6-15 separately, which shows a good consistency between these two tests.

Table 6-3. Poisson's ratio comparison

Mixtures	DGUS	DGMS	DGRS	DGAS	DGBS	DGCS
CDL	0.35	0.30	0.33	0.25	0.32	0.42
IDT strength test	0.37	0.31	0.35	0.27	0.32	0.44

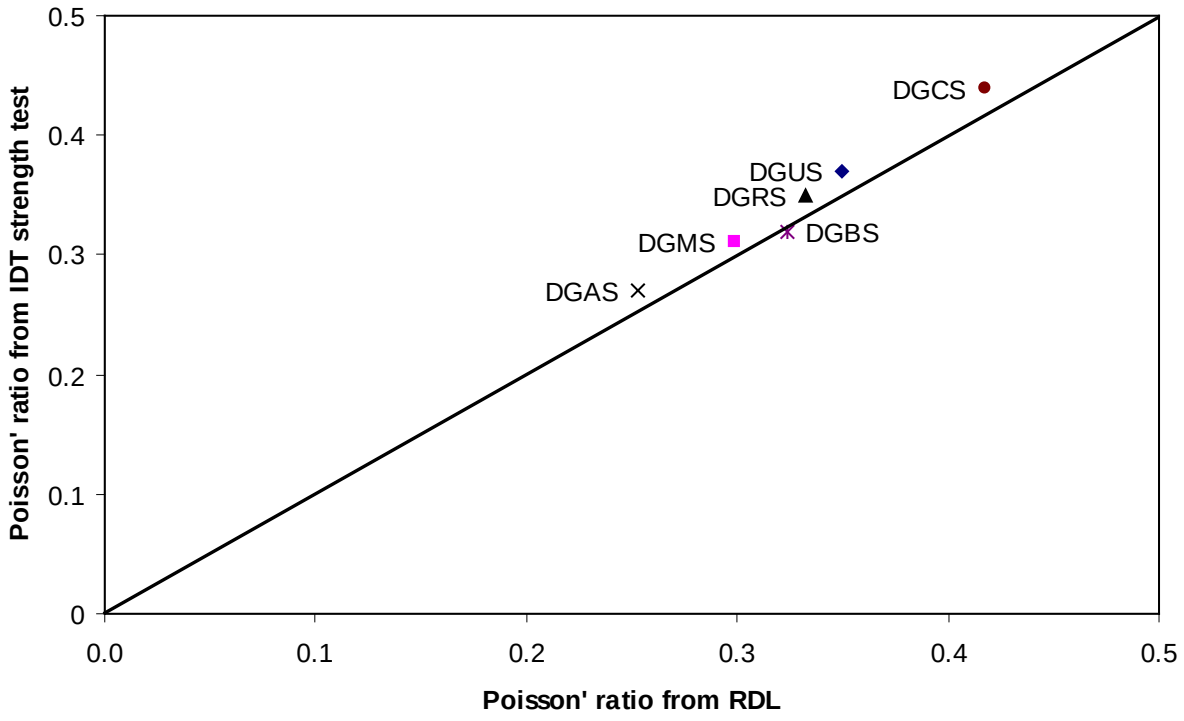

Figure 6-15. Poisson's ratio comparison, 10 ºC

The determination of original resilient modulus of HMA materials form healing test is different from that obtained through IDT resilient modulus test. As of IDT specimens, thanks to the existence of air voids, HMA material's thermal properties and cyclic loading effects, the material will first experience reversal of steric hardening and heat transformed from loading work, as shown in Fig. 6-16. This work induced a jump reduction in the resilient modulus as shown at the beginning of damage phase in Fig. 6-16. After that, the material's resilient modulus exhibited a linear relationship with loading cycles. If this linear relationship was fitted by regression line, the interception of this line and the Y-axis will be the original resilient modulus of the material, which is E_{R0} in Fig. 6-16. A summary of original resilient modulus of the materials from IDT and healing test is shown in Table 6-4 and Fig. 6-17. Although the healing test results underestimated the resilient modulus compared to IDT strength test results, it would not affect the damage and healing rates analysis in the following.

Fig. 6-16 also shows the sketch how damage will affect the materials and how the materials recover from damage. During the damage phase, damage is presented by resilient modulus reduction and the rate of this reduction will be compared for mixtures with different binders. Typically the damage phase takes around 30 minutes to have a nearly 12% reduction in resilient modulus: $\frac{E_{R0} - E_{Rd}}{E_{R0}} \times 100\%$. The damage healing phase will also be described by resilient modulus and the results will be shown in next subchapter. After that, DCSE will be analyzed associated with resilient modulus.

Plotting of resilient modulus changes with loading time were summarized in appendix B. In order to have a direct comparison of the CDL damage effects on

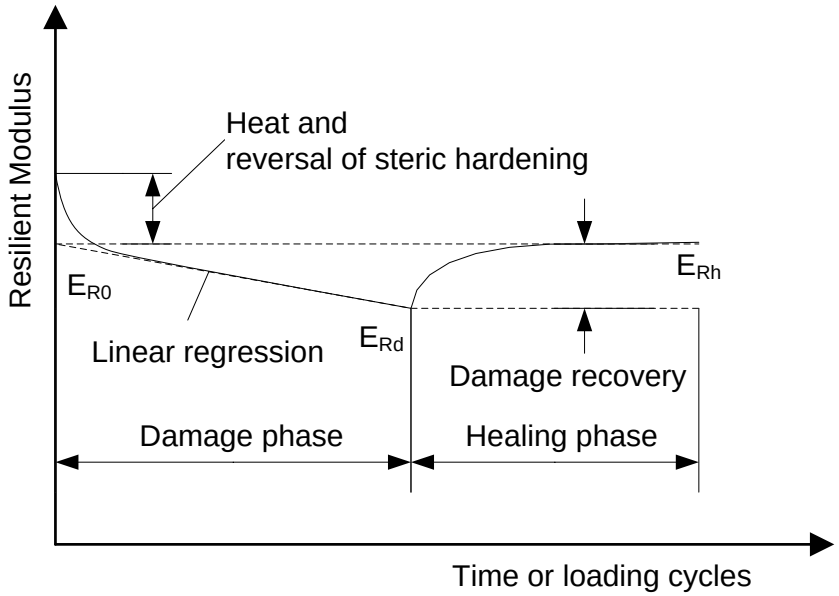

Figure 6-16. Damage and healing interpretation with resilient modulus

mixtures with different binders, the resilient modulus was normalized to original resilient modulus and the results were plotted in Fig. 6-17. Regression was made on the linear parts of these normalized curves and the resultant fitting equations and R square-values were also shown in the figure. Damage rate was defined as percentage of original resilient modulus reduction per minute. The meaning of this parameter to the surface mixtures in the field is related to how fast cracks can be initiated. Damage rates in Fig. 6-17 show that mixtures with different binders exhibit different responses to damages. Apparently mixtures with control binder PG 67-22 appears the worst case: material deteriorates at the fastest rate under CDL, which reflects that the surface dense graded granite mixtures designed with control binder will exhibit cracks at an earlier stage compared to the same mixtures designed with other binders under the same traffic load. There are no apparent differences among mixtures with PG 76-22, hybrid binder B and C, which means some hybrid binders can perform as well as polymer modified binder PG 76-22 with respect to resistance to RDL damage.

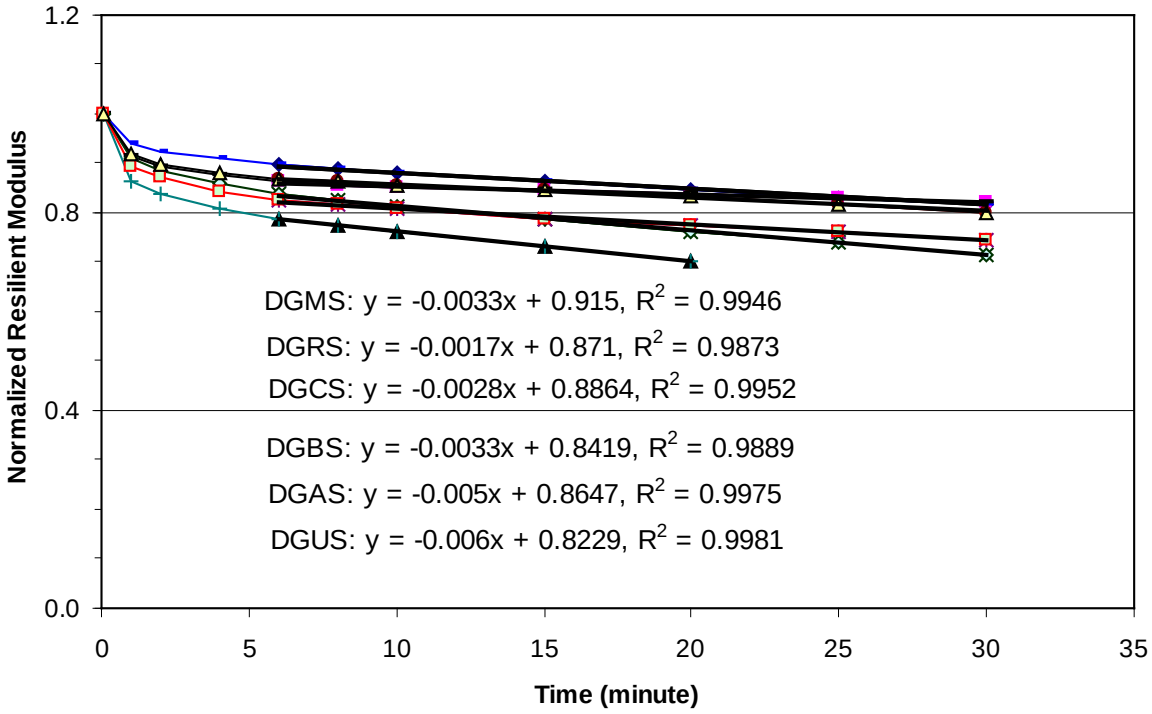

Figure 6-17. DG mixtures normalized resilient modulus at damage phase

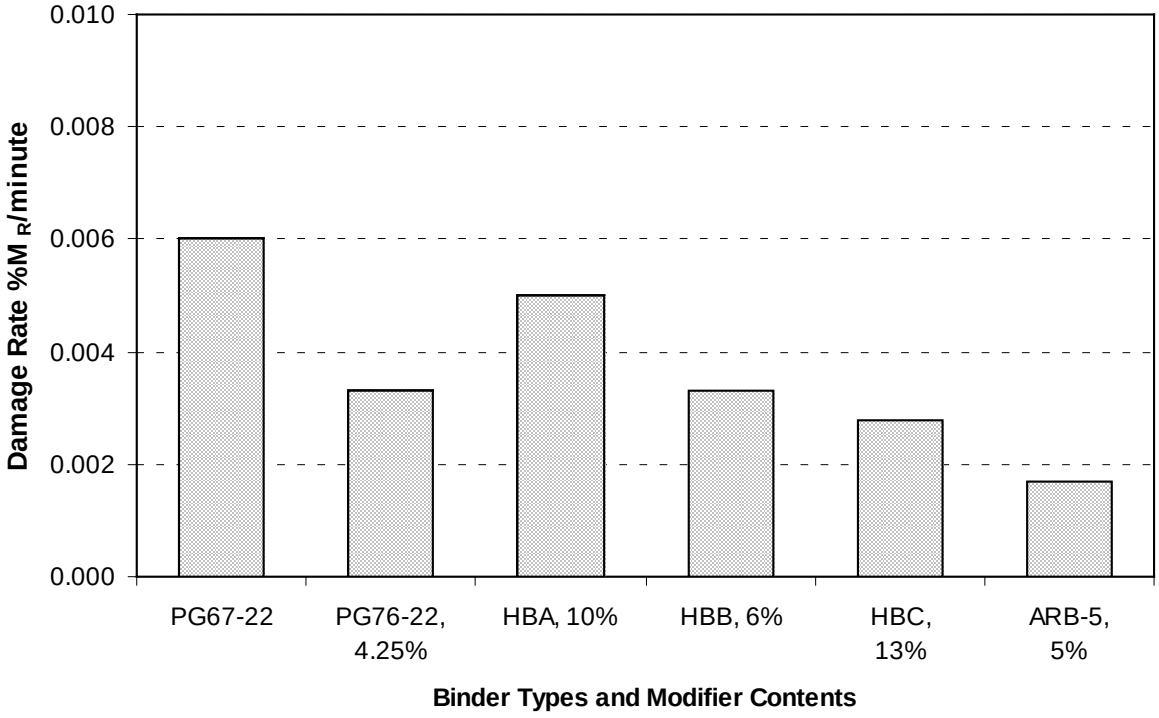

Figure 6-18. Relationship between modifier contents and damage rate

Furthermore, damage rates are plotted with modifiers content in binders in order to check whether there is a relationship between these two parameters. As shown in Fig. 6-19, modifiers (no matter it is CRM or SBS polymers) do decrease damage rate applied to dense graded granite mixtures (STOA). However, whether the CRM or SBS polymer was leading a major role in this case can not be told from this figure.

Healing Analysis of DG Mixtures

The analysis of dense graded granite mixtures' healing performance is similar to that of mixtures' damage performance. One of the few differences is that the modulus in healing phase was normalized to the modulus at the beginning of healing, which is E_{Rd} shown in Fig. 6-16. E_{Rh} is the resilient modulus at the end of healing phase.

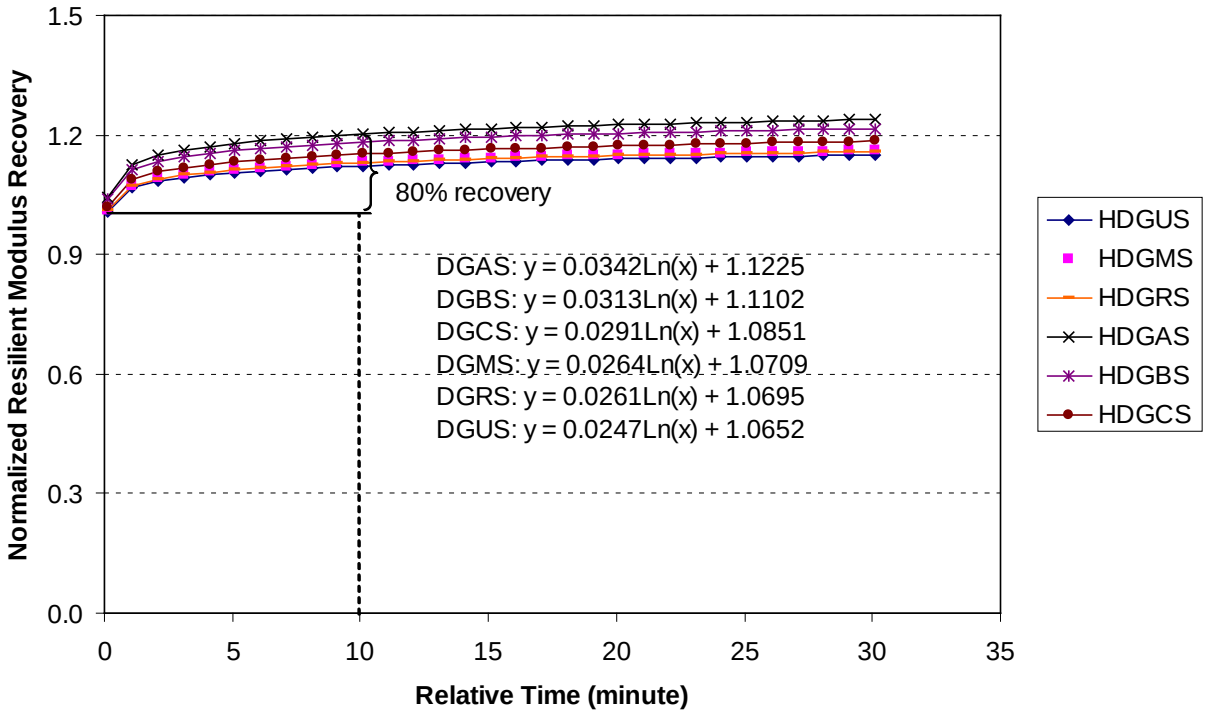

Figure 6-19. Combined regression for healing test

Fig. 6-19 shows the trimmed normalized resilient modulus recovery during the healing phase. From this figure it can be seen that there is no much difference with

respect to healing rates for dense graded mixtures with different binders, no matter the binder was modified or not. An important point should be addressed is that all mixtures recovered 80% of the resilient modulus in 10 minutes after the CDL was removed. This property is independent of damages accumulated from CDL. This figure appears that binders will not significantly affect mixtures healing performance.

A further study was conducted on the relationship between healing rates and damage (DCSE and resilient modulus reduction separately) accumulated at the end of damage phase.

The $DCSE_{applied}/DCSE_f$ is the ratio of the dissipated creep strain energy to the total dissipated creep strain energy at failure during CDL. The calculation of $DCSE_{applied}$ is shown in the following equation:

$$DCSE_{applied} = \frac{1}{20}\sigma_{AVE}^2 D_1 m 1000^{m-1} \times cycles$$

Where:

σ_{AVE}: applied stress

D_1, m: parameters from power model

Parameters D_1, m, and $DCSE_f$ can be obtained from IDT test.

Fig. 6-20 shows that the amount of accumulated DCSE (at 20 minutes loading) in dense graded granite mixtures does not apparently affect healing rates. In Fig. 6-20, the DCSE accumulated in DGRS and DGUS at the end of damage phase almost doubles that of mixtures with other binders, but the healing rates for DGRS and DGUS do not vary much accordingly. This implies that healing rates are independent of accumulated DCSE during damage phase. But if compared with the same accumulated DCSE,

DGAS, followed by DGBS and DGCS, apparently recovers faster than mixture with PG 76-22. We have to notice that although the healing rates are different for mixtures with different binders, more than 80% of damage will be healed in around 10 minutes, which seems to minimize the effects from healing rates.

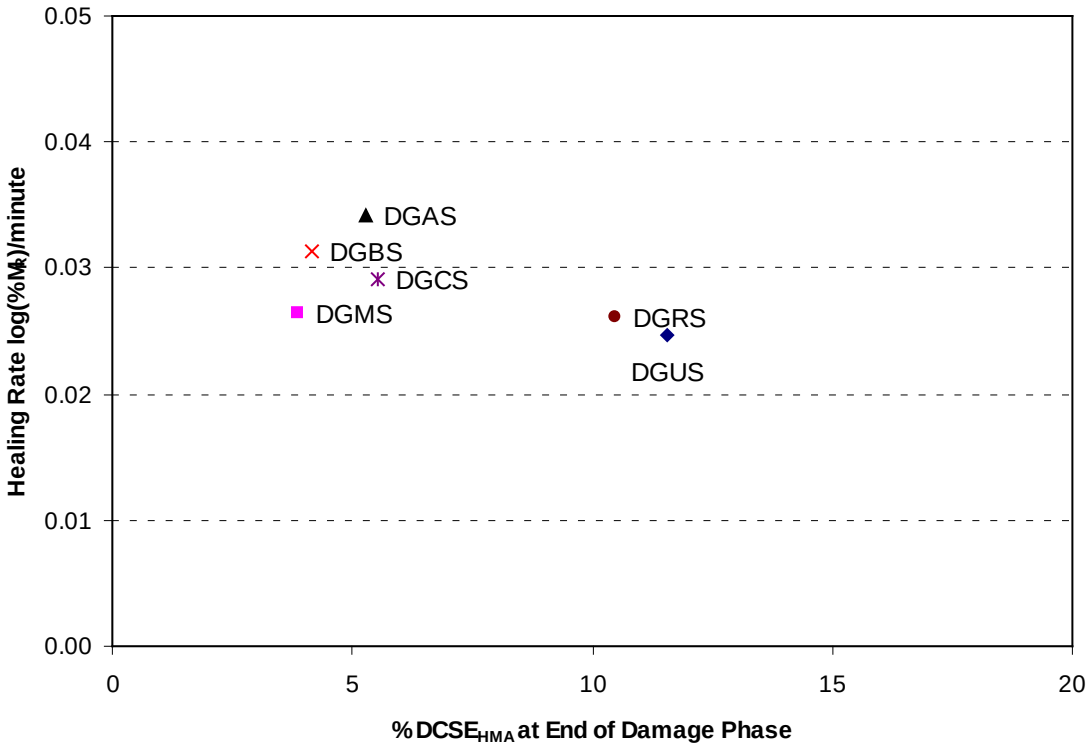

Figure 6-20. Damage (DCSE) and healing rate comparison

Fig. 6-21 shows the relationship between accumulated resilient modulus reduction (at 20 minutes loading) and healing rates for DG mixtures. The approximate trend curves seem to imply that DG mixtures with modified binders heal faster than control binder mixtures. However, the conclusion from this figure needs to be verified with more data at both lower or higher damage zones.

The relationship between accumulated DCSE and reduction in resilient modulus is shown in Table 6-11 and plotted in Fig. 6-22. From Fig. 6-22, it can be seen that mixture

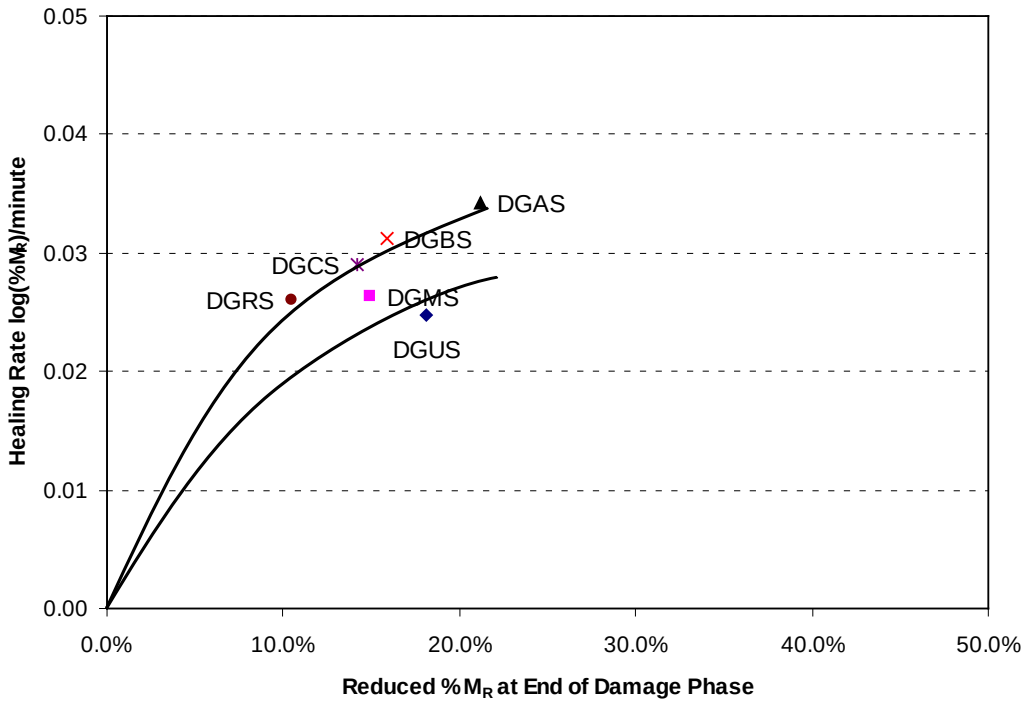

Figure 6-21. Damage (resilient modulus reduction) and healing rate comparison

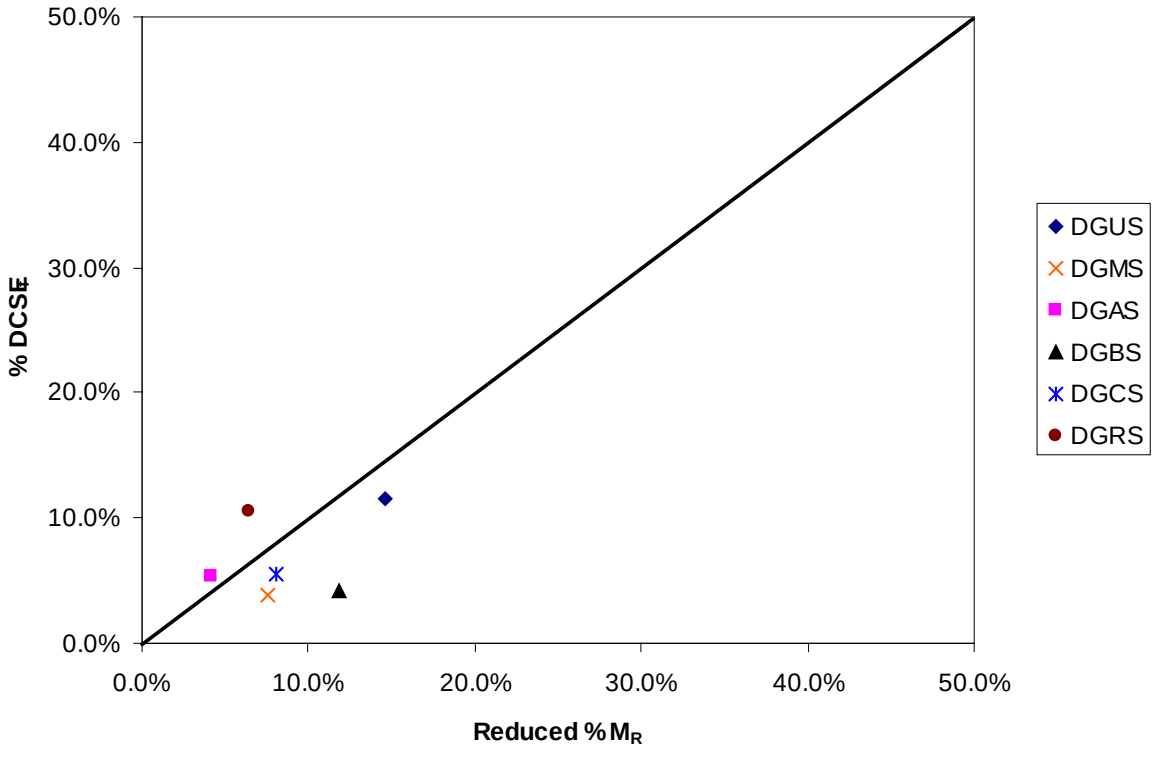

Figure 6-22. Reduced resilient modulus vs reduced DCSE, 20 minutes loading

points below the midline will exhibit more reduction in resilient modulus with less dissipated creep strain energy absorption compared to mixtures above the midline. However, except for DGBS, dense graded granite mixtures appear to have a liner relationship between $DCSE_{applied}$ and reduction in resilient modulus.

Table 6-4. Comparison of DCSE and MR reduction at 20 minutes CDL

Mixutures	% $DCSE_{HMA}$	Reduction % M_{RI}
DGUS	11.56	14.55
DGMS	3.86	7.59
DGAS	5.30	4.11
DGBS	4.17	11.78
DGCS	5.55	8.05
DGRS	10.48	6.45

Summary

In general, HMA mixtures damage and healing performance can be evaluated through their resilient modulus changes. Cyclic damage loading mode provides not only a convenient way to interpret damages through resilient modulus, but also allows delayed elasticity recovery, which removes difficulty of differentiating delayed elasticity and permanent deformation. Furthermore, CDL makes it easier to control dissipated creep strain energy by monitoring loading cycles.

Considered damage phase during healing test, the damage rate showed that dense graded mixtures with hybrid binders after STOA exhibited similar behavior with SBS polymer modified binders (PG76-22). All mixtures with modified binders presented better performances compared to unmodified base binder (PG 67-22). The modified binders apparently slower down damages to dense graded granite mixtures.

If considered from healing phase during healing test, binder types turned out no effects on healing performances of dense graded granite mixtures. Most of all, 80% of

damages will be recovered in about 10 minutes in this healing test, which minimized the importance of healing rates.

In a word, modified binders, especially SBS modified and hybrid binders will definitely decrease damage rates and performs better than unmodified binders in dense graded granite mixtures. Healing rates could not differentiate binder components effects on healing potentials of dense graded granite mixtures after STOA.

CHAPTER 7
CLOSURE AND RECOMMENDATIONS

Summary

Binder and mixture tests were performed to evaluate the relative performance of a PG 67-22 base binder and six other binders produced by modifying the same base binder with the following modifiers: one SBS polymer, three commercially available hybrid binders composed of different percentages of rubber and SBS polymer, and two asphalt rubber binders (5% and 12 % rubber: ARB-5 and ARB-12). The primary goal was to evaluate whether commercially available hybrid binder could exceed the performance characteristics of the base and asphalt rubber binders, as well as approach, meet or exceed the performance characteristics of the SBS polymer modified binder. Secondary goals were to determine whether available binder tests and characterization methods are suitable for specifying hybrid binder. Key findings from the study are summarized below:

- Mixture tests indicated that cracking performance characteristics of dense-graded mixtures (granite and limestone) produced with the commercially available hybrid binders used in this study exceeded the cracking performance characteristics of mixtures produced with the base binder and the ARB-5 binder, and were about the same as the cracking performance characteristics of the SBS polymer modified binder.
- Results of tests on open-graded friction course (OGFC) mixtures (granite and limestone) indicated that except for one special case (granite OGFC mixture with hybrid binder C), the commercially available hybrid binders used in this study exhibited cracking performance characteristics that were about the same as those exhibited by mixtures produced with SBS polymer modified binder and ARB-12. It was concluded that hybrid binder C, which included the finer grained rubber, may not have maintained appropriate consistency to achieve and maintain uniform distribution within the smoother textured and less absorptive granite OGFC during mixing and compaction. The resulting non-uniformity is the most probable cause of the anomalous result (lower cracking performance characteristics). Addition of fibers or mixing and compaction at lower temperatures would likely have resulted in better distribution and cracking performance characteristics.

- The two hybrid binders produced with coarser grained rubber (hybrid binders A and B), as well as the two asphalt rubber binders (ARB-5 and ARB-12) did not meet FDOT's solubility specification, indicating that the rubber may not have been fully digested in the base binder. Consequently, test results on these binders determined from the dynamic shear rheometer (DSR), including G*/sinδ, G*sinδ, and parameters derived from the newly proposed MSCR test, were considered suspect, because the presence of particulates in the binder is well known to affect DSR results. The binders produced with the coarser grained rubber met, and in most cases far exceeded requirements for PG76-22 binder, resulting in binder performance parameters that indicated better performance characteristics than all other binders evaluated, including the SBS polymer modified binder. These results were not consistent with relative cracking performance characteristics determined from mixture tests.

- Hybrid binders A and B were also found to result in significantly lower absorption than all other binders in OGFC mixtures. This indicated that the combination of coarser rubber particles and polymer affected absorption into the aggregate. Differences in absorption were taken into account when determining the effective asphalt content, which was the same for all binder-mixture combinations.

- Hybrid binder C, which was produced with finer grained rubber, did meet FDOT's solubility specification, indicating that the rubber was fully digested in the base binder, thereby making it suitable for DSR testing. This binder also met all requirements for PG76-22 binder with the exception of maximum phase angle (an additional FDOT requirement).

- None of the existing or currently proposed intermediate temperature binder tests, including DSR (G*sinδ), Elastic Recovery (ER), and Force-Ductility (FD) were found to provide parameters that consistently correlated with the relative cracking performance of mixtures.

- Parameters obtained from the new multiple stress creep recovery (MSCR) test and from Elastic Recovery (ER) distinguished the SBS polymer modified binder, but not hybrid binder C, from the base binder. Therefore, it appears questionable whether either of these tests is suitable in their present form to specify hybrid binder.

- Only the elongation at failure from either the ER or FD tests was able to clearly distinguish the observed relative cracking performance of the SBS polymer modified and hybrid binders from that of the asphalt rubber binders. The asphalt rubber binders were more brittle (less elongation to failure) than the SBS and hybrid binders.

- Considered damage phase during healing test, the damage rate showed that dense graded mixtures with hybrid binders after STOA exhibited similar behavior with SBS polymer modified binders (PG76-22). All mixtures with modified binders presented better performances compared to unmodified base binder (PG 67-22).

The modified binders apparently slower down damages to dense graded granite mixtures.

- If considered from healing phase during healing test, binder types turned out no effects on healing performances of dense graded granite mixtures. Most of all, 80% of damages will be recovered in about 10 minutes in this healing test, which minimized the importance of healing rates.

Conclusions

The following conclusions may be drawn on the basis of the research findings:

Hybrid binders produced commercially, consisting of crumb rubber and SBS polymer (more rubber than SBS), can approach, meet or exceed the cracking performance characteristics of the SBS polymer modified binder.

Although all the hybrid binders in this study did not meet all the Superpave binder tests, it appears that hybrid binder can be suitably specified using existing specification requirements for PG76-22 binder and solubility (to distinguish it from asphalt rubber binder and to assure the validity of DSR test results).

Hybrid binder specified in this manner has the potential to replace three binders currently used by FDOT in hot mix asphalt: SBS polymer modified asphalt, ARB-5, and ARB-12. This would result in the following benefits:

- Continued and probably increased use of tire rubber in asphalt.
- The ground tire rubber will not settle out like asphalt rubber binders.
- Eliminate a method recipe specification asphalt rubber for performance related hybrid binder.
- Simplify storage of binders at the hot mix plant by replacing three currently used asphalt binders.
- Improved cracking, and probably rutting, resistance of dense-graded friction courses (FC9.5 and FC12.5)

Recommendations

As indicated above, hybrid binder specified in a proper manner, has the potential to replace three binders currently used by FDOT in hot mix asphalt: SBS polymer modified asphalt, ARB-5, and ARB-12. It also appears that a benefit may be derived by taking this course of action (i.e. eventually specifying hybrid binder exclusively for use in FDOT hot mix asphalt). Therefore, it is recommended that FDOT develop a transition plan to accomplish this. This should involve an assessment of impact and cost, development of a draft specification and strategy for implementation. Consideration should be given to first allowing the use of hybrid binder as an alternate binder, then eventually requiring its use.

Hybrid Binders have never been used on an actual project in Florida. The implementation process should include a number of demonstration projects where the hybrid binder is specifically specified in addition to the polymer modified binder for the project. The asphalt suppliers' timeline to supply hybrid binder to Florida will have to be taken into account, and suppliers will need to know the level of Florida's commitment to this product before making the necessary investments.

Finally, it is recommended that FDOT pursue development and evaluation of the new binder direct tension test configuration for eventual use in performance based specification of hybrid binder, particularly since not even the newest MSCR test was successful in identifying its benefits.

Further healing test is also recommended to find aging effects on healing characteristics on both dense graded and open graded mixtures. Resilient modulus is a good parameter to interpret damage and healing performance of HMA mixtures, but

further relationship of resilient modulus and dissipated creep strain energy needs to be verified and analyzed.

APPENDIX A
BINDER TEST RESULTS

Table A-1. G*/sinδ and δ at 67 ºC (152.6 F)

Binders	Original binders		RTFOT residue	
	G*/sinδ (kPa)	δ (°)	G*/sinδ (kPa)	δ (°)
PG 67-22	1.65	84.05	3.95	78.55
PG 76-22	n/a	n/a	n/a	n/a
HB A	n/a	n/a	n/a	n/a
HB B	n/a	n/a	n/a	n/a
HB C	n/a	n/a	n/a	n/a
ARB-5	3.36	76.60	n/a	n/a
ARB-12	5.98	75.40	n/a	n/a

Table A-2. G*/sinδ and δ at 70 ºC (158 F)

Binders	Original binders		RTFOT residue	
	G*/sinδ (kPa)	δ (°)	G*/sinδ (kPa)	δ (°)
PG 67-22	1.14	84.80	2.73	79.80
PG 76-22	n/a	n/a	n/a	n/a
HB A	n/a	n/a	n/a	n/a
HB B	n/a	n/a	n/a	n/a
HB C	n/a	n/a	n/a	n/a
ARB-5	2.40	78.40	6.14	67.55
ARB-12	4.46	77.05	12.27	59.35

Table A-3. G*/sinδ and δ at 76 ºC (168.8 F)

Binders	Original binders		RTFOT residue	
	G*/sinδ (kPa)	δ (°)	G*/sinδ (kPa)	δ (°)
PG 67-22	0.59	86.60	1.39	82.30
PG 76-22	1.52	71.95	3.19	65.80
HB A	3.03	71.65	5.83	65.45
HB B	2.25	75.90	4.28	69.10
HB C	1.15	82.55	2.83	77.20
ARB-5	1.34	81.15	3.52	70.60
ARB-12	2.30	80.65	6.91	63.00

Table A-4. G*/sinδ and δ at 82 ºC (179.6 F)

Binders	Original binders		RTFOT residue	
	G*/sinδ (kPa)	δ (°)	G*/sinδ (kPa)	δ (°)
PG 67-22	n/a	n/a	n/a	n/a
PG 76-22	0.91	74.25	1.88	68.15
HB A	1.70	74.95	3.34	68.60
HB B	1.26	79.25	2.44	72.40

Table A-4. Continued

Binders	Original binders		RTFOT residue	
	G*/sinδ (kPa)	δ (^{o})	G*/sinδ (kPa)	δ (^{o})
HB C	0.64	83.55	1.49	80.20
RB-12	1.27	82.90	4.10	66.40

Table A-5. G*/sinδ and δ at 88 ºC (190.4 F)

Binders	Original binders		RTFOT residue	
	G*/sinδ (kPa)	δ (^{o})	G*/sinδ (kPa)	δ (^{o})
PG 67-22	n/a	n/a	n/a	n/a
PG 76-22	n/a	n/a	n/a	n/a
HB A	1.03	77.30	1.99	70.90
HB B	0.77	81.60	1.39	76.10
HB C	n/a	n/a	n/a	n/a
ARB-5	n/a	n/a	n/a	n/a
ARB-12	1.27	84.85	4.10	70.60

Table A-6. G*/sinδ and δ at 90 ºC (194 F)

Binders	Original binders		RTFOT residue	
	G*/sinδ (kPa)	δ (^{o})	G*/sinδ (kPa)	δ (^{o})
PG 67-22	n/a	n/a	n/a	n/a
PG 76-22	n/a	n/a	n/a	n/a
HB A	0.86	78.20	n/a	n/a
HB B	n/a	n/a	n/a	n/a
HB C	n/a	n/a	n/a	n/a
ARB-5	n/a	n/a	n/a	n/a
ARB-12	n/a	n/a	n/a	n/a

Table A-7. G*sinδ and δ at 25 ºC (77 F)

Binders	100^{o}C PAV residue		110^{o}C PAV residue	
	G*sinδ (kPa)	δ (^{o})	G*sinδ (kPa)	δ (^{o})
PG 67-22	3255.5	49.8	4508.0	44.3
PG 76-22	3192.0	48.2	3633.0	44.0
HB A	2969.0	43.5	3626.5	38.9
HB B	2828.5	45.3	3372.0	40.8
HB C	3693.0	46.3	4692.5	42.1
ARB-5	2770.5	46.6	3750.0	41.8
ARB-12	2139.5	44.9	2604.5	40.5

Table A-8. G*sinδ and δ at 22 ºC (71.6 F)

Binders	100^{o}C PAV residue		110^{o}C PAV residue	
	G*sinδ (kPa)	δ (^{o})	G*sinδ (kPa)	δ (^{o})

Table A-8 Continued

PG 67-22	4901.5	46.9	6446.0	41.7
PG 76-22	4812.5	46.0	5238.0	41.8
HB A	4193.5	41.2	4976.5	36.8
HB B	4122.5	42.9	4749.0	38.8
HB C	5475.5	43.8	6655.5	39.7
ARB-5	4074.0	44.1	5226.5	39.7
ARB-12	3047.5	42.8	3566.5	38.7

Table A-9. G*sinδ and δ at 19 ºC (66.2 F)

Binders	100°C PAV residue		110°C PAV residue	
	G*sinδ (kPa)	δ (°)	G*sinδ (kPa)	δ (°)
PG 67-22	7053.0	44.2	n/a	n/a
PG 76-22	6962.0	43.2	n/a	n/a
HB A	5921.0	38.9	6705.0	34.8
HB B	5877.0	40.7	6542.0	36.8
HB C	n/a	n/a	n/a	n/a
ARB-5	5946.0	41.6	n/a	n/a
ARB-12	4246.5	40.6	4868.0	37.0

Table A-10. G*sinδ and δ at 16 ºC (60.8 F)

Binders	100°C PAV residue		110°C PAV residue	
	G*sinδ (kPa)	δ (°)	G*sinδ (kPa)	δ (°)
PG 67-22	n/a	n/a	n/a	n/a
PG 76-22	n/a	n/a	n/a	n/a
HB A	n/a	n/a	n/a	n/a
HB B	n/a	n/a	n/a	n/a
HB C	n/a	n/a	n/a	n/a
ARB-5	n/a	n/a	n/a	n/a
ARB-12	5867.5	35.1	6459.5	34.9

Table A-11. BBR test results at -12 ºC (10.4 F)

Binders	100°C PAV residue creep stiffness, S (MPa)	m-value	110°C PAV residue creep stiffness, S (MPa)	m-value
PG 67-22	159.5	0.365	182.5	0.339
PG 76-22	144.0	0.362	170.0	0.334
HB A	137.5	0.322	154.5	0.301
HB B	147.0	0.336	155.5	0.318
HB C	166.5	0.337	185.0	0.315
ARB-5	138.0	0.345	155.5	0.318
ARB-12	109.0	0.337	127.5	0.316

Table A-12. BBR test results at -18 ºC (0.4 F)

Binders	100°C PAV residue creep stiffness, S (MPa)	m-value	110°C PAV residue creep stiffness, S (MPa)	m-value
PG 67-22	341.5	0.291	400.5	0.276
PG 76-22	331.0	0.295	356.5	0.279
HB A	298.0	0.262	313.5	0.252
HB B	303.0	0.279	303.5	0.269
HB C	358.5	0.274	373.5	0.265
ARB-5	281.0	0.287	302.0	0.270
ARB-12	231.0	0.288	241.5	0.274

Table A-13. Multiple stress creep recovery, %, RTFOT residue

Binders	67 ºC (152.6 F)			76 ºC (168.8 F)		
	3.2 kPa	0.1 kPa	Rdiff	3.2 kPa	0.1 kPa	Rdiff
PG 67-22	3.73	13.27	71.88	0.68	6.16	88.93
PG 76-22	64.25	71.79	10.50	31.87	54.24	41.25
HB A	51.11	67.38	24.14	23.08	53.05	56.46
HB B	40.52	54.15	25.15	16.85	38.75	56.58
HB C	13.13	27.23	51.71	3.05	13.84	78.01
ARB-5	25.03	46.02	45.61	6.81	32.27	78.86
ARB-12	56.64	74.97	24.52	20.30	58.37	65.21

Table A-14. Non-recoverable creep compliance, kPa^{-1}, RTFOT residue

	67 ºC (152.6 F)			76 ºC (168.8 F)		
Binders	$J_{nr}3.2$	$J_{nr}0.1$	Diff. %	$J_{nr}3.2$	$J_{nr}0.1$	Diff. %
PG 67-22	2.06	1.66	24.51	7.05	5.65	24.84
PG 76-22	0.24	0.19	29.30	1.34	0.81	65.54
HB A	0.21	0.13	63.20	1.02	0.51	103.42
HB B	0.34	0.25	36.17	1.51	0.92	63.76
HB C	0.78	0.61	28.85	3.02	2.25	34.46
ARB-5	0.58	0.38	0.53	2.42	1.35	0.7919
ARB-12	0.15	0.08	0.87	0.87	0.36	1.4319

Table A-17. Elastic recovery at 25 ºC (77 F) (RTFOT residue)

Binders	Replicate A (%)	Replicate B (%)	Average (%)
PG 67-22	7.41	4.94	6.18
PG 76-22	75.00	75.00	75.00
HB A	66.25	67.50	66.88
HB B	72.50	72.50	72.50
HB C	23.75	25.00	24.38

Table A-18. Force ductility test result

Binders	f2/f1 (10 ºC)	f2/f1 (RTFOT residue, 10 ºC)	f2/f1 (PAV residue, 25 ºC)
PG 67-22	0.04	0.04	0.03
PG 76-22	0.53	0.43	0.26
HB A	0.46	0.36	0.40
HB B	0.42	0.40	0.40
HB C	0.17	0.20	0.13
ARB-5	0.20	0.32	0.24
ARB-12	0.24	0.51	0.18

Table A-19. Smoke point, flash point and solubility of original binders

Binders	Smoke Point (F)	Flash Point (F)	Solubility (%)
PG 67-22	322.5	545.0	99.995
PG 76-22	330.0	552.5	99.975
HB A	325.0	557.5	92.760
HB B	320.0	550.0	96.905
HB C	320.0	495.0	99.860
ARB-5	315.0	545.0	93.835
ARB-12	320.0	547.5	88.765

Table A-20. Mass loss after RTFOT at 163 ºC (325.4 F)

Binders	Replicate A (%)	Replicate B (%)	Average (%)
PG 67-22	-0.423	-0.412	-0.418
PG 76-22	-0.370	-0.369	-0.370
HB A	-0.341	-0.340	-0.341
HB B	-0.359	-0.319	-0.339
HB C	-0.525	-0.522	-0.524
ARB-5	-0.429	-0.433	-0.431
ARB-12	-0.463	-0.472	-0.468

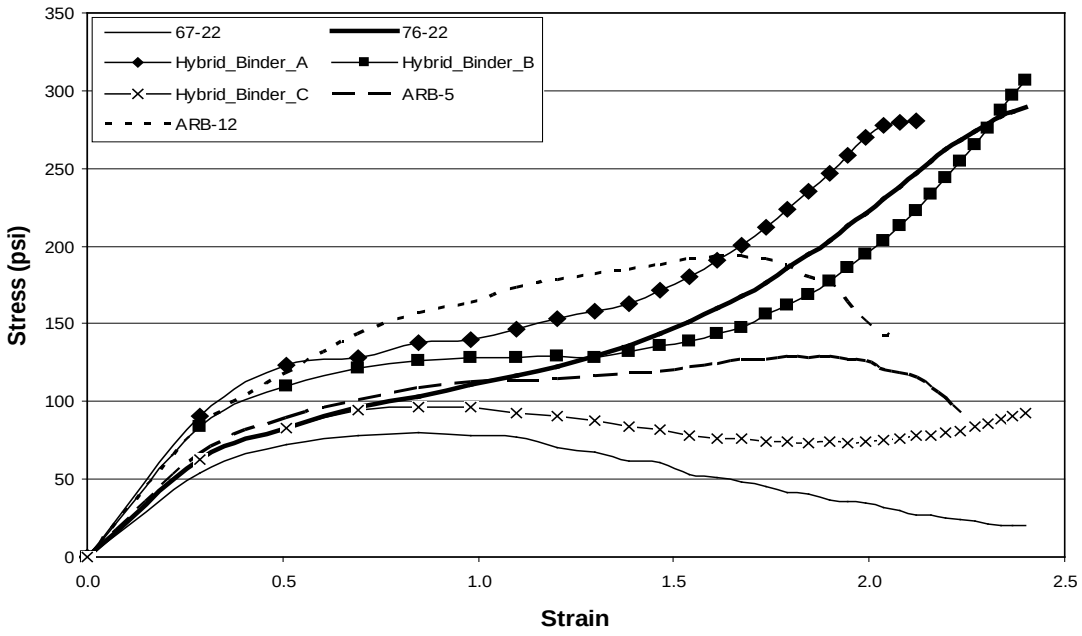

Figure A-1. Original binders stress-strain diagram, 10 ºC (50 F)

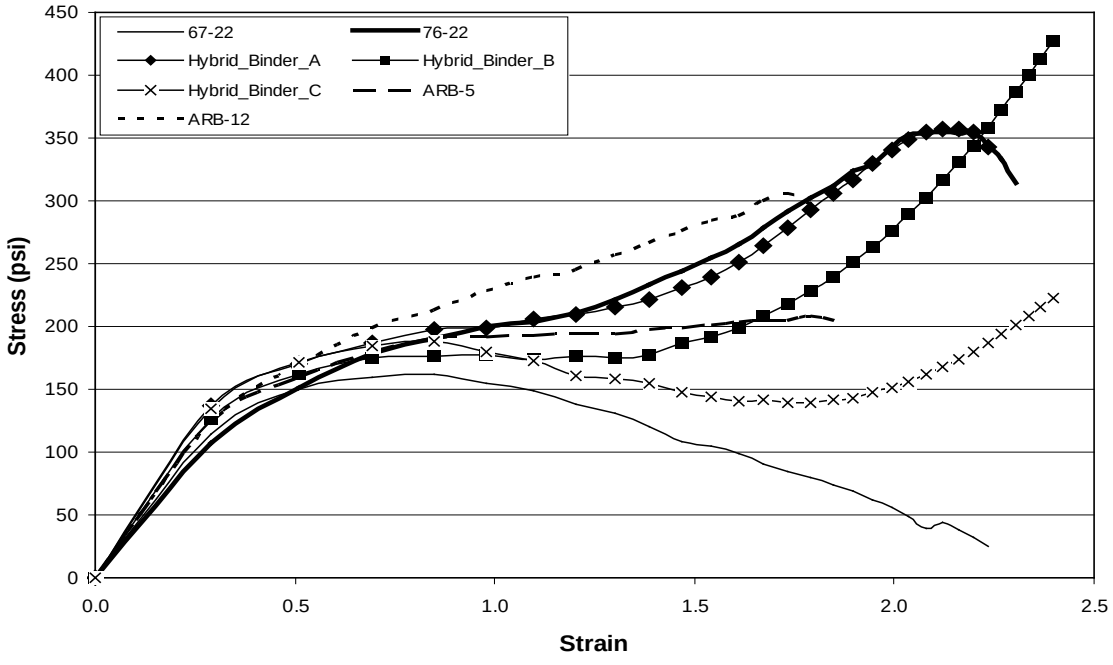

Figure A-2. RTFOT residues stress-strain diagram, 10 ºC (50 F)

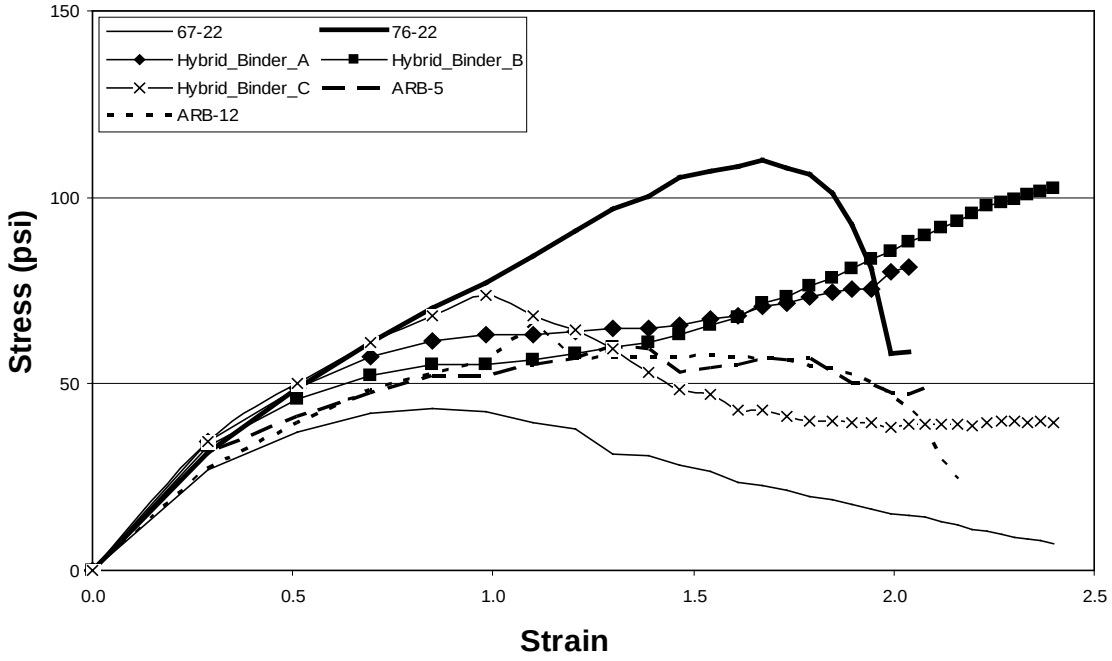

Figure A-3. PAV residues' stress-strain diagram, 25 ºC (77 F)

APPENDIX B
HEALING TEST RESULTS

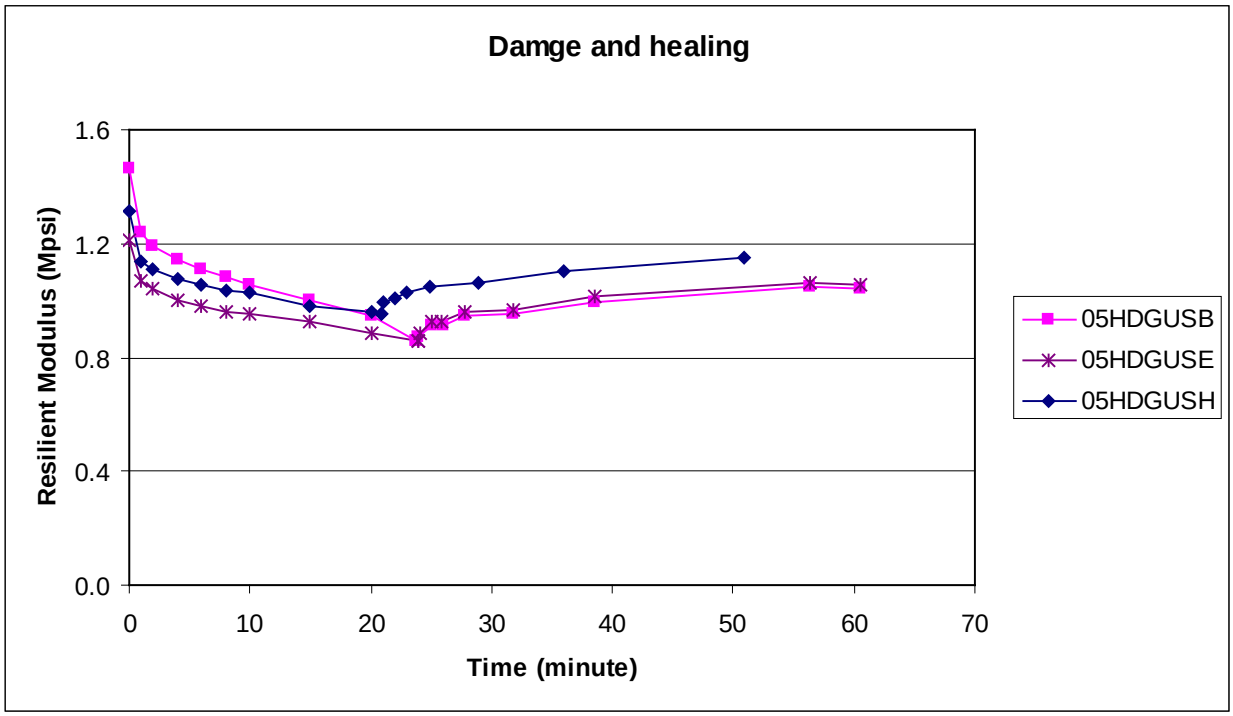

Figure B-1. M_{RDGUS} at damage and healing, 10 ºC

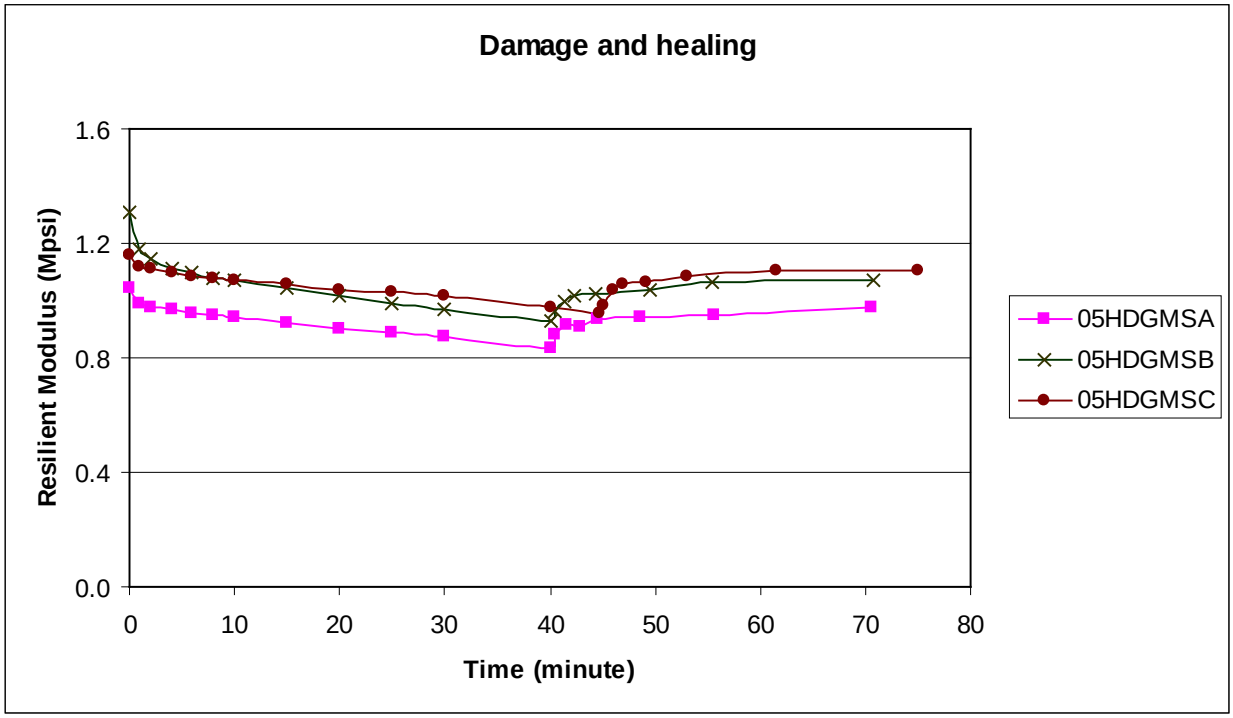

Figure B-2. M_{RDGMS} at damage and healing, 10 ºC

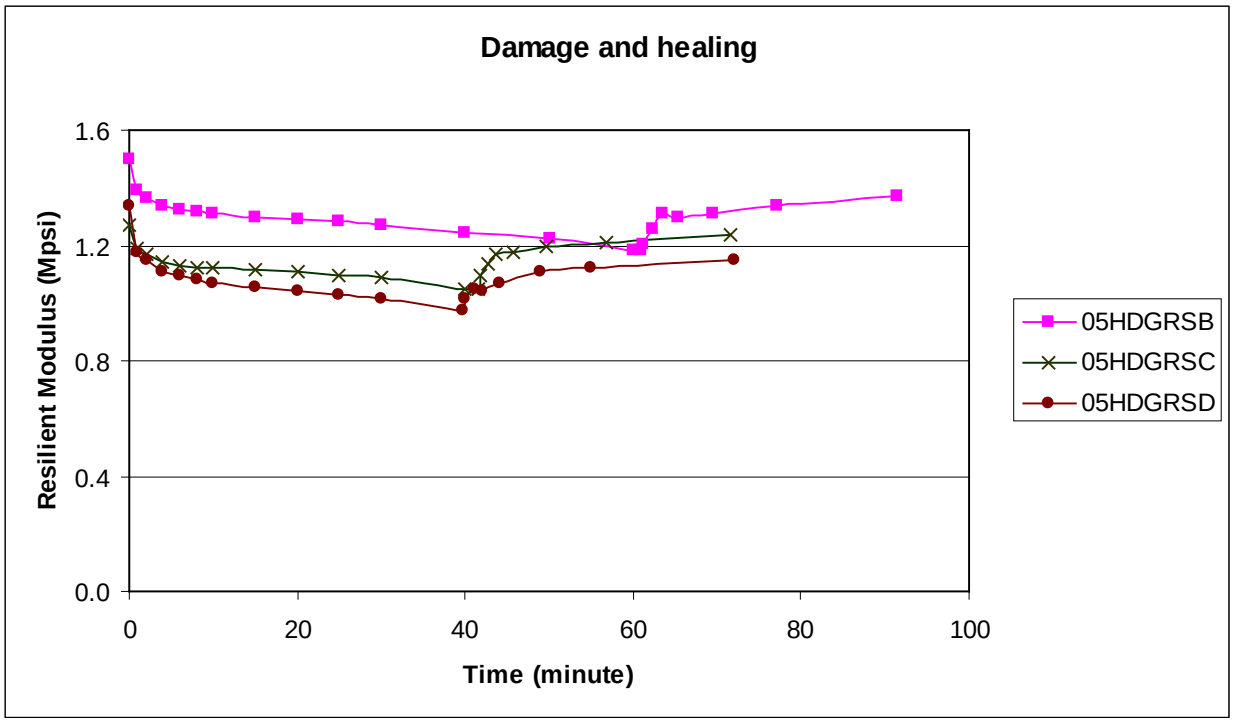

Figure B-3. M_{RDGRS} at damage and healing, 10 ºC

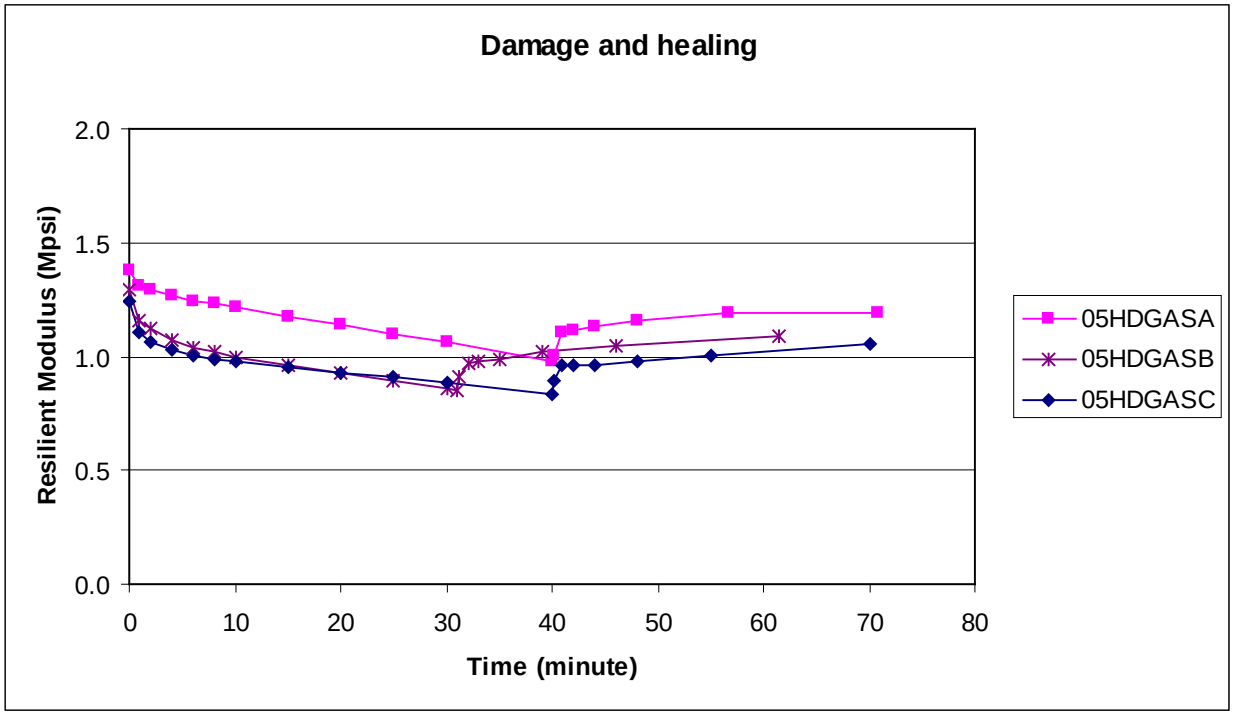

Figure B-4. M_{RDGAS} at damage and healing, 10 ºC

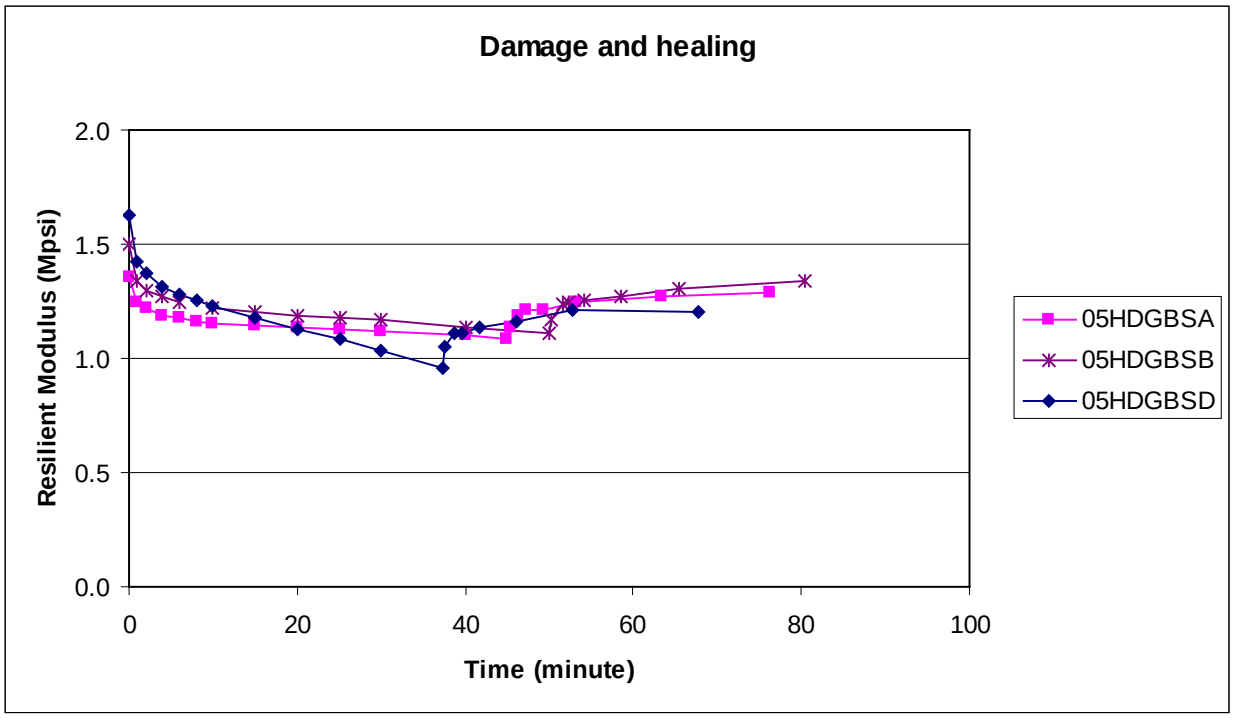

Figure B-5. M_{RDGBS} at damage and healing, 10 ºC

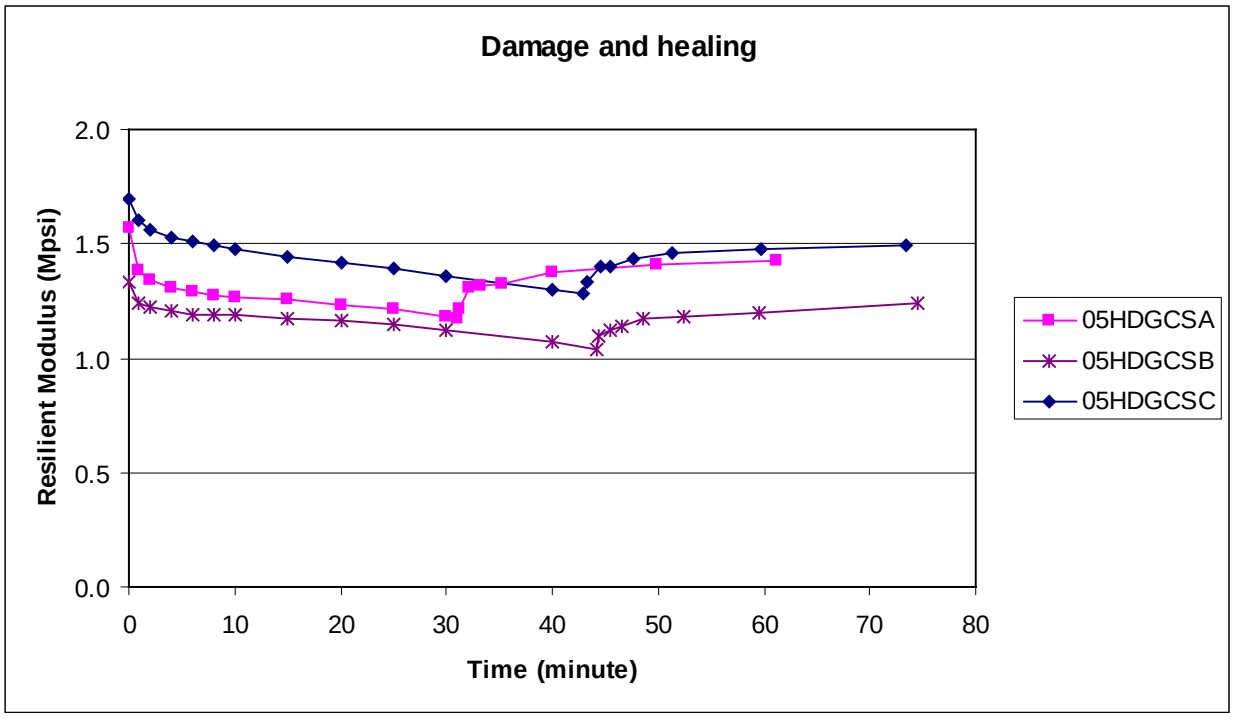

Figure B-6. M_{RDGCS} at damage and healing, 10 ºC

APPENDIX C
CITGO CERTIFICATES OF ANALYSIS

Certificate of Analysis

Supplier:	CITGO Asphalt Refining Co	Phone:	856-224-7409
Terminal:	Savannah Refinery	Fax:	856-423-7289
Address:	Savannah, GA 31408		

Date Sampled	7/5/2007	Grade	67-22	Specification	AASHTO M-320
Date Tested	7/5/2007	Tank #	52 Lot # 7	Sampled By	Jerome Hall
Date Received	7/5/2007	Volume	tons	DOT #	

TEST	METHOD	TEST LAB	SPECIFICATION REQUIREMENTS	TEST RESULTS
Unaged Binder				
Spot Test	AASHTO T 102		Negative	Negative
Absolute Viscosity @ 140°F	AASHTO T 202		Report	3310
Sp. Gravity @ 15.6°C, gm/cm³	AASHTO T 228		Report	1.043
Sp. Gravity @ 25.0°C, gm/cm³	AASHTO T 228		Report	1.037
Smoke Point	Fla Specs		> 125°C	177
Flash Point, °C	AASHTO T 48		> 230°C	277
Viscosity @ 135°C, Pa-s	AASHTO T 316		< 3.0 Pa-s	0.585
Viscosity @ 165°C, Pa-s	AASHTO T 316		Report	0.165
Lab Mixing Temp,°C			Max: 169 Min: 162	
Lab Compaction Temp,°C			Max: 155 Min: 150	
G*/sin(delta) (kPa) 67°C	AASHTO T 315	CICS	> 1.00 kPa	1.346
Phase Angle, δ	AASHTO T 315	CICS		84.9
RTFOT				
G*/sin(delta) (kPa) 67°C	AASHTO T 315	CICS	> 2.20 kPa	3.226
RTFOT Mass Change (%)	AASHTO T 240	CICS	< 0.500 %	-0.347
PAV				
G*sin(delta) (kPa) 25°C	AASHTO T 315	CICS	< 5,000 kPa	3529
Stiffness (MPa) @ 60 s -12°C	AASHTO T 313	CICS	< 300 MPa	157
m-value @ 60 s -12°C	AASHTO T 313.	CICS	> 0.300	0.360

This Binder classifies as a PG67-22

This material meets requirements set forth in AASHTO M320 and ASTM D6373 and FLDOT Specification Section 916-1.1

By providing this data under my signature, I attest to the accuracy and validity of the data contained on this form and certify that no deliberate misrepresentation of test results, in any manner, has occurred.

Remarks Solubility = 99.98 %

Testing Laboratory:
CITGO Savannah
Savannah, GA
AASHTO #: 1303

Responsible Technician:
Jerome Hall
Signature:

Person responsible for certification:
Larry Bristow 7/6/2007
Signature:

Certificate of Analysis

Supplier:	CITGO Asphalt Refining Co	Phone:	856-224-7409
Terminal:	Savannah Refinery	Fax:	856-423-7289
Address:	Savannah, GA 31408		

Date Sampled	7/6/2007	Grade	76-22	Specification	AASHTO M-320
Date Tested	7/6/2006	Tank #	18 Lot # 7	Sampled By	Jerome Hall
Date Received	7/6/2007	Volume	2,091 tons	DOT #	QC-0200162

TEST	METHOD	TEST LAB	SPECIFICATION REQUIREMENTS	TEST RESULTS
Unaged Binder				
Sp. Gravity @ 15.6°C, gm/cm³	AASHTO T 228		Report	1.039
Sp. Gravity @ 25.0°C, gm/cm³	AASHTO T 228		Report	1.033
Flash Point, °C	AASHTO T 48		> 230°C	282
Smoke Point, °C	FM-5-519		> 230°C	177
Spot Test	AASHTO T102		Negative	Negative
Viscosity @ 135°C, Pa-s	AASHTO T 316		< 3.0 Pa-s	1.515
Viscosity @ 165°C, Pa-s	AASHTO T 316		Report	0.425
Lab Mixing Temp,°C			Max: 163	Min: 157
Lab Compaction Temp,°C			Max: 157	Min: 152
G*/sin(delta) (kPa) 76°C	AASHTO T 315	CICS	> 1.00 kPa	1.347
Phase Angle, δ	AASHTO T 315	CICS		72.8
RTFOT				
G*/sin(delta) (kPa) 76°C	AASHTO T 315	CICS	> 2.20 kPa	2.965
RTFOT Mass Change (%)	AASHTO T 240	CICS	< 0.500 %	-0.341
PAV				
G*sin(delta) (kPa) 31°C	AASHTO T 315	CICS	< 5,000 kPa	1365
G*sin(delta) (kPa) 25°C	AASHTO T 315	CICS	< 5,000 kPa	3006
Stiffness (MPa) @ 60 s -12°C	AASHTO T 313	CICS	< 300 MPa	146
m-value @ 60 s -12°C	AASHTO T 313.	CICS	> 0.300	0.362

This Binder classifies as a PG76-22

This product conforms to the specifications of AASHTO M-320, ASTM D-6373, The State of Georgia's Provision: Section 820.01, and The State of Florida's Provision: Section 916-1 for Superpave Asphalt Binders.

By providing this data under my signature, I attest to the accuracy and validity of the data contained on this form and certify that no deliberate misrepresentation of test results, in any manner, has occurred.

Remarks Solubilty = 99.98%

Testing Laboratory:	Responsible Technician:	Person responsible for certification:
CITGO Savannah	Jerome Hall	Larry Bristow 7/7/2007
Savannah, GA	Signature:	Signature:
AASHTO #: 1303		

LIST OF REFERENCES

Abdelrahman, M. (2006). "Controlling performance of crumb rubber-modified binders through addition of polymer modifiers." *Transportation research record*, Washington, D.C., 64-70.

Bouldin, M.G. and Collins, J.H. (1992). "Influence of binder rheology on rut resistance of polymer modified and unmodified hot mix asphalt," *Polymer Modified Asphalt binders*, ASTM STP 1108, 50-60.

Buttlar, W. G. and Roque, R. (1994). "Experimental development and evaluation of the new SHRP measurement and analysis system for indirect tensile testing of asphalt mixtures at low temperatures." *Association of Asphalt Paving Technologists*, 1994.

Choubane, B., Sholar, G. A.; Musselman, J. A.; and Page, G. C. (1999). "Ten-year performance evaluation of asphalt-rubber surface mixes," *Transportation Research Record* (TRB), No.1681, 10-18.

Cook, M. C., Bressette, T., Holikatti, S., Zhou, H. and Hicks, R. G. (2006). "Laboratory evaluation of asphalt rubber modified mixes," *Proceedings of the Asphalt Rubber 2006 Conference*, Palm Springs, USA, 599-618.

Cui, Z. (2003). "Use of binder rheology to predict the cracking performance of SBS-modified mixture," *Doctoral thesis*, University of Florida, Florida.

D'Angelo, J., Dongre, R. N. (2009). "Practical Use of Multiple Stress Creep Recovery Test: Characterization of Styrene-Butadiene-Styrene Dispersion and Other Additives in PMA Binders," *Transportation Research Board 88th Annual Meeting*, Washington DC, USA.

Hicks, R.G., Lundy, J.R., Leahy, R.B., Hanson, D., and Epps, J. (1995). "Crumb rubber modifiers (CRM) in asphalt pavements: Summary of practices in Arizona, California, and Florida," Transportation Research Institute, Oregon State University, *Report* No. FHWA-SA-95-056.

Fleckenstein, L.J., Mahboub, K., and Allen, D.L. (1992). "Performance of polymer modified asphalt mixes in kentucky," Polymer Modified Asphalt Binders, ASTM STP 1108, *American Society for Testing and Materials*, Philadelphia, USA

Kim, B., Roque, R. and Birgisson, B. (2003) "Laboratory evaluation of the effect of modifier on cracking resistance of asphalt mixture," *Annual Meeting of the Transportation Research Board*, Washington D.C.

Moseley, H. L., Page, G., Musselman, J. A., Scholar, G. A., Upshaw, P. B. (2003). "Laboratory mixture and binder rutting study," *Research Report*, FL/DOT/SMO/03-465.

Page, G C; Ruth, B E; West, R C. (1992) “Florida’s approach using ground tire rubber in asphalt concrete mixtures.” *Transportation Research Record* (TRB), No.1339, 16-22.

Page, G C. (1992). “Florida's initial experience utilizing ground tire rubber in asphalt concrete mixes,” *Association of Asphalt Paving Technologists* (AAPT), Vol. 61, 446.

Roberts, F. L., Kandhal, P. S., Brown, E. R., Lee, D. and Kennedy, T. W. (1996). “Hot mix asphalt materials, mixture design and construction.” *National Asphalt Pavement Association Research and Education Foundation*, Lanham, Maryland, Second edition.

Romagosa, H., Corun, R. and Berkley, R.(2008). “SBS polymer supply outlook,” *Association of Modified Asphalt Producers (AMAP)’s Updated White Paper on the SBS Supply Outlook*, St. Louis, MO.

Rogge, D.F., Terrel, R.L. and George A.J. (1992). “Polymer modified hot mix asphalt—Oregon experience.” *Polymer Modified Asphalt Binder*, ASTM STP 1108, Kenneth R. *Testing and Materials*, Philadelphia.

Roque, R., Birgisson, B., Drakos, C. and Dietrich, B. (2004). “Development and field evaluation of energy-based criteria for top-down cracking performance of Hot Mix Asphalt,” *Journal of the Association of Asphalt Paving Technologists*, Vol. 73, 229-260.

Roque, R., and Buttlar, W.G.(1992). “The development of a measurement and analysis system to accurately determine asphalt concrete properties using the indirect tensile test.” *Association of Asphalt Paving Technologists* (AAPT), Vol. 73, 395.

Shuler, T. S., Collins, J. H., and Kirkpatrick, J. P., “Polymer modified asphalt properties related to asphalt concrete performance.” *Asphalt Rheology: Relationship to Mixture, ASTM STP 941*, O. E. Briscoe, American Society for Testing and Materials, Philadelphia, 1987, pp. 179-193.

Sousa, J., Way, G. B. and Zareh, A. (2006). “Asphalt-rubber gap graded mix design concepts.” *Proceedings of the Asphalt Rubber 2006 Conference*, Palm Springs, USA, 523-543.

The Balmoral Group. (2008). “2008 Strategic resource evaluation update: highway construction materials.” the Balmoral Group, Maitland, FL.

Tia, M.; Roque, R.; Sirin, O. and Kim, H-J. (2002). “Evaluation of superpave mixtures with and without polymer modification by means of Accelerated Pavement Testing,” *Report to FDOT*, UF PN 49104504801-12.

Xiao, F., Putman, B. J. and Amirkhaniam, S. N.(2006). “Laboratory investigation of dimensional changes of crumb rubber reacting with asphalt binder,” *Proceedings Asphalt Rubber 2006 Conference*, Palm Springs, USA, 693-713.

BIOGRAPHICAL SKETCH

Weitao Li was born in a small town, Julu, which lies in south part of Hebei province in north China. He grew up there and finished all his preliminary school, middle school and high school years in that town.

In 1997, he was admitted by Jilin University, Changchun and awarded Bachelor Degree of Drilling and Exploration Engineering in the year of 2001. Thanks to his exceptional overall performance in school, he was titled Outstanding Graduate by the university on the Graduation Ceremony and in the same year, he was recommended to pursue the master degree of geological engineering in the same college with waiver of entrance exams. Three years later, he finished his graduate study and was awarded the degree Master of Geological Engineering in 2004.

In August of the year 2005, he came to the U.S. to pursue a Ph.D. degree in the Department of Civil and Coastal Engineering at UF under the supervision of professors Dr. Reynaldo Roque and Dr. Bjorn Birgisson. Except for the academia, he also actively took part in volunteering activities in the University of Florida to help other students. He worked as the President of Friendship Association of Chinese Students and Scholars at the University of Florida during the school year of 2008 to 2009. After completing his Ph.D., he plans to work in industrial companies in Civil Engineering to continue his dedication to this field.